Guias de Onda e Fibras Óticas

Ondas eletromagnéticas

Ondas electromagnéticas

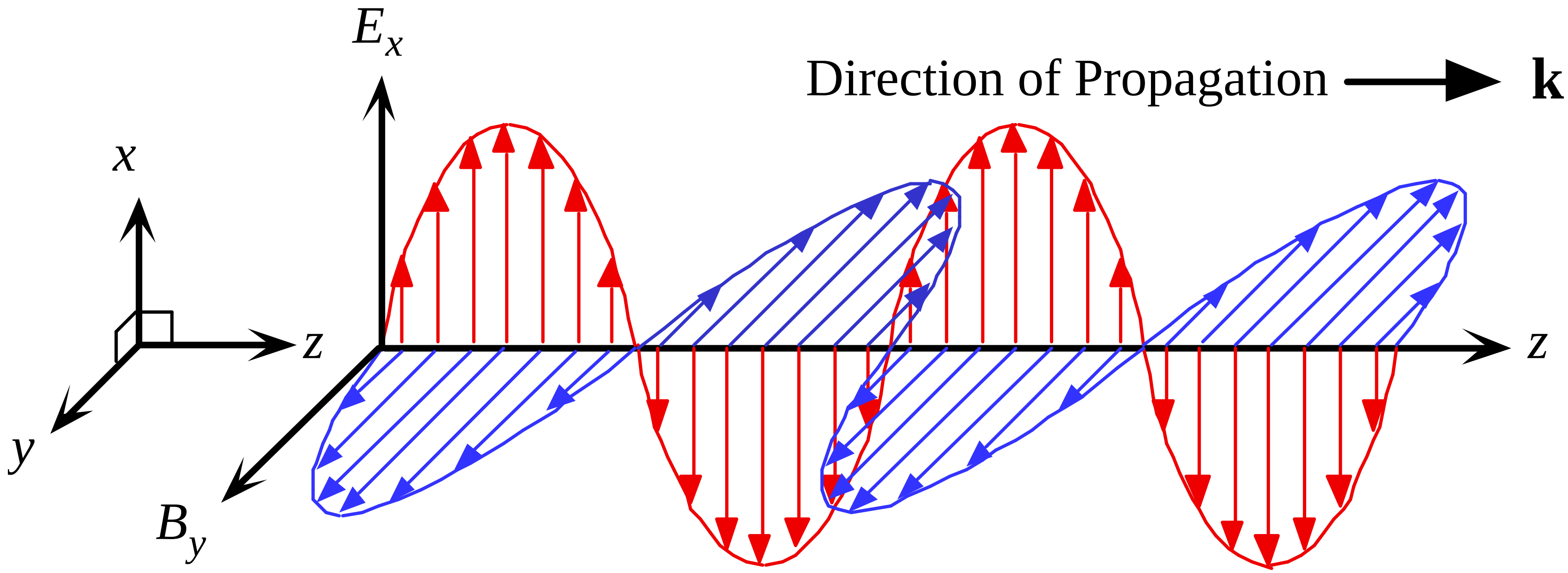

An electromagnetic wave is a travelling wave which has time varying electric and magnetic fields which are perpendicular to each other and the direction of propagation, *z*.

Wave fronts– regions with the same phase

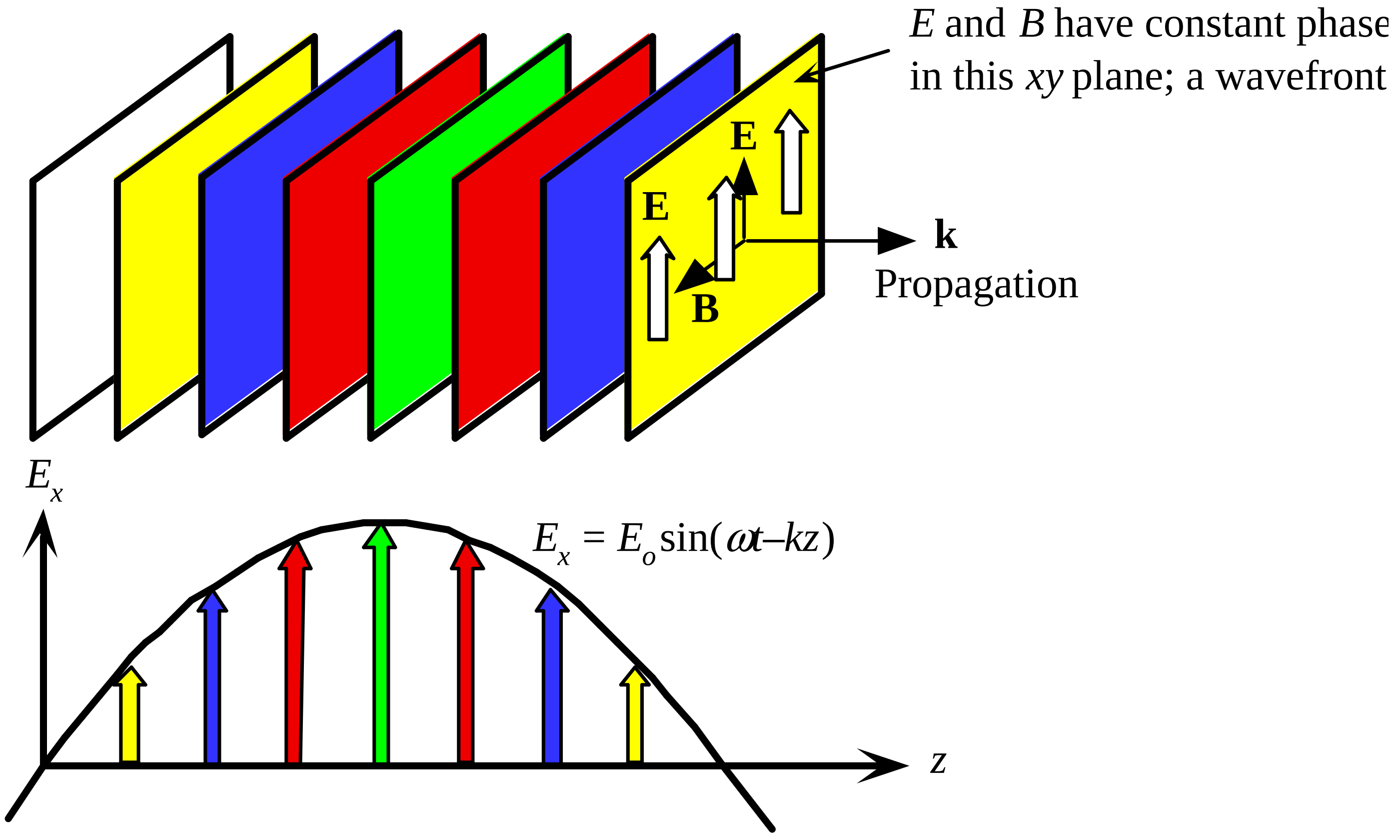

A plane EM wave travelling along z, has the same E_x (or B_y) at any point in a given xy plane. All electric field vectors in a given xy plane are therefore in phase. The xy planes are of infinite extent in the x and y directions.

Vector de Poynting

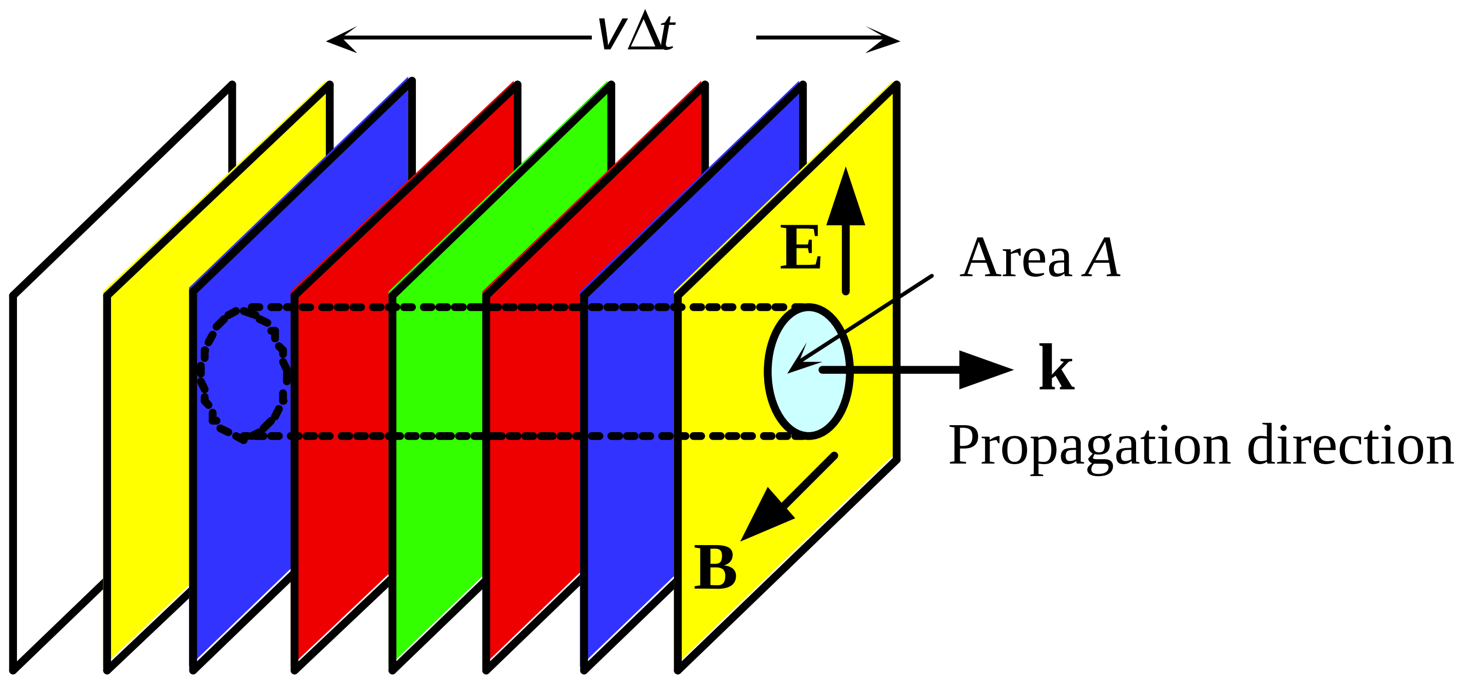

A plane EM wave travelling along **k** crosses an area A at right angles to the direction of propagation. In time Δt, the energy in the cylindrical volume $Av\Delta t$ (shown dashed) flows through A .

Wave vector - Vector de onda

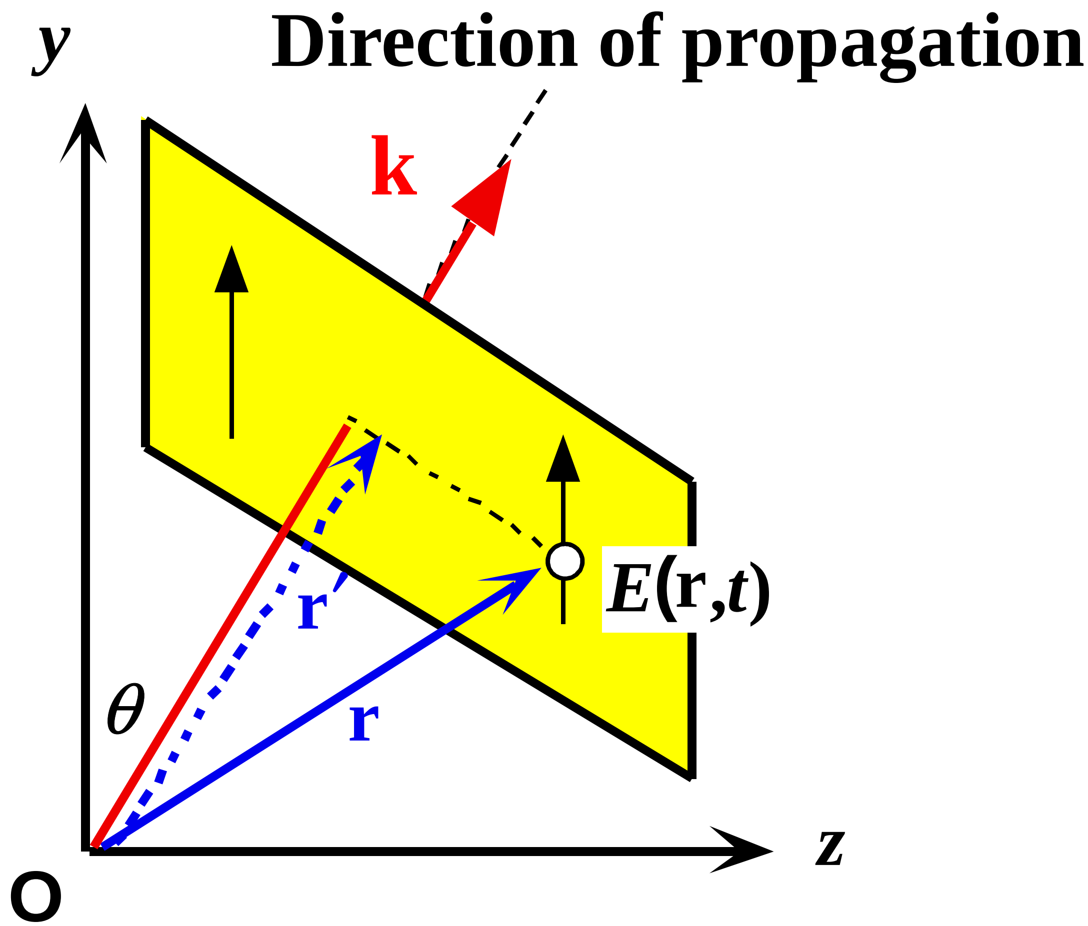

A travelling plane EM wave along a direction k.

Examples of electromagnetic wave fronts

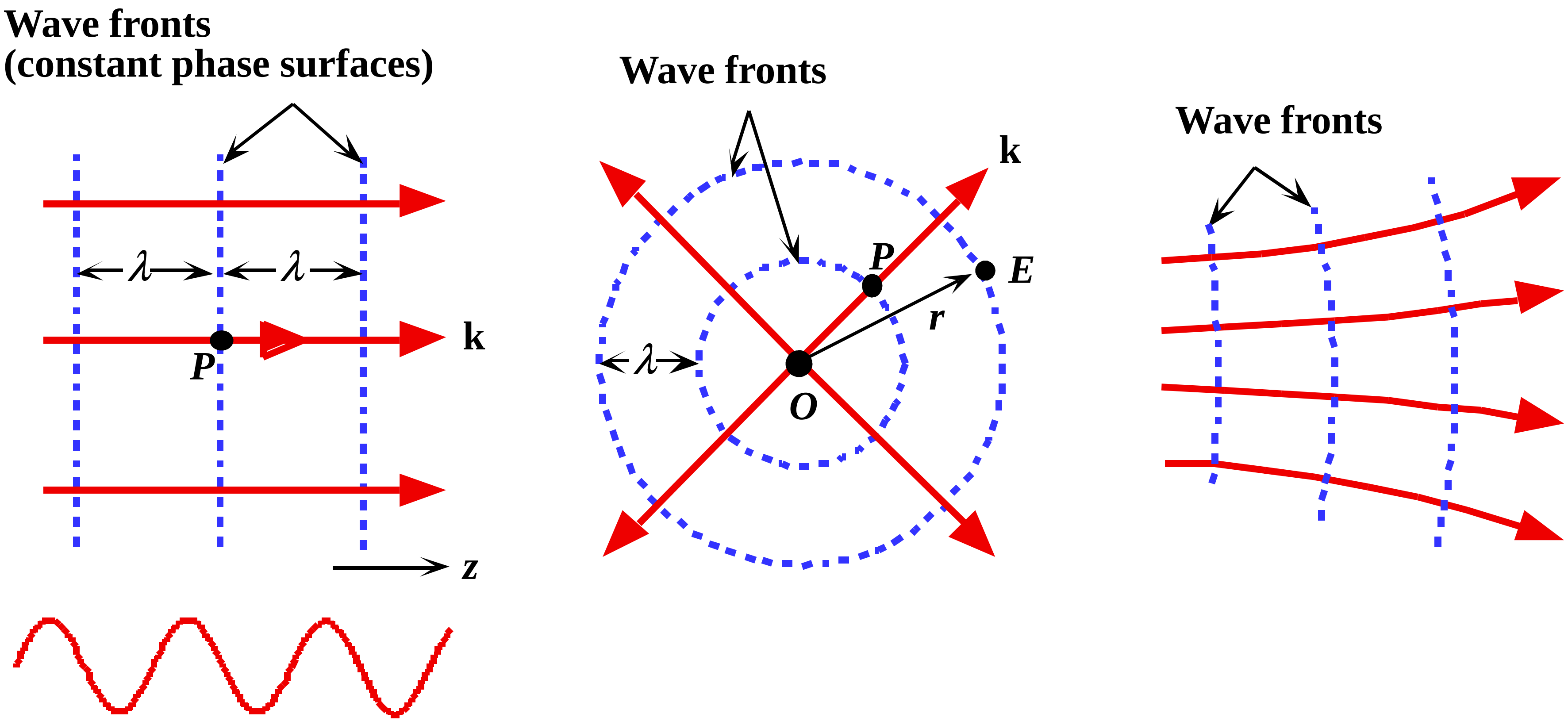

A perfect plane wave

(a)

A perfect spherical wave

(b)

A divergent beam

(c)

Examples of possible EM waves

Ondas electromagnéticas – Gaussian beam

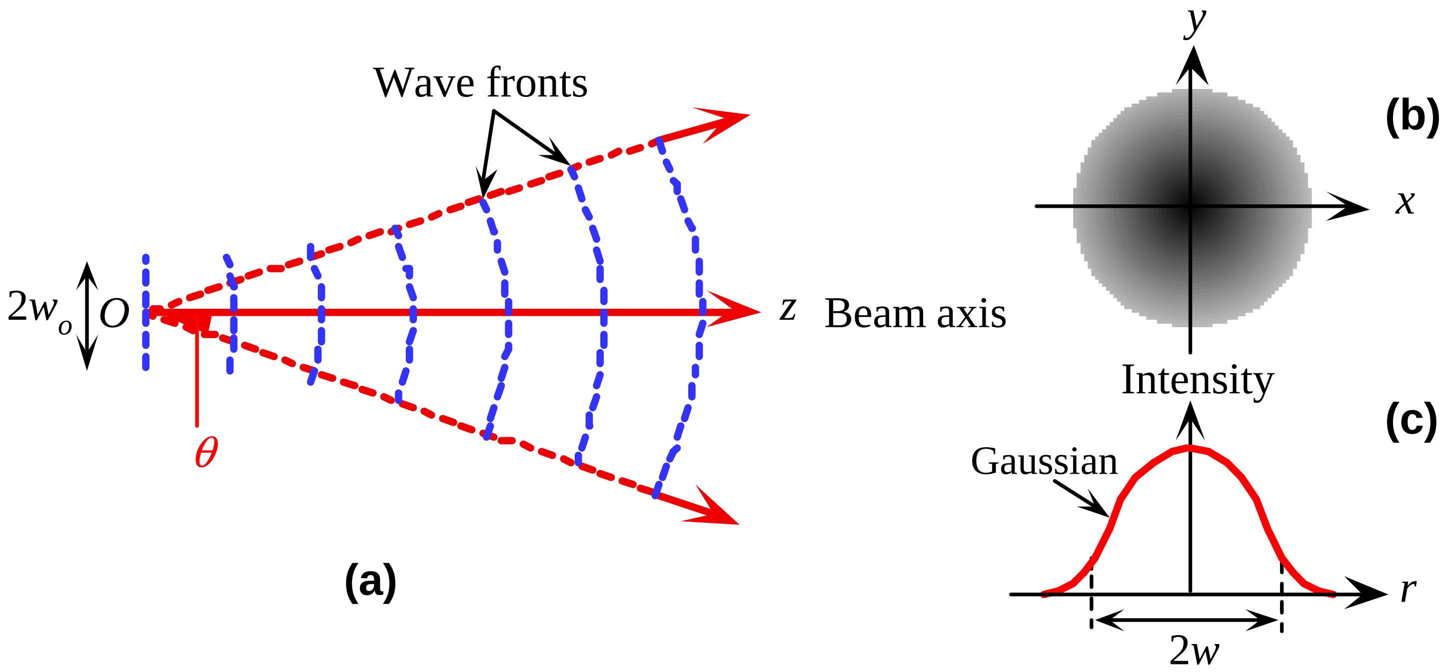

(a) Wavefronts of a Gaussian light beam. (b) Light intensity across beam cross section. (c) Light irradiance (intensity) vs. radial distance *r* from beam axis (*z*).

Group velocity

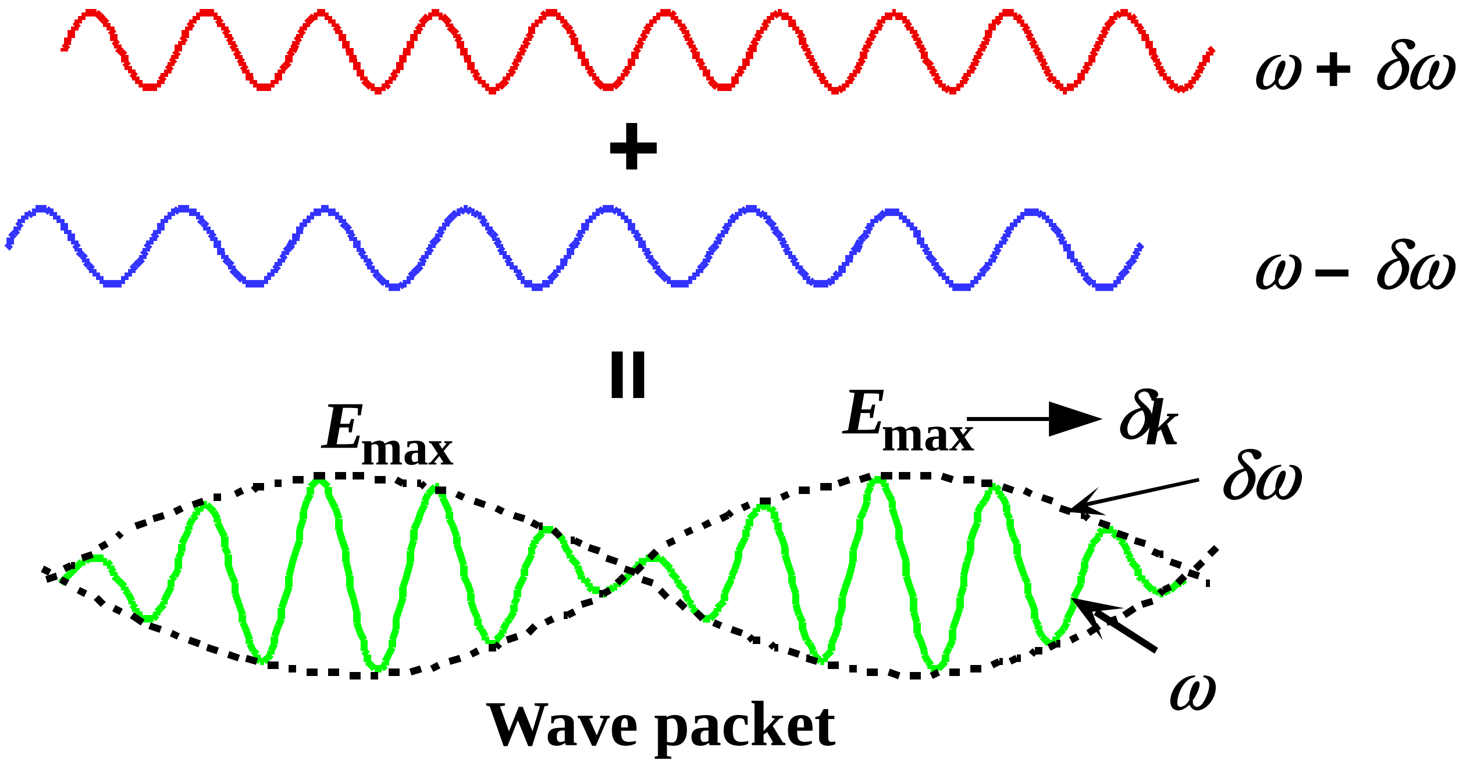

Two slightly different wavelength waves travelling in the same direction result in a wave packet that has an amplitude variation which travels at the group velocity.

Índice de refracção de grupo

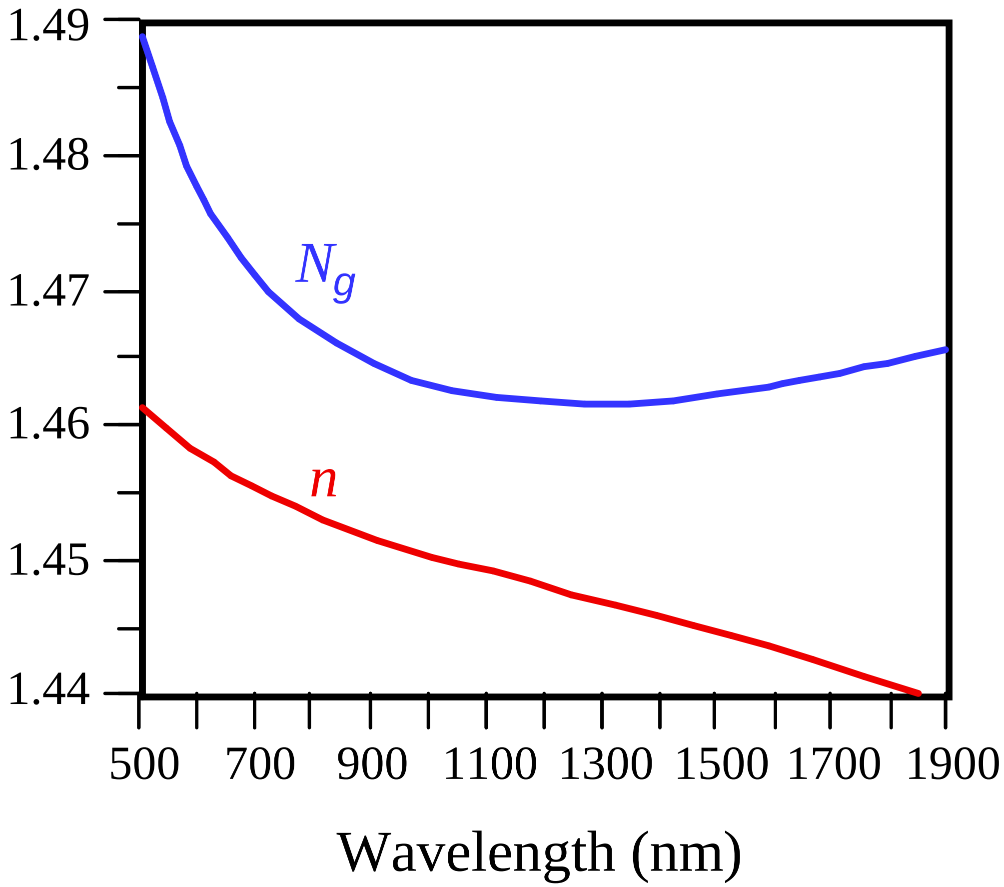

Refractive index n and the group index N_g of pure SiO_2 (silica) glass as a function of wavelength.

Coerência temporal e espacial

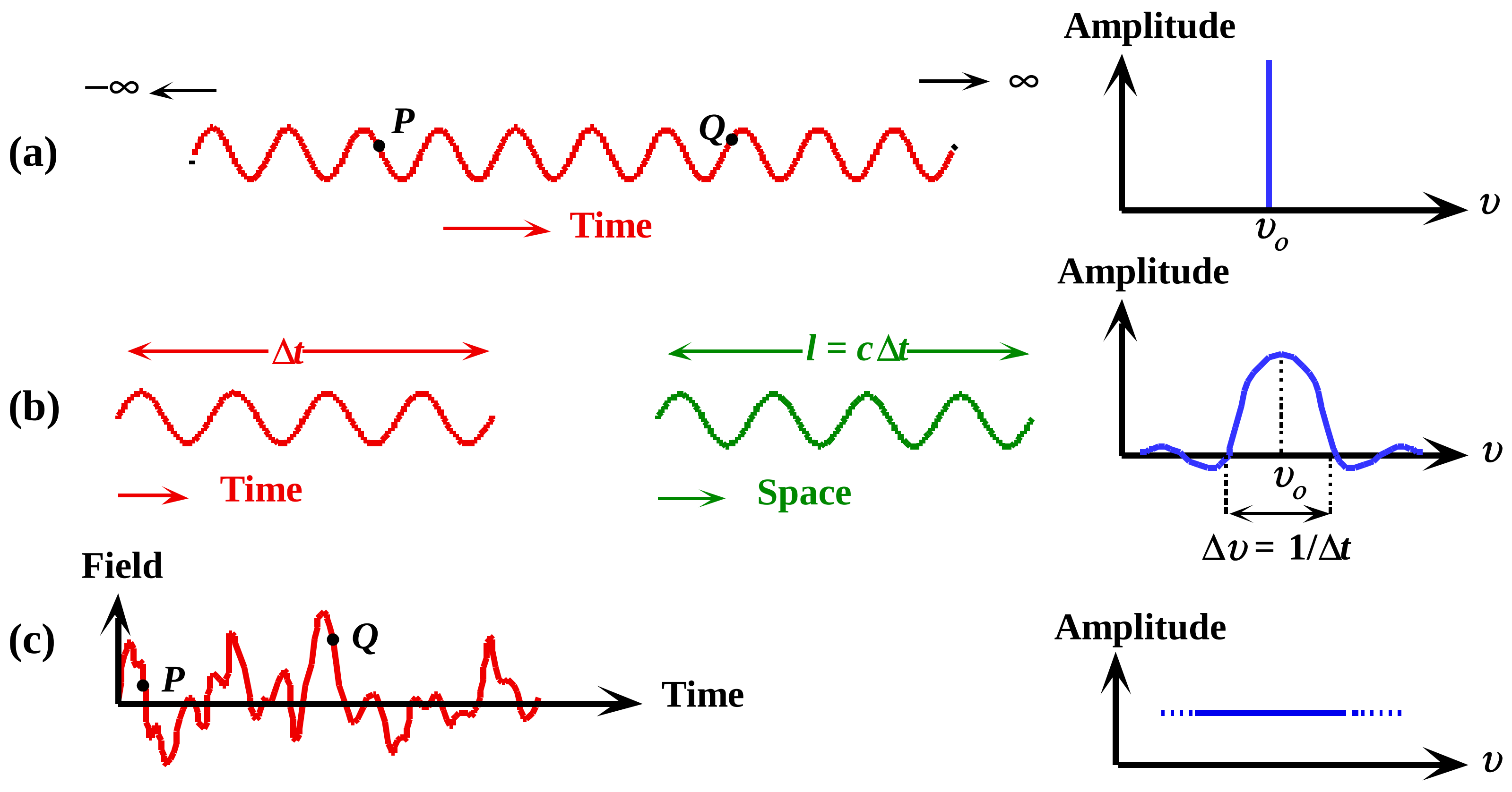

(a) A sine wave is perfectly coherent and contains a well-defined frequency υ_o. (b) A finite wave train lasts for a duration Δt and has a length l. Its frequency spectrum extends over $\Delta\upsilon = 1/\Delta t$. It has a coherence time Δt and a coherence length l. (c) White light exhibits practically no coherence.

Coerência temporal e espacial e o fenómeno de interferência

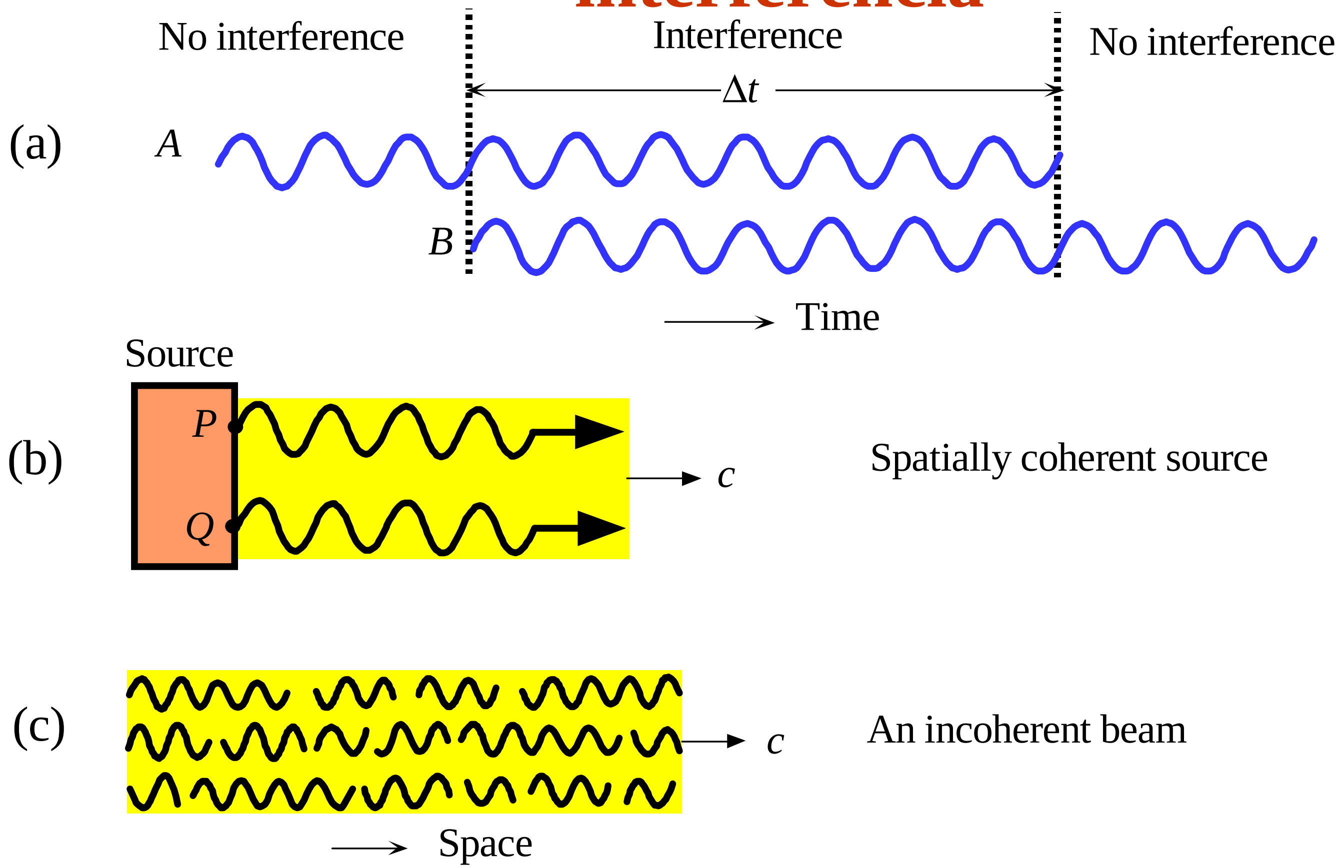

(a) Two waves can only interfere over the time interval Δt. (b) Spatial coherence involves comparing the coherence of waves emitted from different locations on the source. (c) An incoherent beam.

Fenómeno da reflexão interna total

Reflexão e refracção

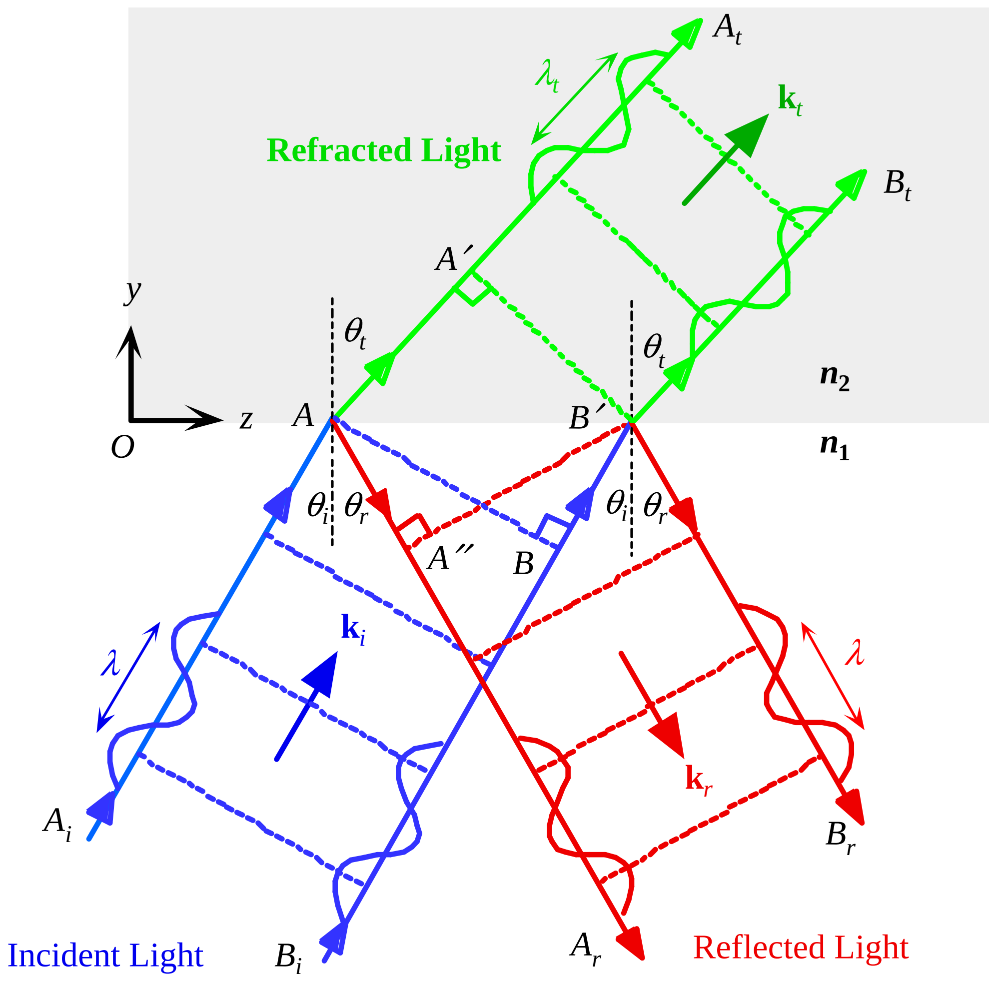

A light wave travelling in a medium with a greater refractive index $(n_1 > n_2)$ suffers reflection and refraction at the boundary.

Leis de Snell

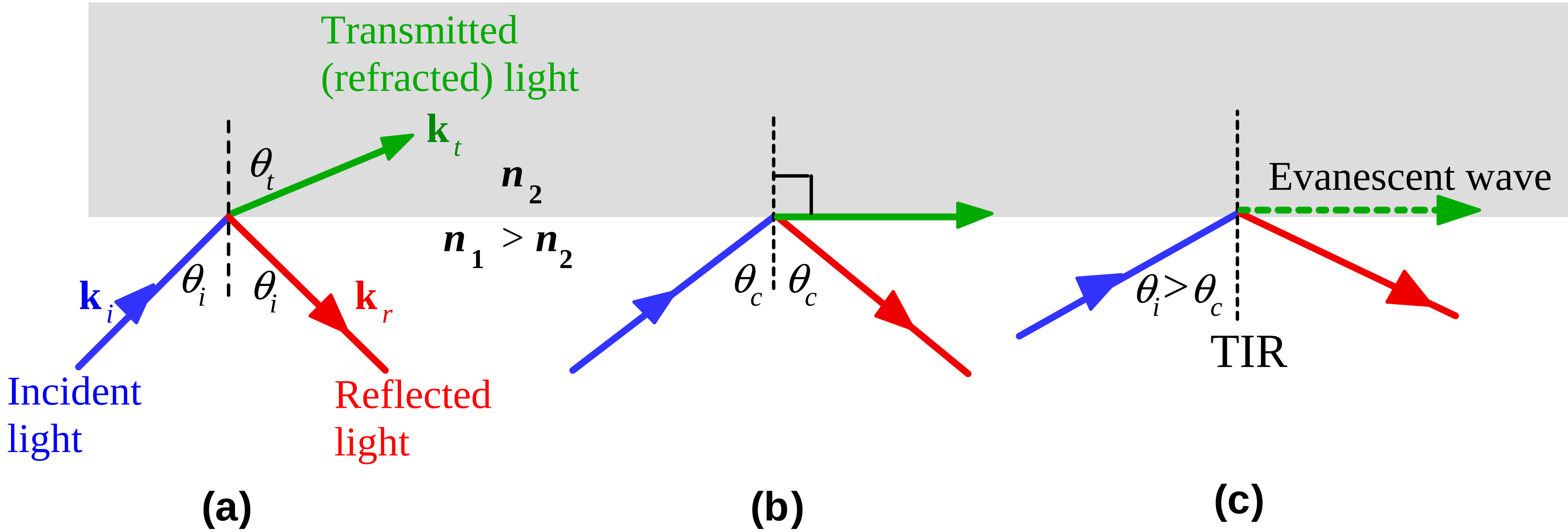

Light wave travelling in a more dense medium strikes a less dense medium. Depending on the incidence angle with respect to θ_c, which is determined by the ratio of the refractive indices, the wave may be transmitted (refracted) or reflected. (a) $\theta_i < \theta_c$ (b) $\theta_i = \theta_c$ (c) $\theta_i > \theta_c$ and total internal reflection (TIR).

Equações de Fresnel

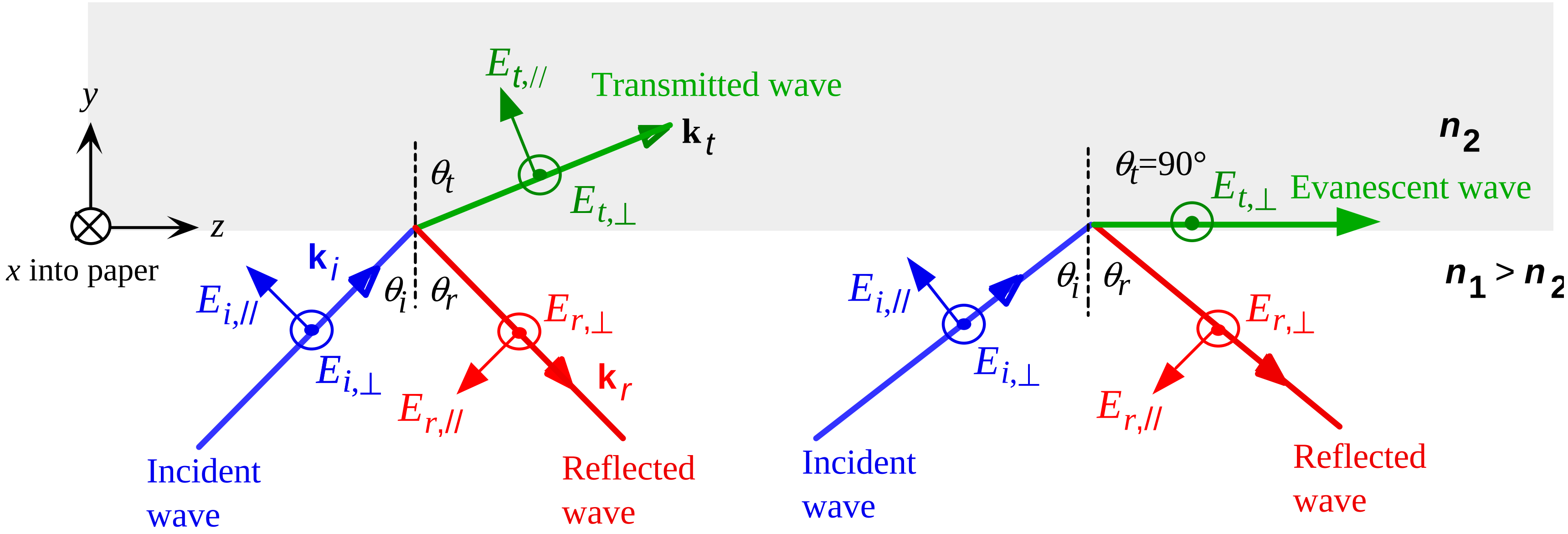

(a) $\theta_i < \theta_c$ then some of the wave is transmitted into the less dense medium. Some of the wave is reflected.

(b) $\theta_i > \theta_c$ then the incident wave suffers total internal reflection. However, there is an evanescent wave at the surface of the medium.

Light wave travelling in a more dense medium strikes a less dense medium. The plane of incidence is the plane of the paper and is perpendicular to the flat interface between the two media. The electric field is normal to the direction of propagation . It can be resolved into perpendicular (⊥) and parallel (//) components

Coeficientes de reflexão e variação da fase

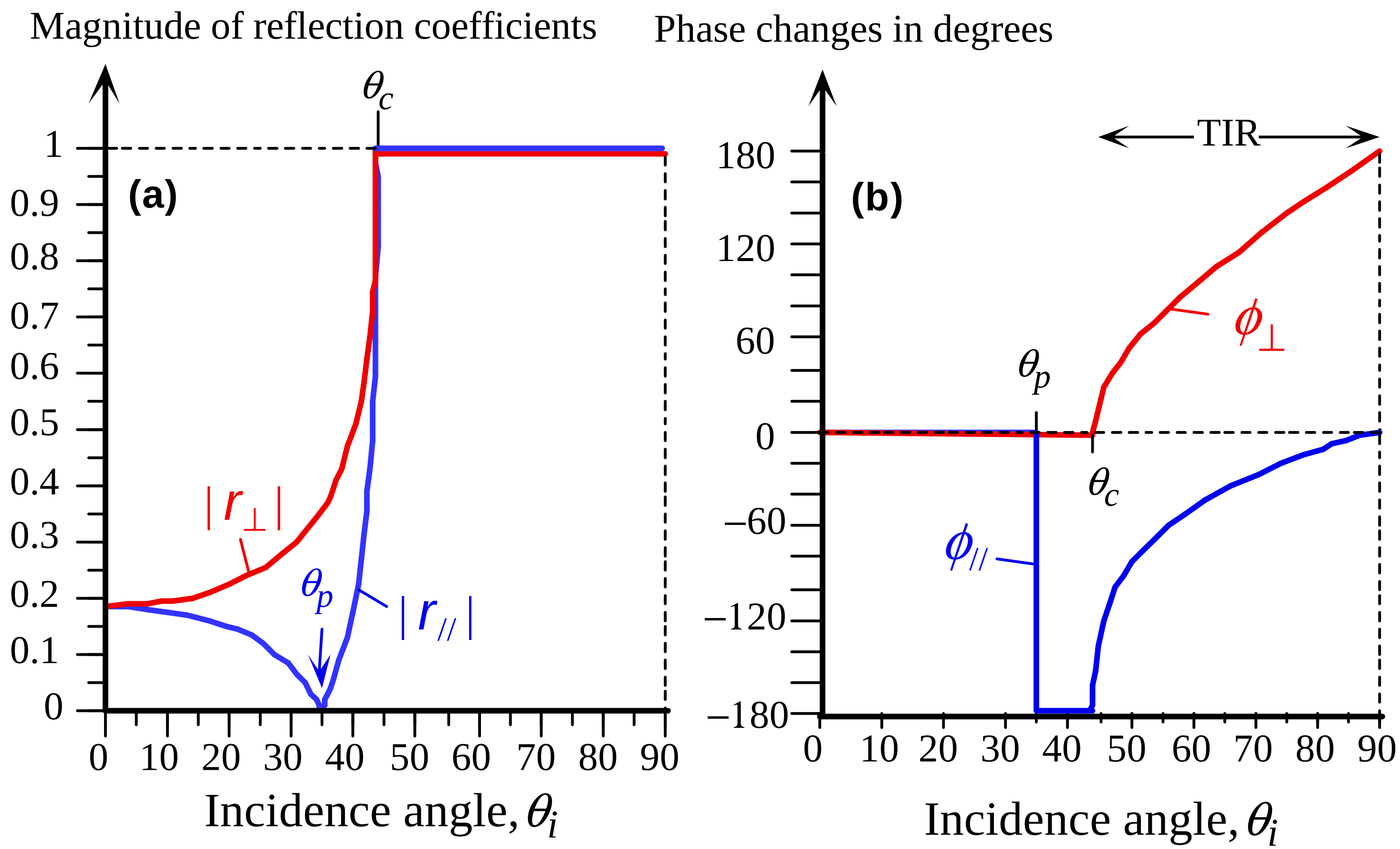

Internal reflection: (a) Magnitude of the reflection coefficients $r_{//}$ and $r_{\perp}$ vs. angle of incidence θ_i for n_1 = 1.44 and n_2 = 1.00. The critical angle is 44°. (b) The corresponding phase changes $\phi_{//}$ and $\phi_{\perp}$ vs. incidence angle

Coeficientes de reflexão

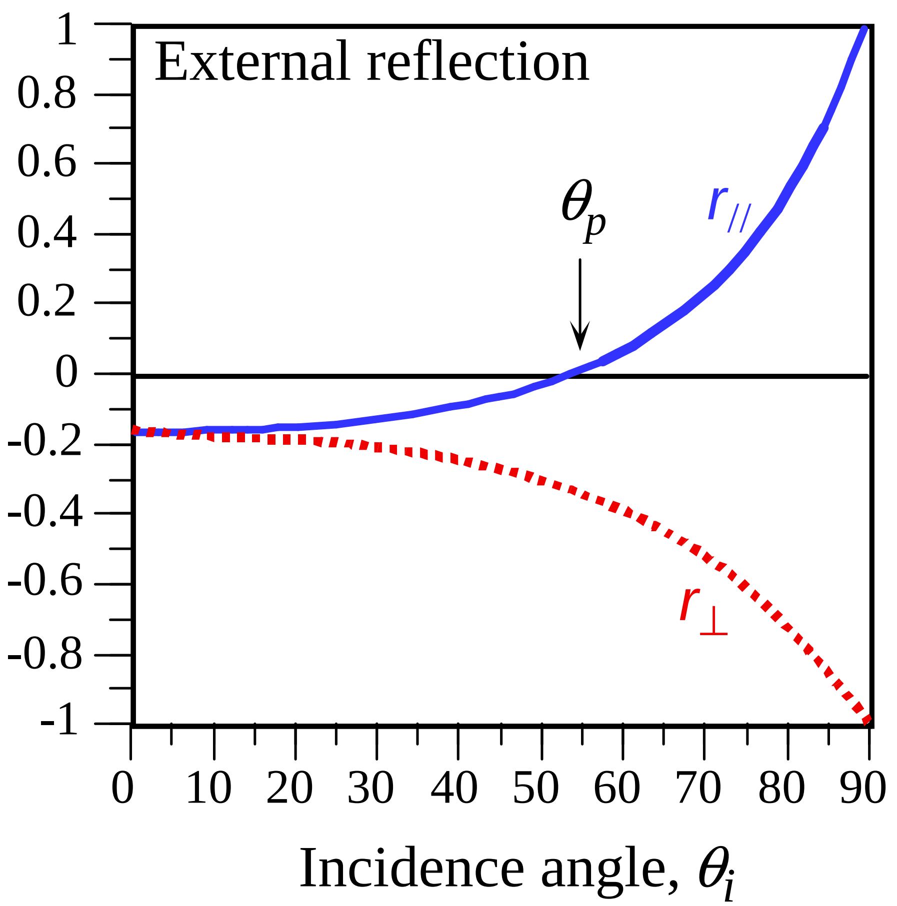

The reflection coefficients $r_{//}$ and $r_{\perp}$ vs. angle of incidence θ_i for $n_1 = 1.00$ and $n_2 = 1.44$.

Reflexão total: profundidade de penetração

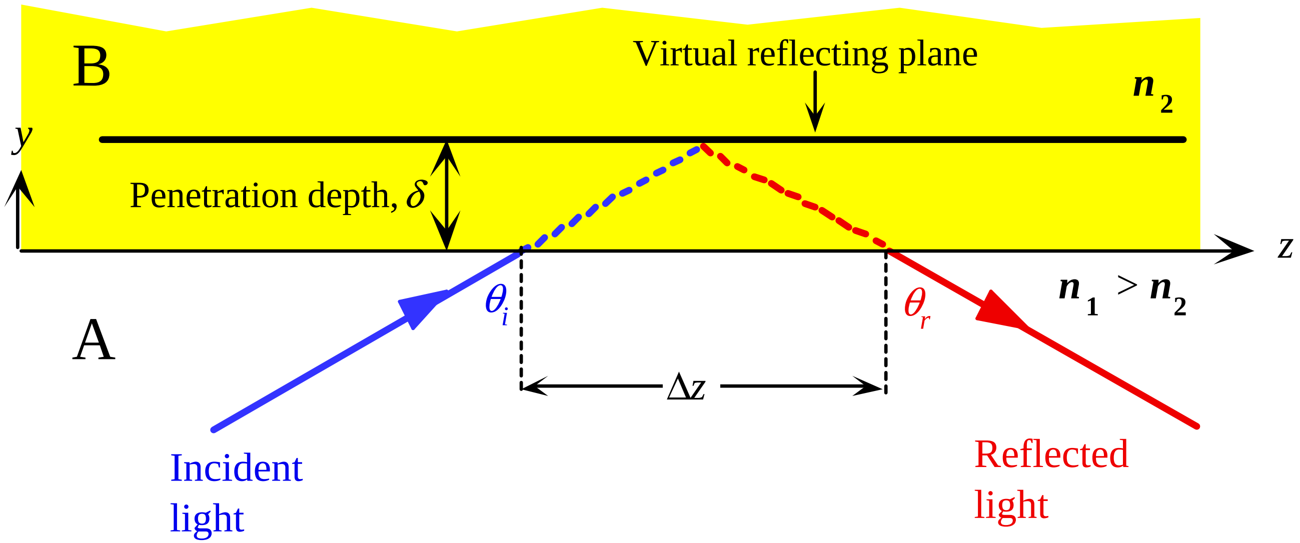

The reflected light beam in total internal reflection appears to have been laterally shifted by an amount Δz at the interface.

Efeito de túnel óptico

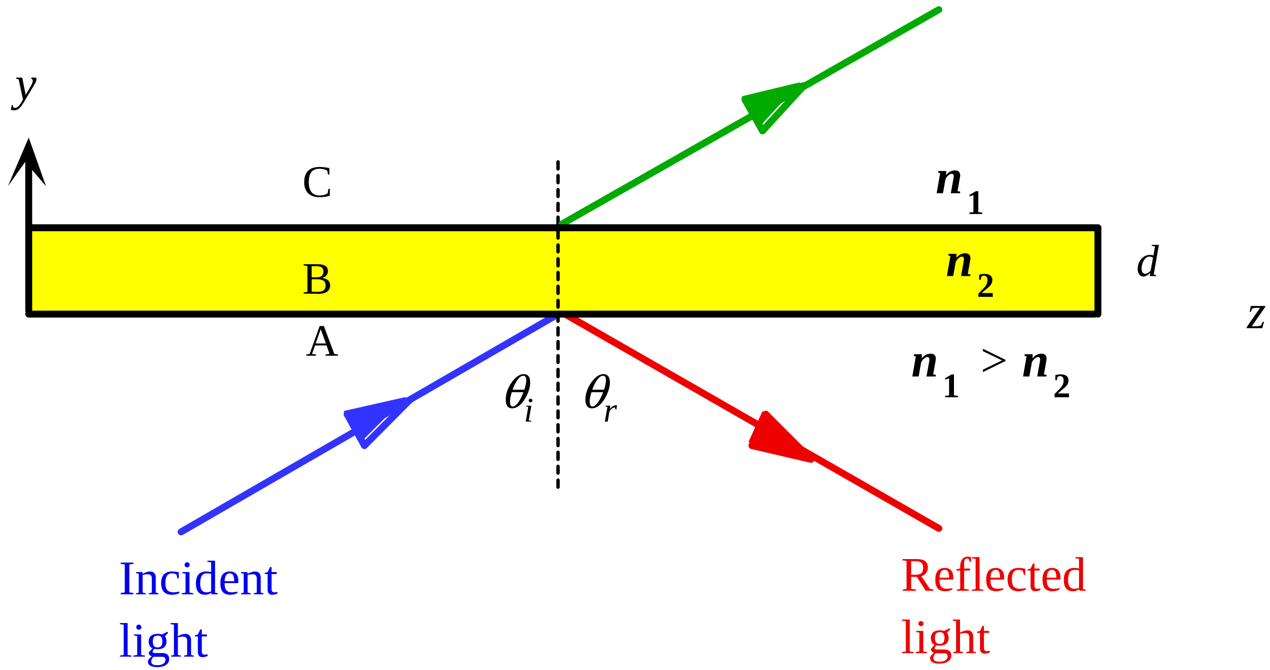

When medium B is thin (thickness d is small), the field penetrates to the BC interface and gives rise to an attenuated wave in medium C. The effect is the tunnelling of the incident beam in A through B to C.

Reflexão interna total frustrada

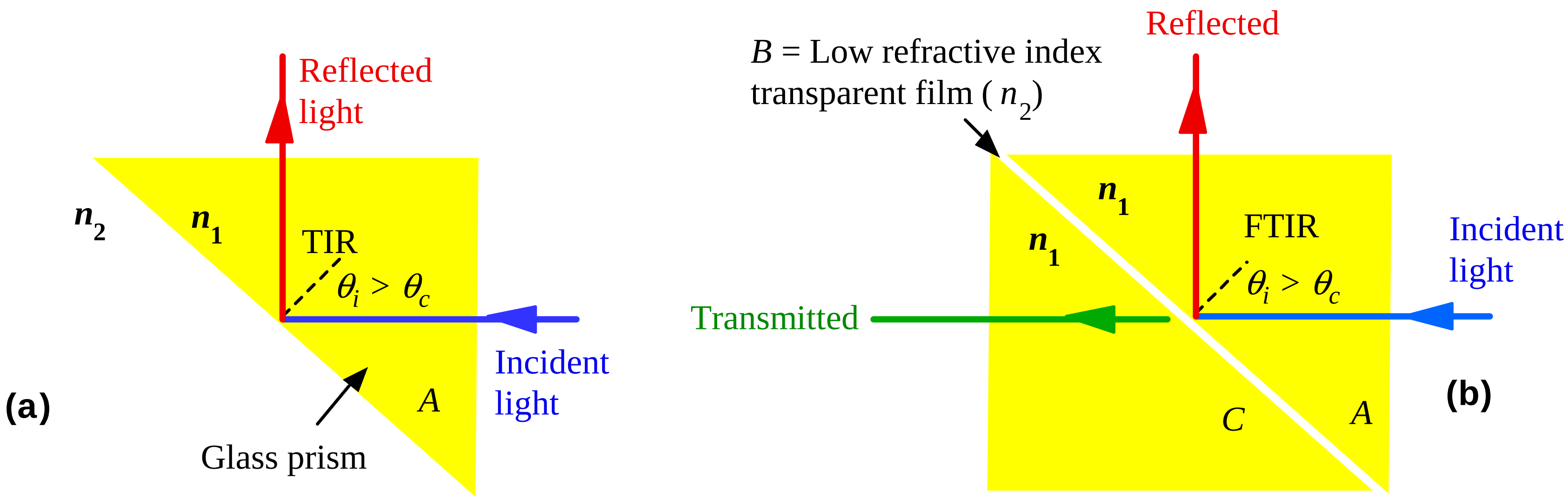

(a) A light incident at the long face of a glass prism suffers TIR; the prism deflects the light.
(b) Two prisms separated by a thin low refractive index film forming a beam-splitter cube. The incident beam is split into two beams by FTIR.

Filme fino – camada anti-reflectora

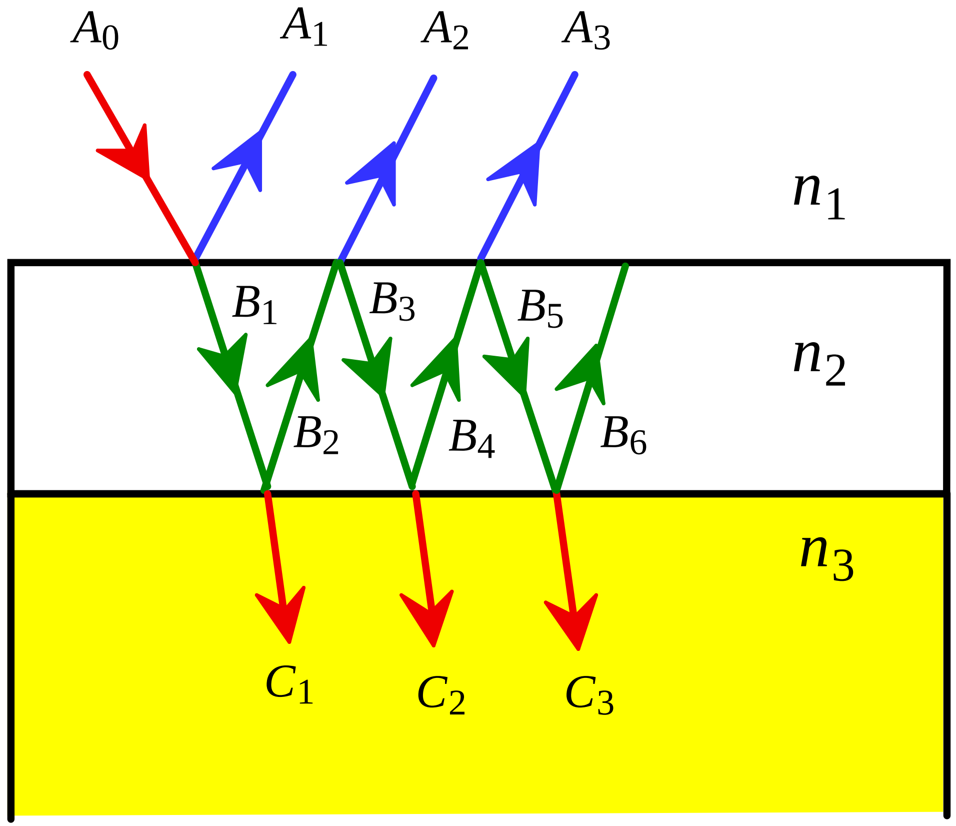

Thin film coating of refractive index n_2 on a semiconductor device

Princípio de funcionamento de uma camada anti-reflectora

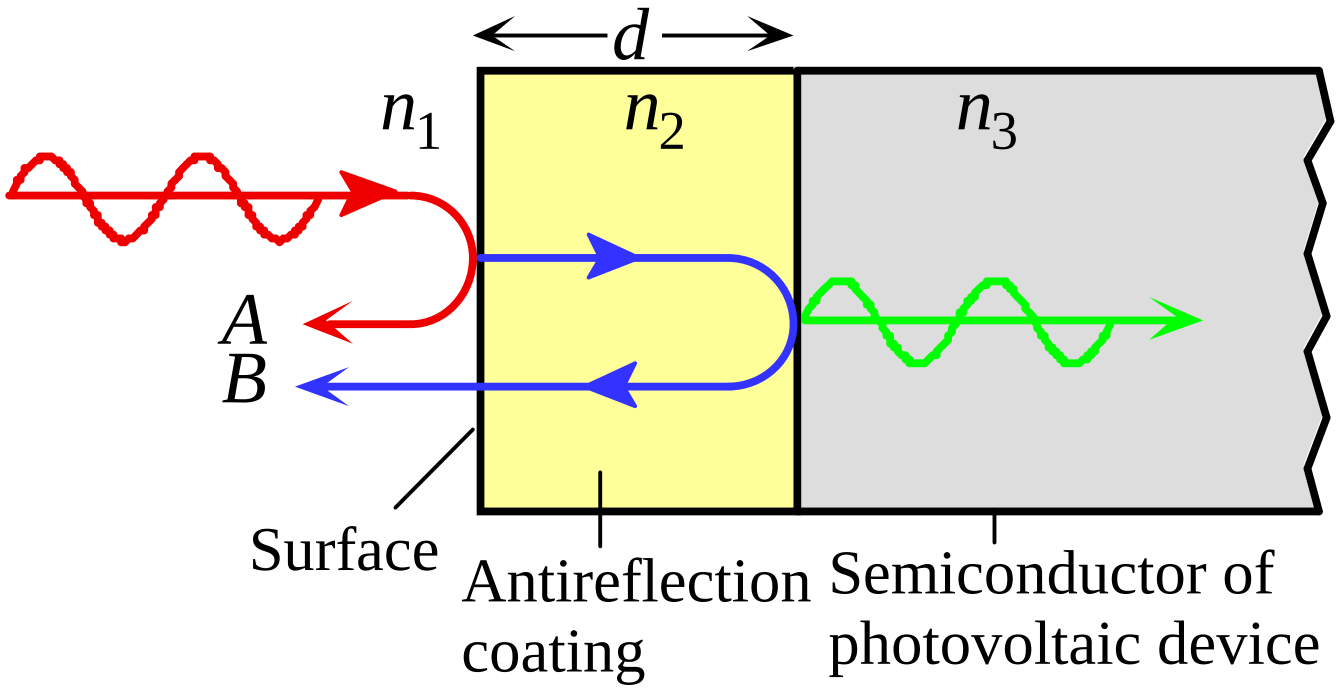

Illustration of how an antireflection coating reduces the reflected light intensity

Espelho dieléctrico

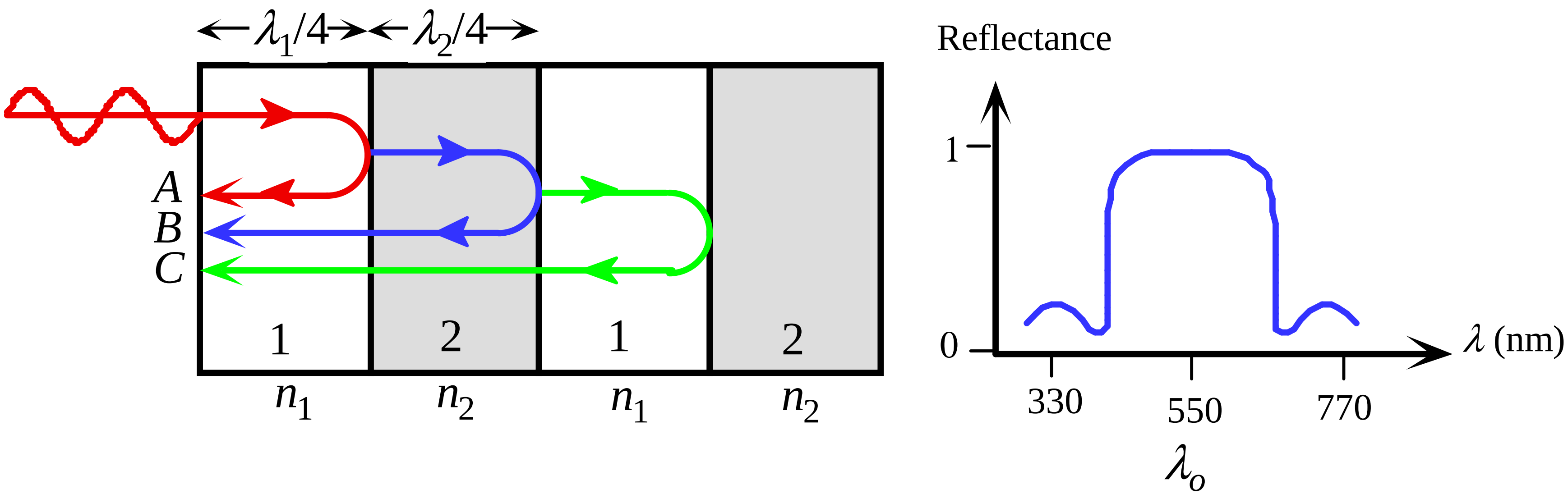

Schematic illustration of the principle of the dielectric mirror with many low and high refractive index layers and its reflectance.

Cavidade Fabry-Perot

Cavidade óptica Fabry-Perot

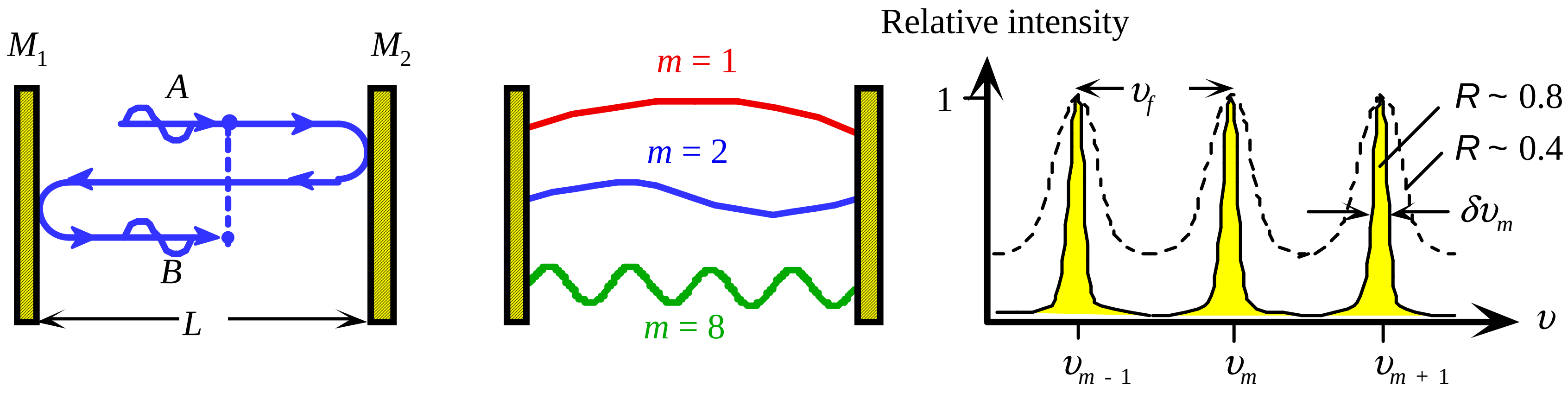

(a) (b) (c)

Schematic illustration of the Fabry-Perot optical cavity and its properties. (a) Reflected waves interfere. (b) Only standing EM waves, *modes*, of certain wavelengths are allowed in the cavity. (c) Intensity vs. frequency for various modes. R is mirror reflectance and lower R means higher loss from the cavity.

Filtro Fabry-Perot

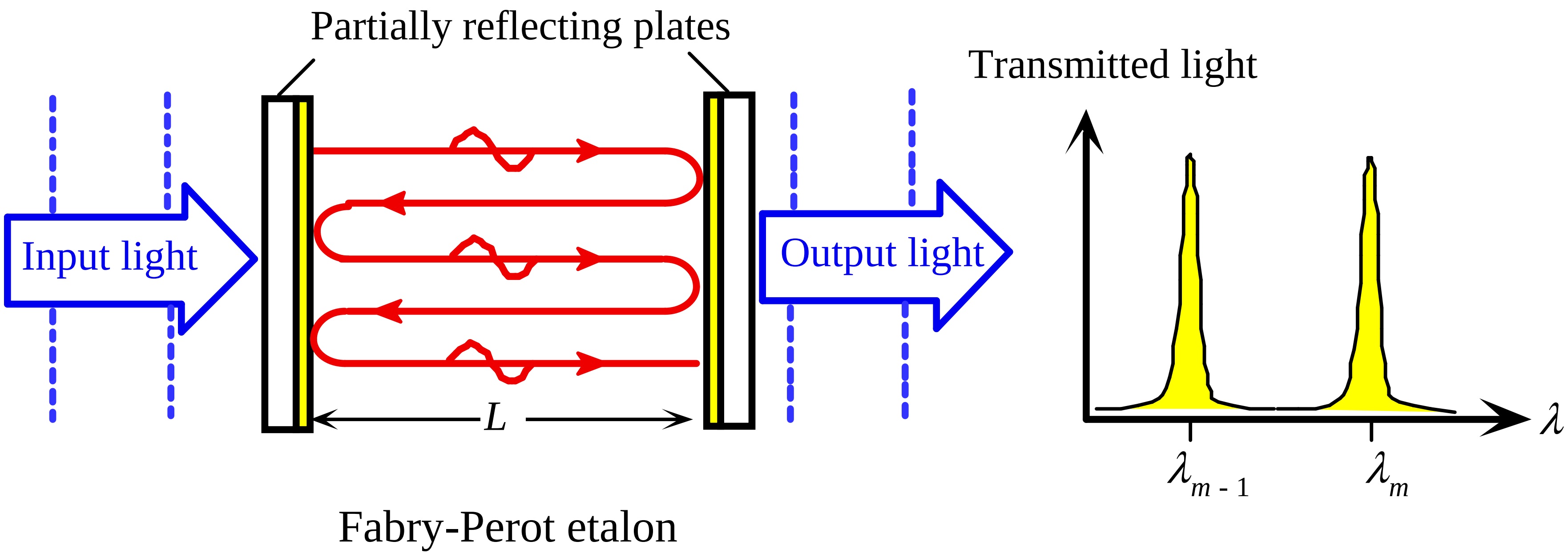

Transmitted light through a Fabry-Perot optical cavity.

Interferómetro Fabry-Perot

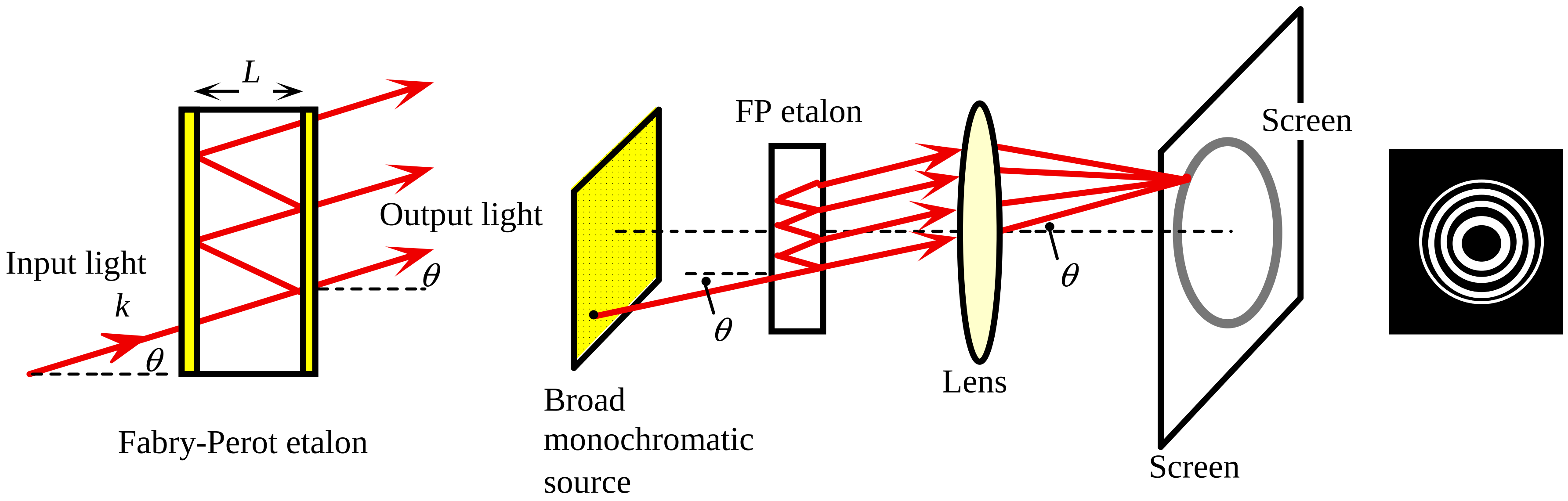

Fabry-Perot optical resonator and the Fabry-Perot interferometer (schematic)

Polarização e birrefringência

Grelha polarizadora

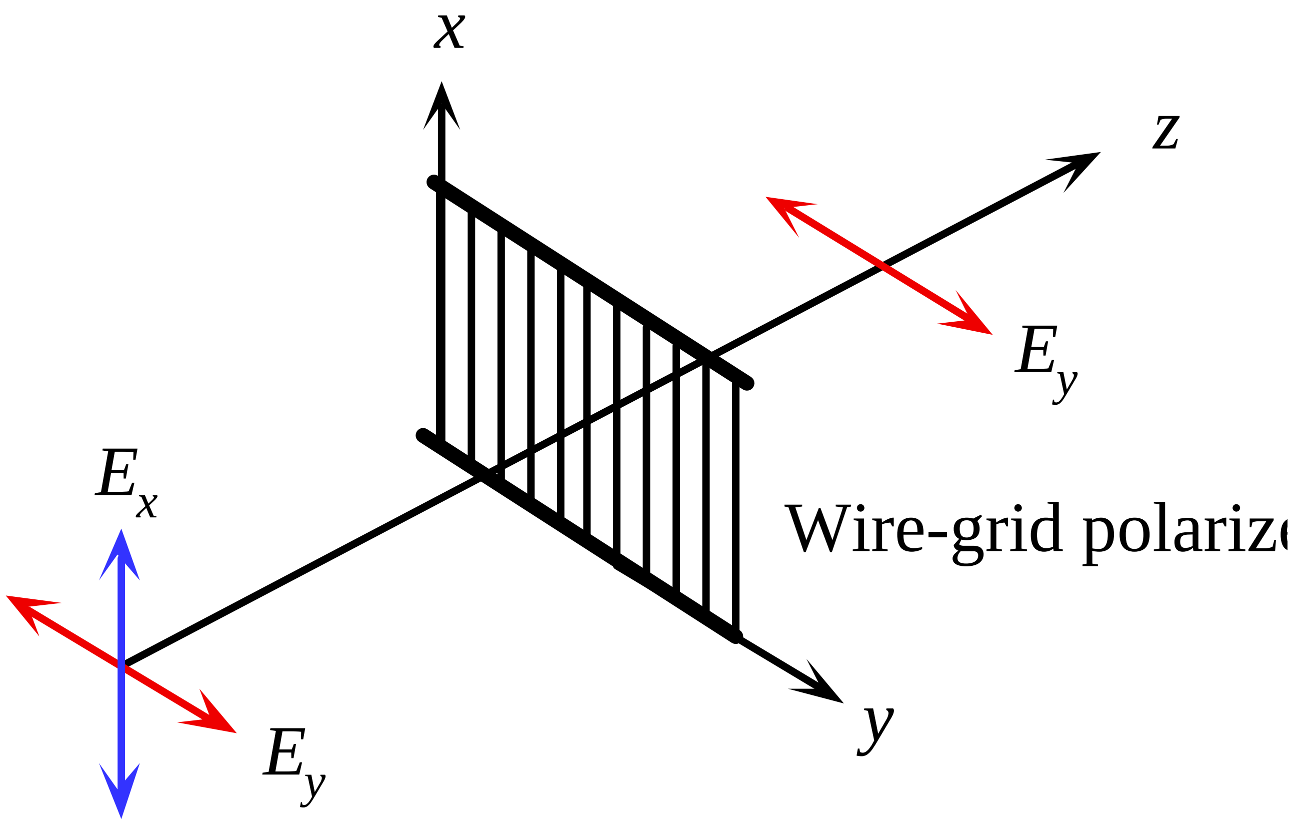

The wire grid-acts as a polarizer

Luz linearmente polarizada

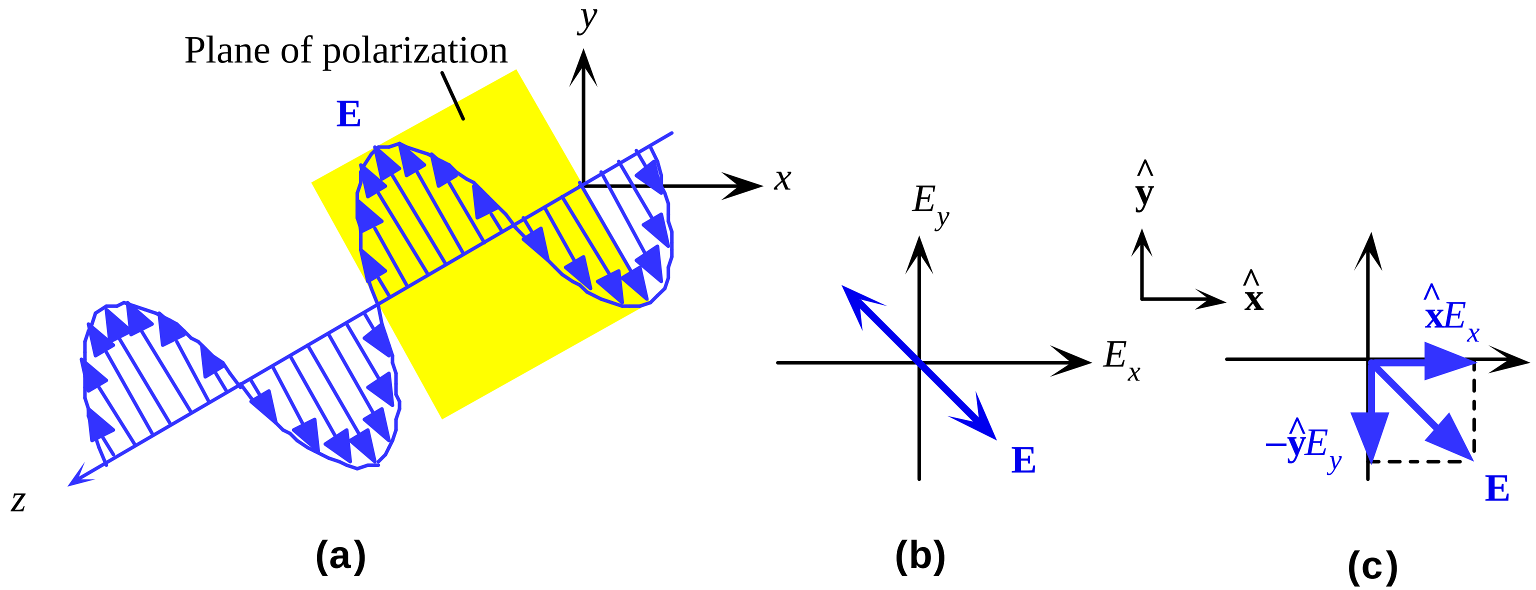

(a) A linearly polarized wave has its electric field oscillations defined along a line perpendicular to the direction of propagation, z. The field vector **E** and z define a *plane of polarization*. (b) The E-field oscillations are contained in the plane of polarization. (c) A linearly polarized light at any instant can be represented by the superposition of two fields E_x and E_y with the right magnitude and phase.

Polarização circular direita

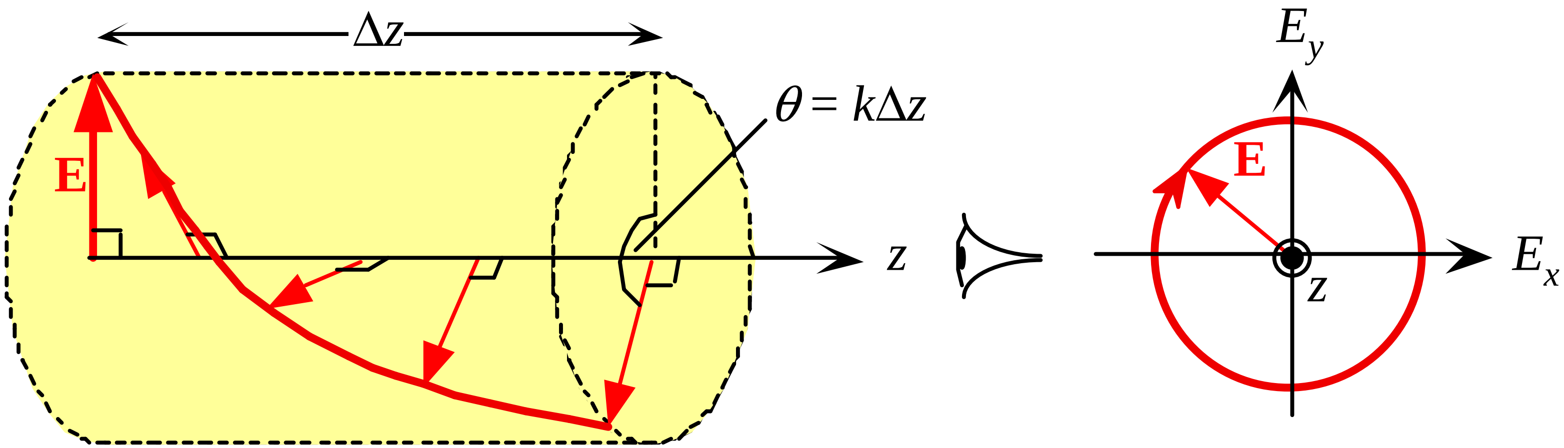

A *right circularly polarized light*. The field vector **E** is always at right angles to *z* , rotates clockwise around *z* with time, and traces out a full circle over one wavelength of distance propagated.

Estados de polarização

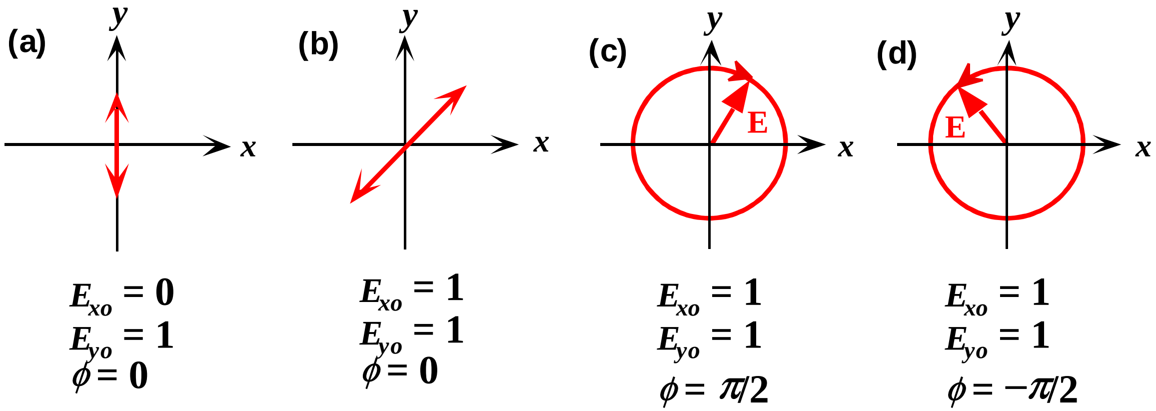

Examples of linearly, (a) and (b), and circularly polarized light (c) and (d); (c) is right circularly and (d) is left circularly polarized light (as seen when the wave directly approaches a viewer)

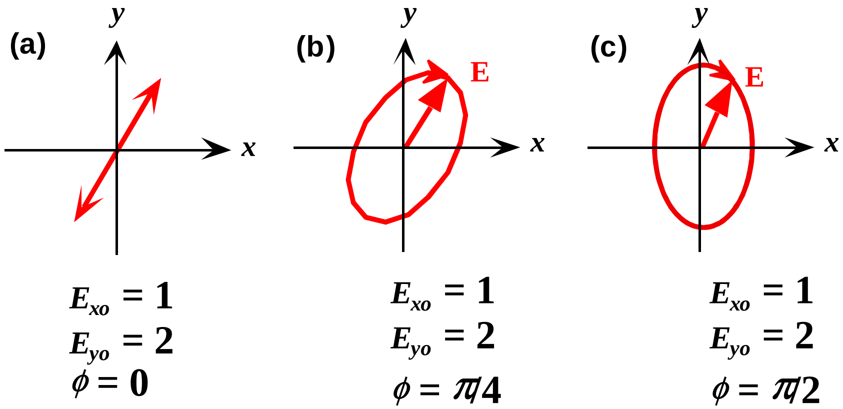

(a) Linearly polarized light with $E_{yo} = 2E_{xo}$ and $\phi = 0$. (b) When $\phi = \pi/4$ (45°), the light is right elliptically polarized with a tilted major axis. (c) When $\phi = \pi/2$ (90°), the light is right elliptically polarized. If E_{xo} and E_{yo} were equal, this would be right circularly polarized light.

Lei de Malus

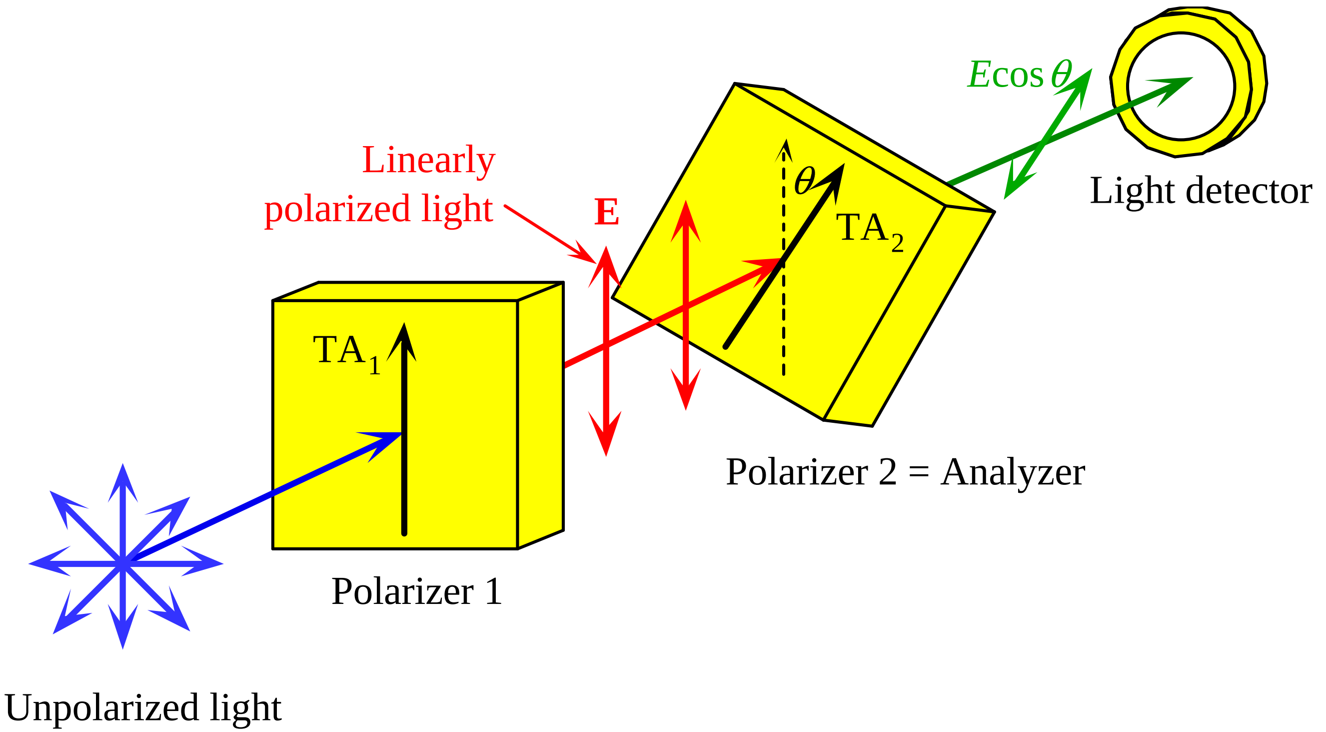

Randomly polarized light is incident on a Polarizer 1 with a transmission axis TA_1. Ligh emerging from Polarizer 1 is linearly polarized with **E** along TA_1, and becomes incident on Polarizer 2 (called "analyzer") with a transmission axis TA_2 at an angle θ to TA_1. A detector measures the intensity of the incident light. TA_1 and TA_2 are normal to the light direction.

Anisotropia óptica – birrefringência

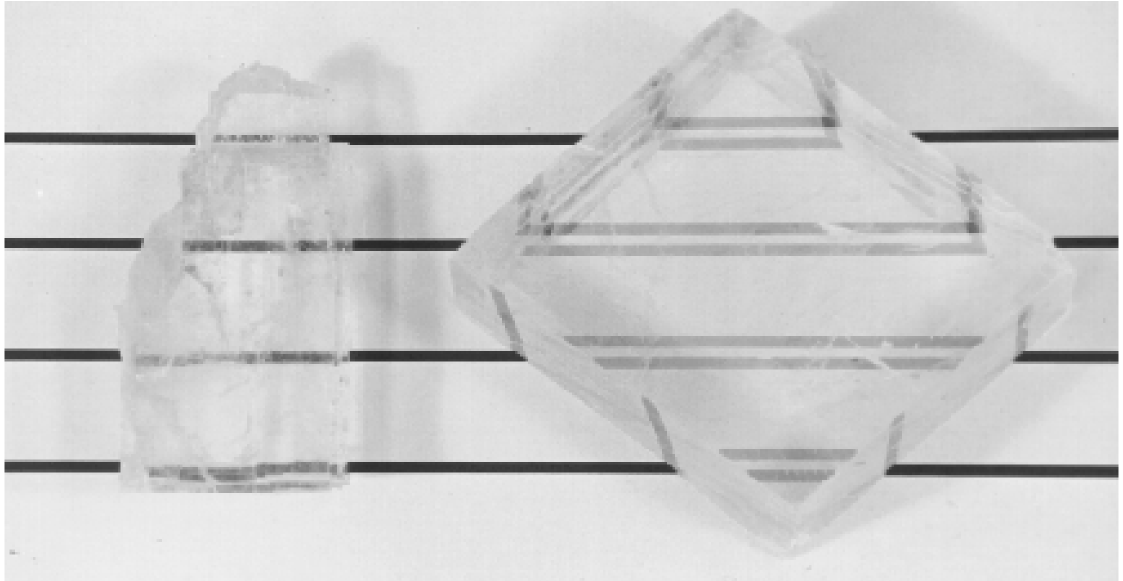

A line viewed through a cubic sodium chloride (halite) crystal (optically isotropic) and a calcite crystal (optically anisotropic).

Birrefringência e polarização

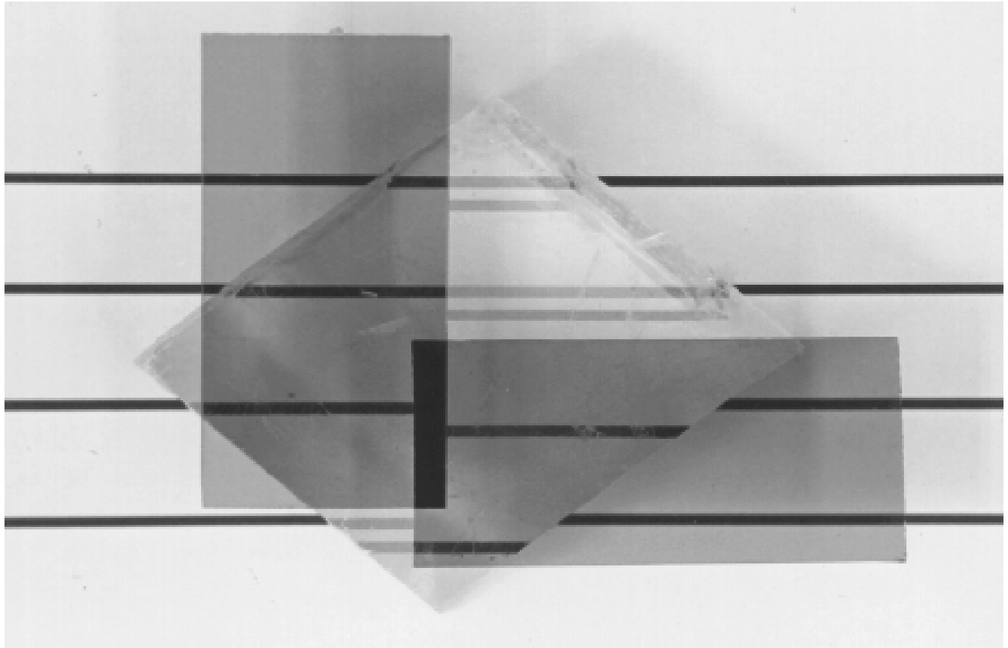

Two polaroid analyzers are placed with their transmission axes, along the long edges, at right angles to each other. The ordinary ray, undeflected, goes through the left polarizer whereas the extraordinary wave, deflected, goes through the right polarizer. The two waves therefore have orthogonal polarizations.

Birrefringência e polarização

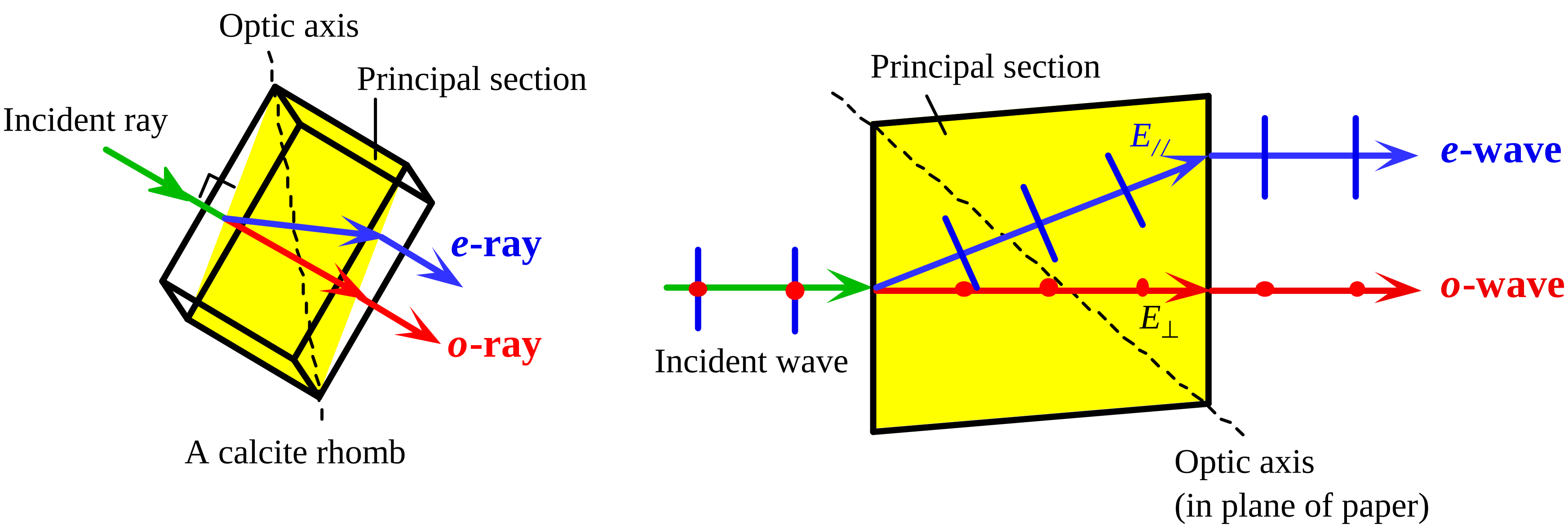

An EM wave that is off the optic axis of a calcite crystal splits into two waves called ordinary and extraordinary waves. These waves have orthogonal polarizations and travel with different velocities. The *o*-wave has a polarization that is always perpendicular to the optical axis.

Birrefringência e polarização

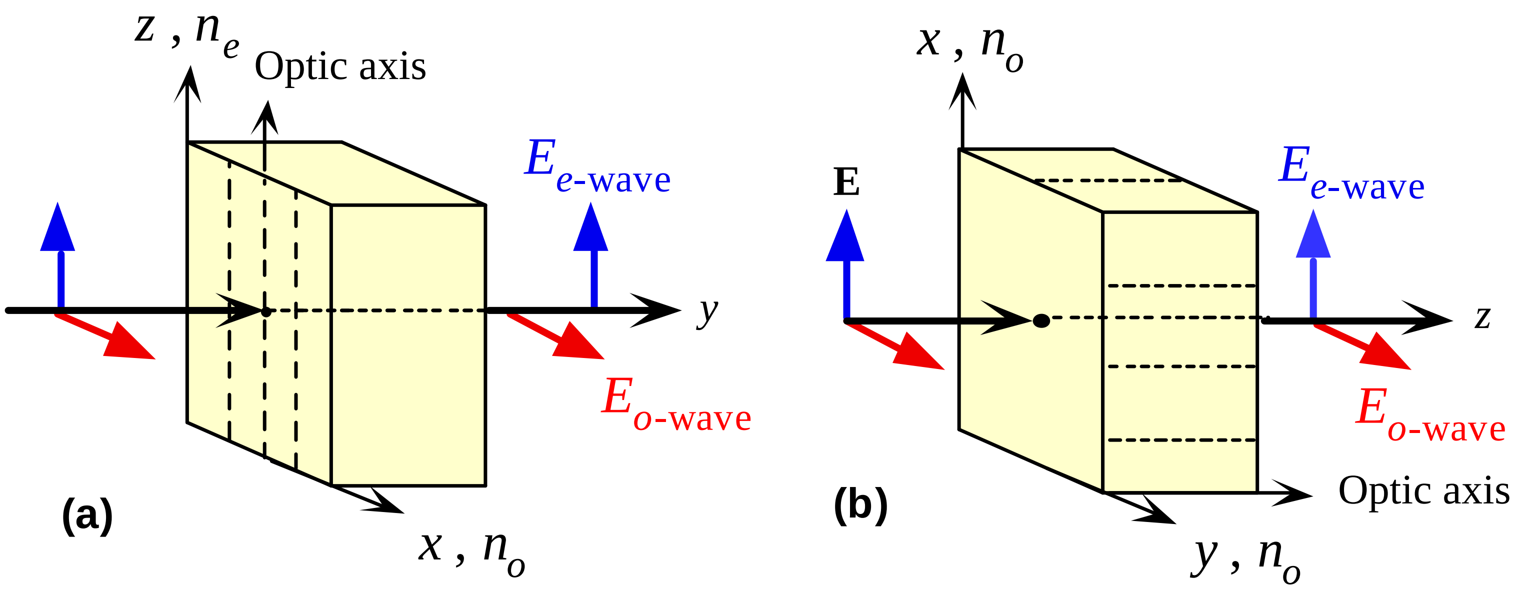

(a) A birefringent crystal plate with the optic axis parallel to the plate surfaces. (b) A birefringent crystal plate with the optic axis perpendicular to the plate surfaces.

Dispositivos baseados na birrefringência – lâminas de atraso

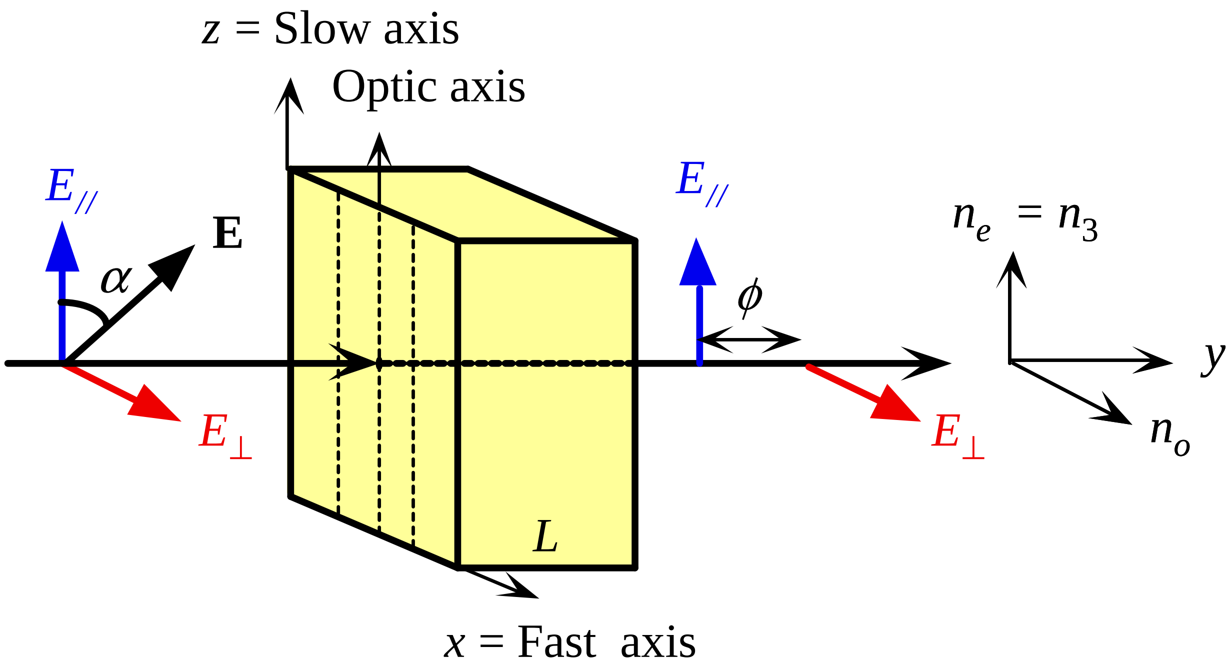

A retarder plate. The optic axis is parallel to the plate face. The *o*- and *e*-waves travel in the same direction but at different speeds.

Lâminas de atraso

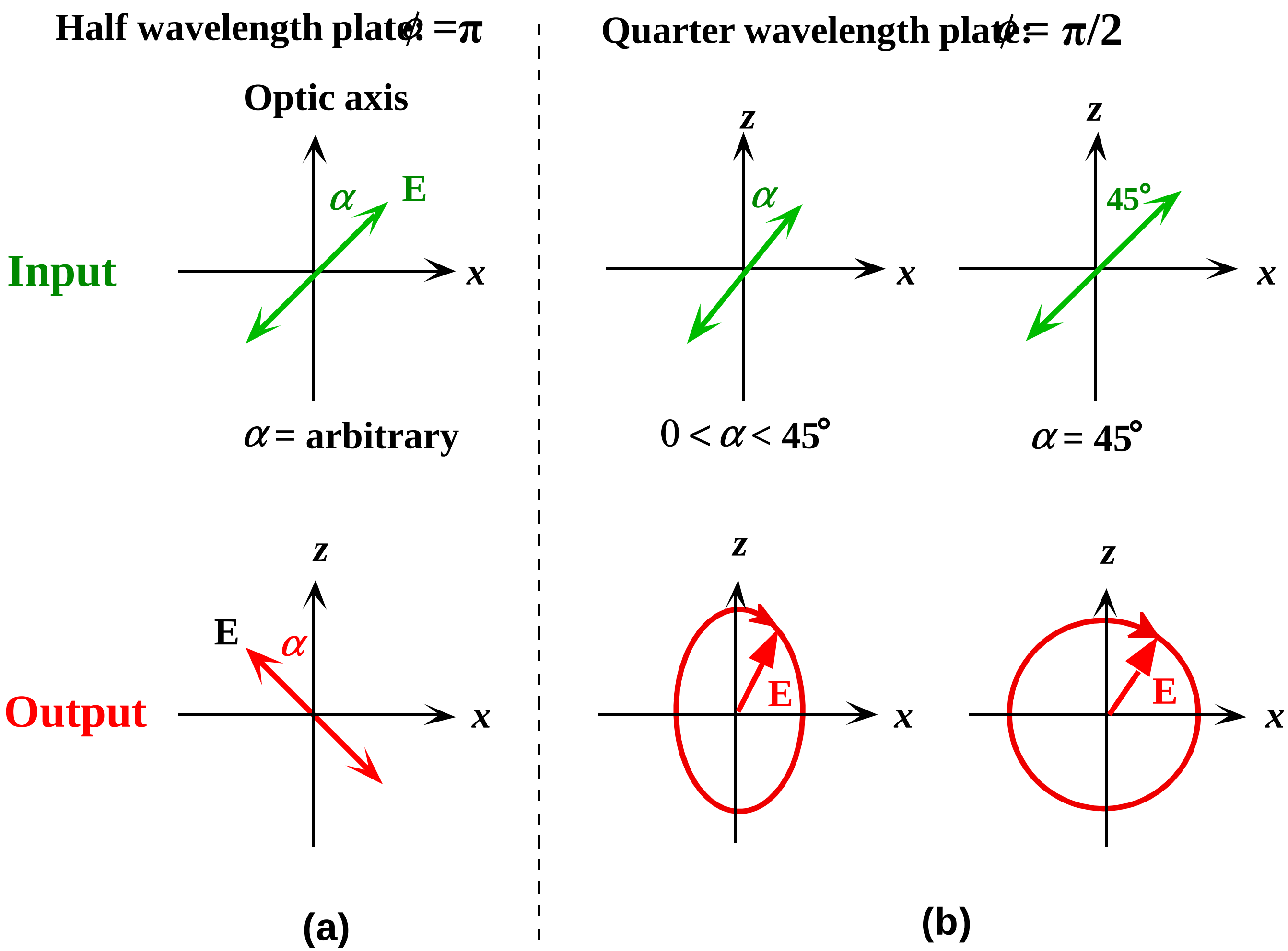

Input and output polarizations of light through (a) a half-wavelength plate and (b) through a quarter-wavelength plate.

Dispositivos de atraso variável

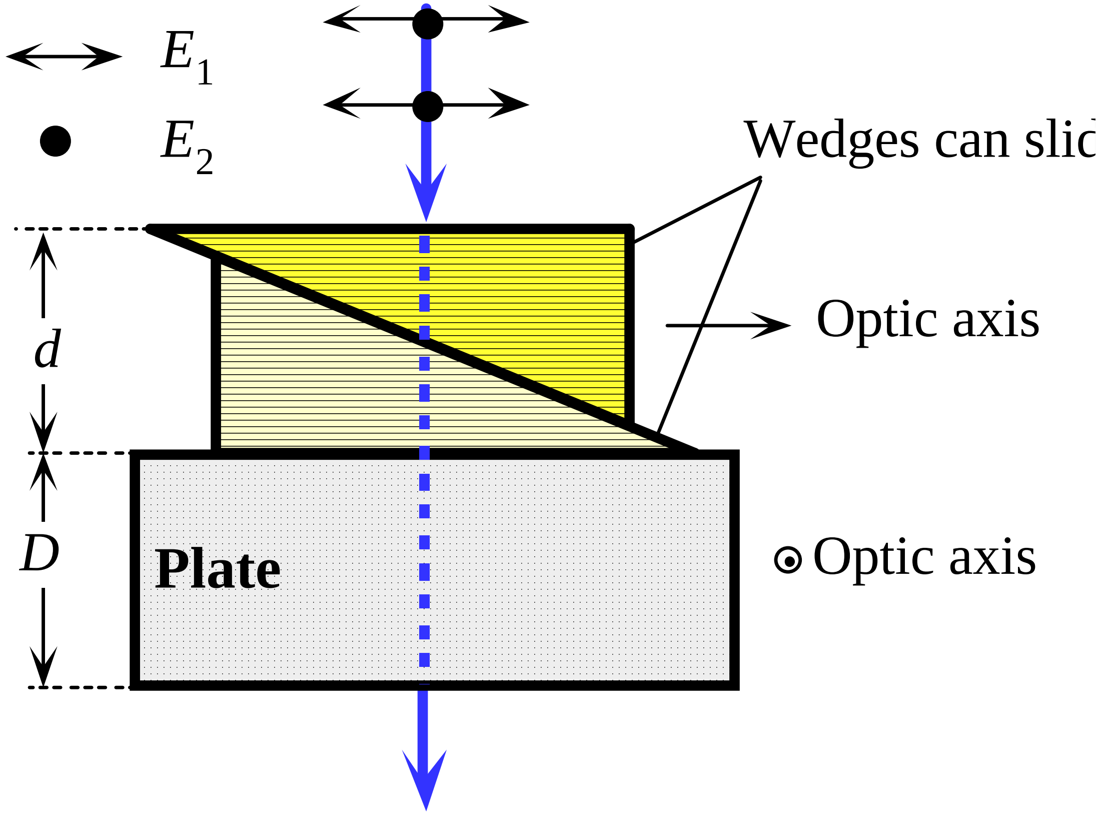

Soleil-Babinet Compensator

Prismas birrefringentes

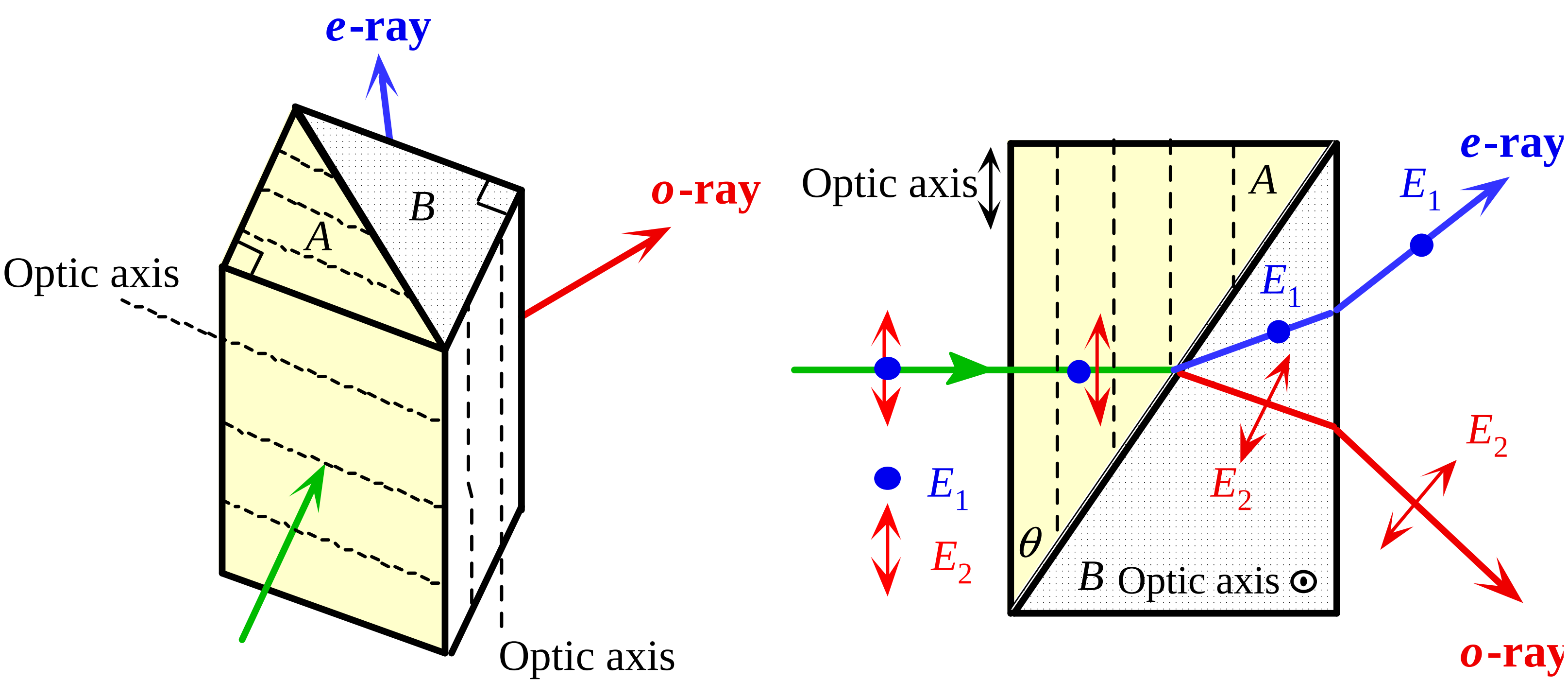

The Wollaston prism is a beam polarization splitter. E_1 is orthogonal to the plane of the paper and also to the optic axis of the first prism. E_2 is in the plane of the paper and orthogonal to E_1.

Guias de Onda Dielétricos

Princípio do guia de onda e acoplamento de luz

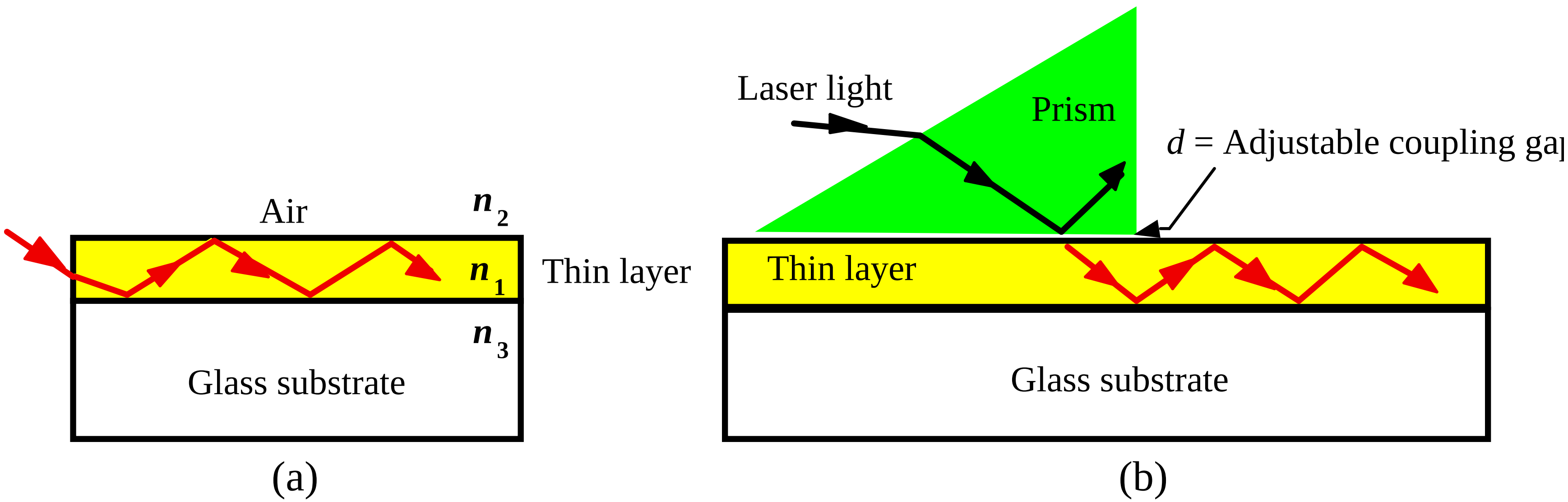

(a) Light propagation along an optical guide. (b) Coupling of laser light into a thin layer - optical guide - using a prism. The light propagates along the thin layer.

Guia de onda planar

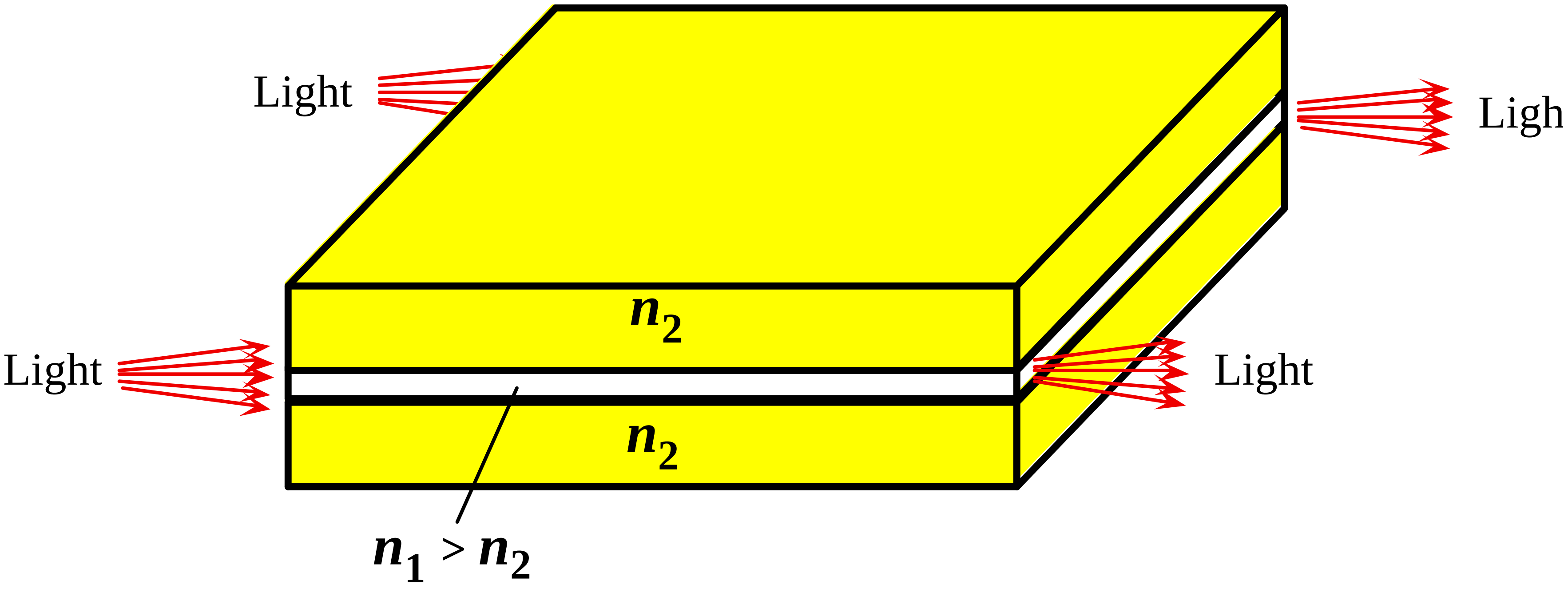

A planar dielectric waveguide has a central rectangular region of higher refractive index n_1 than the surrounding region which has a refractive index n_2. It is assumed that the waveguide is infinitely wide and the central region is of thickness $2a$. It is illuminated at one end by a monochromatic light source.

Ângulo de aceitação máxima

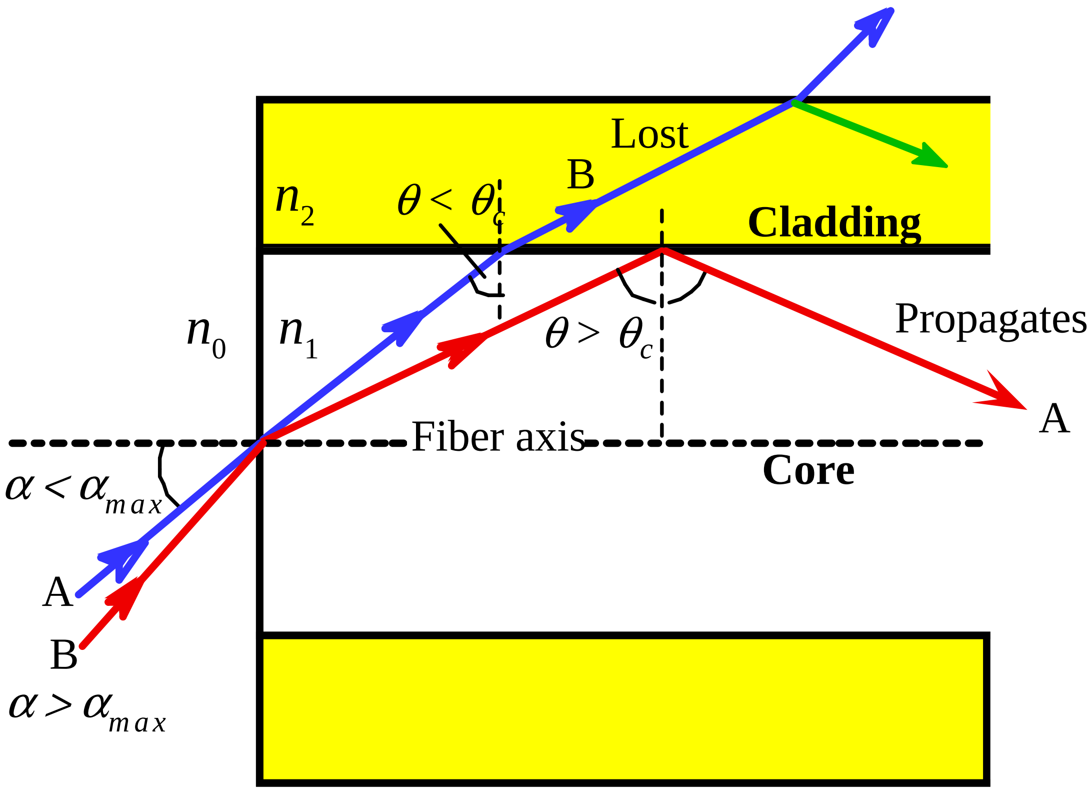

Maximum acceptance angle α_{max} is that which just gives total internal reflection at the core-cladding interface, i.e. when $\alpha = \alpha_{max}$ then $\theta = \theta_c$. Rays with $\alpha > \alpha_{max}$ (e.g. ray B) become refracted and penetrate the cladding and ar eventually lost.

Propagação da luz num guias de onda planar

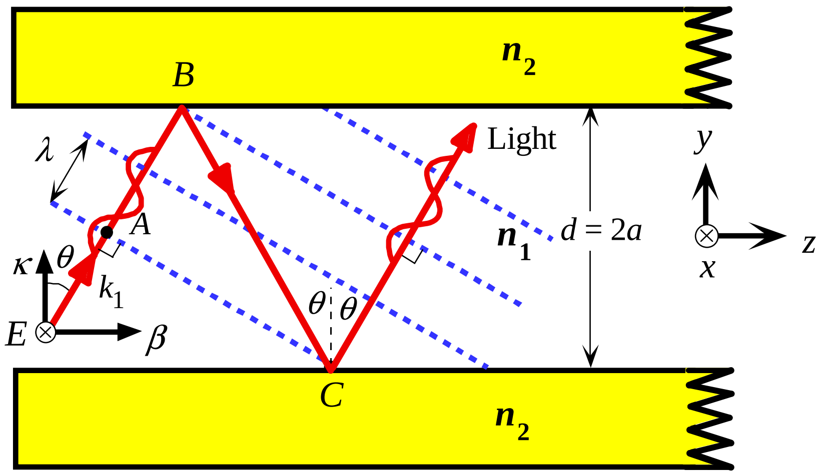

A light ray travelling in the guide must interfere constructively with itself to propagate successfully. Otherwise destructive interference will destroy the wave.

Propagação da luz num guias de onda planar

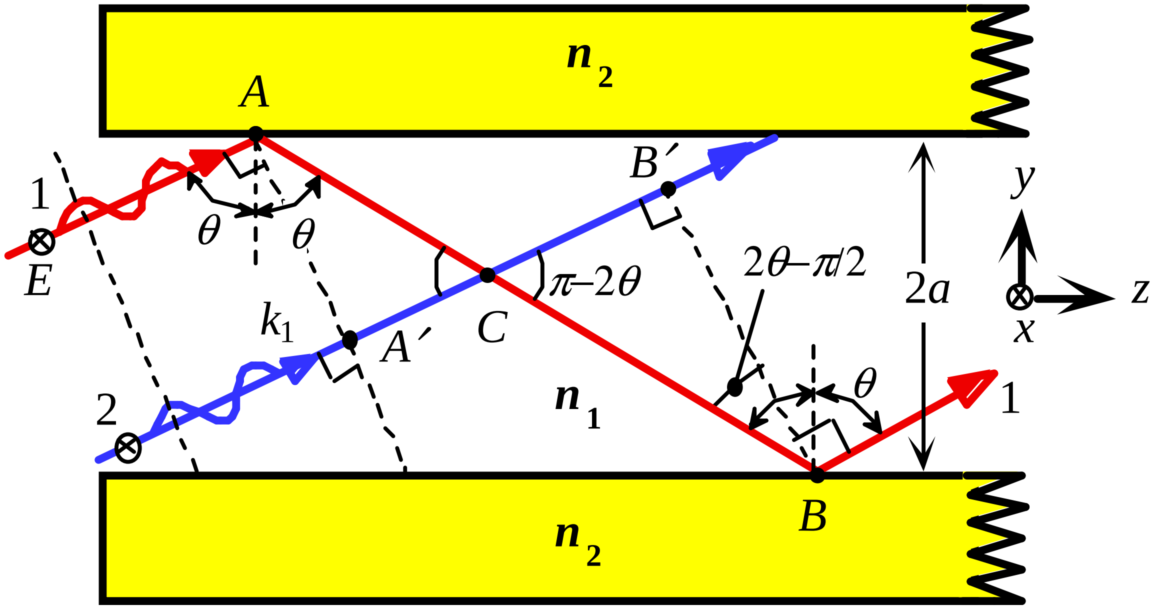

Two arbitrary waves 1 and 2 that are initially in phase must remain in phase after reflections. Otherwise the two will interfere destructively and cancel each other.

Propagação da luz num guias de onda planar

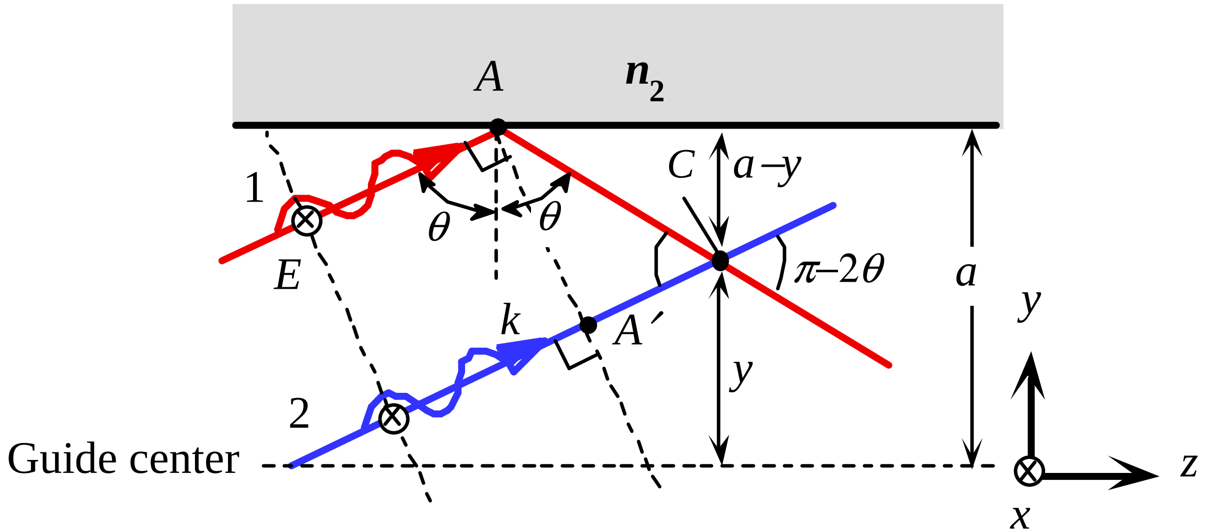

Interference of waves such as 1 and 2 leads to a standing wave pattern along the *y*-direction which propagates along *z*.

Ilustração da propagação da luz num guia de onda

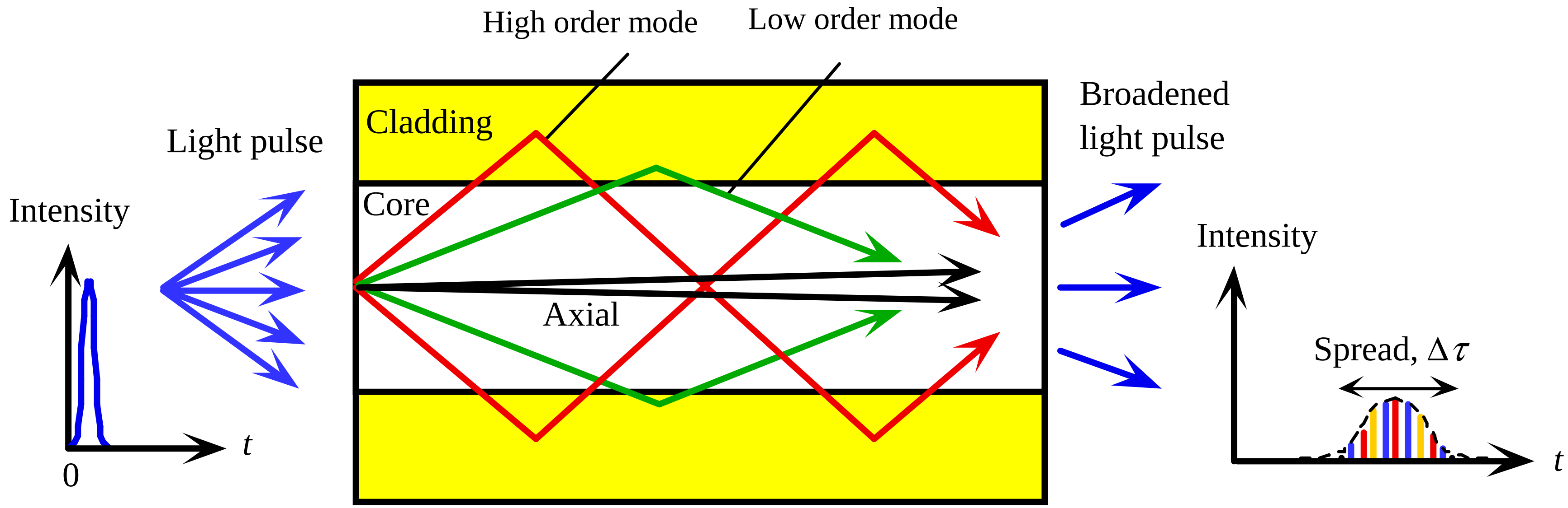

Schematic illustration of light propagation in a slab dielectric waveguide. Light pulse entering the waveguide breaks up into various modes which then propagate at different group velocities down the guide. At the end of the guide, the modes combine to constitute the output light pulse which is broader than the input light pulse.

Distribuição do campo eléctrico do primeiro modo

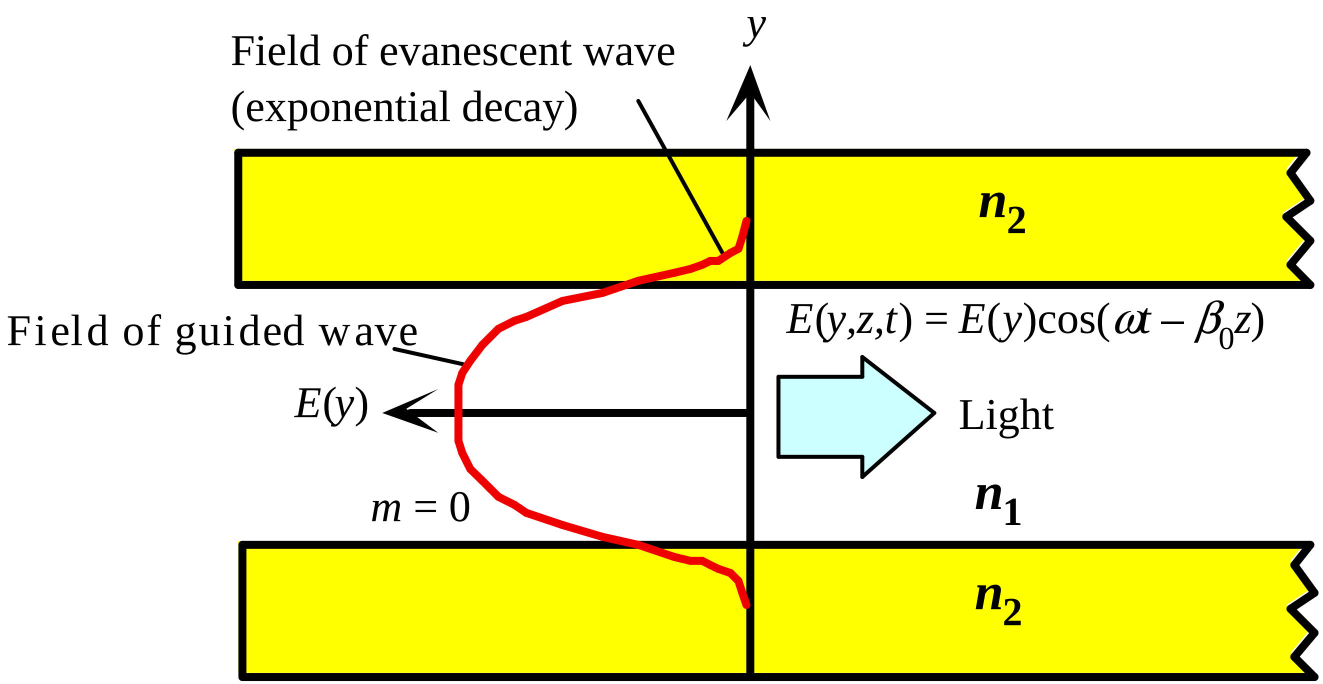

The electric field pattern of the lowest mode traveling wave along the guide. This mode has $m = 0$ and the lowest θ. It is often referred to as the glazing incidence ray. It has the highest phase velocity along the guide.

© 1999 S.O. Kasap, *Optoelectronics* (Prentice Hall)

Distribuição do campo eléctrico dos 3 1ºs modos

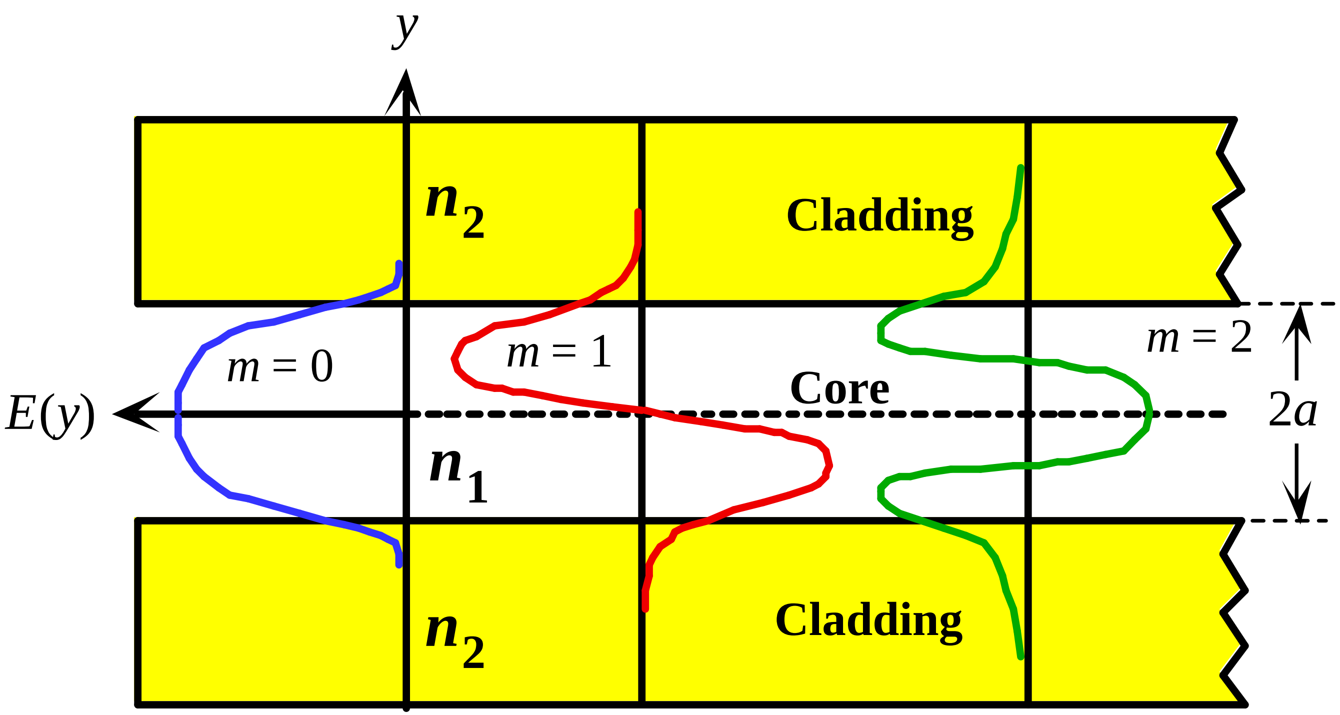

The electric field patterns of the first three modes (m = 0, 1, 2) traveling wave along the guide. Notice different extents of field penetration into the cladding.

Dispersão intramodal

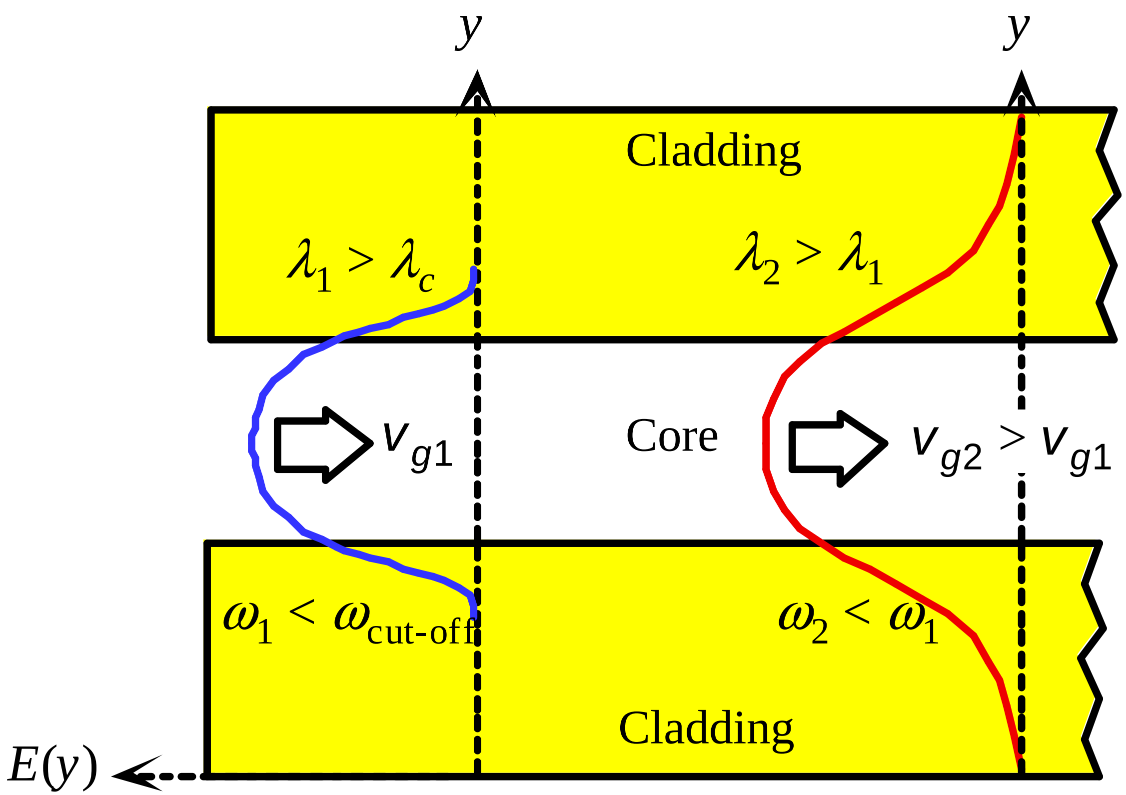

The electric field of TE_0 mode extends more into the cladding as the wavelength increases. As more of the field is carried by the cladding, the group velocity increases.

Determinação do numero de modos num guia de onda

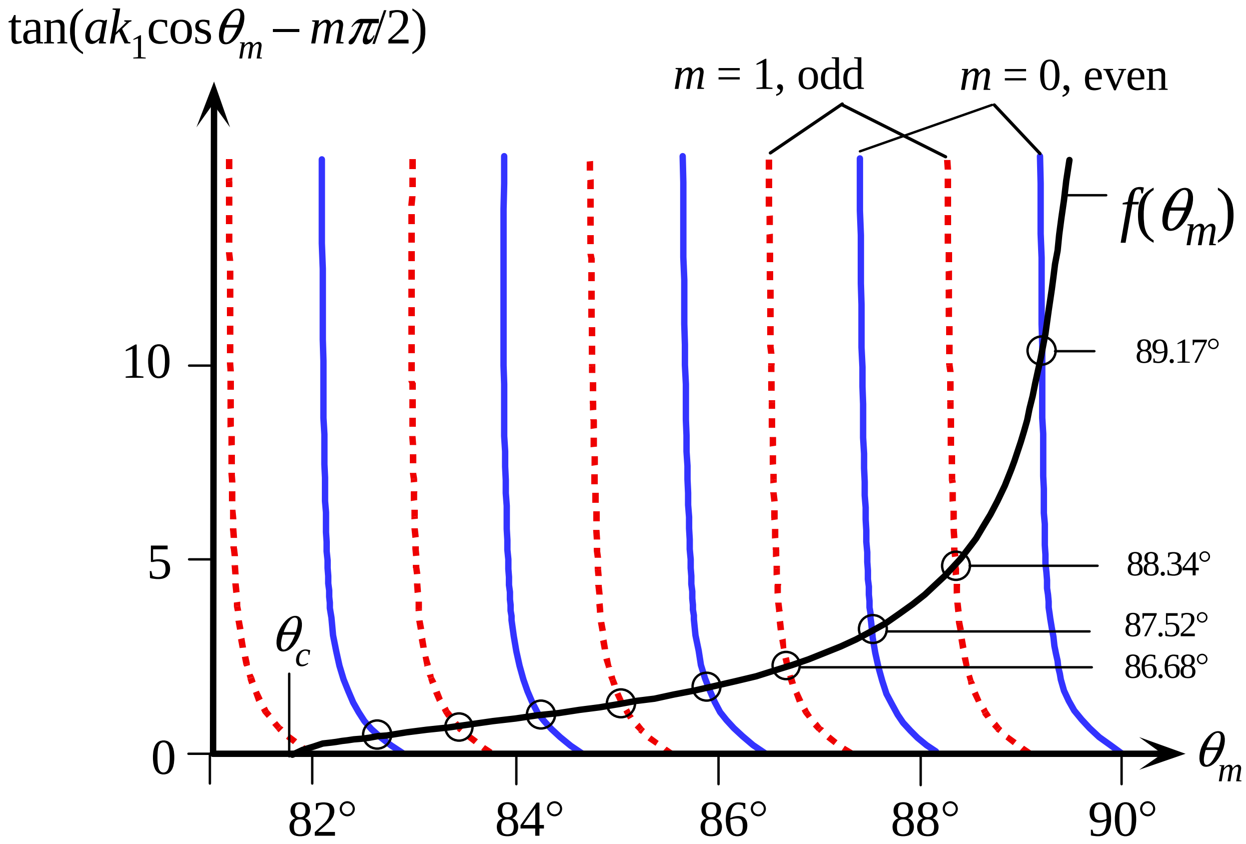

Modes in a planar dielectric waveguide can be determined by plotting the LHS and the RHS of eq. (11).

Dispersão modal

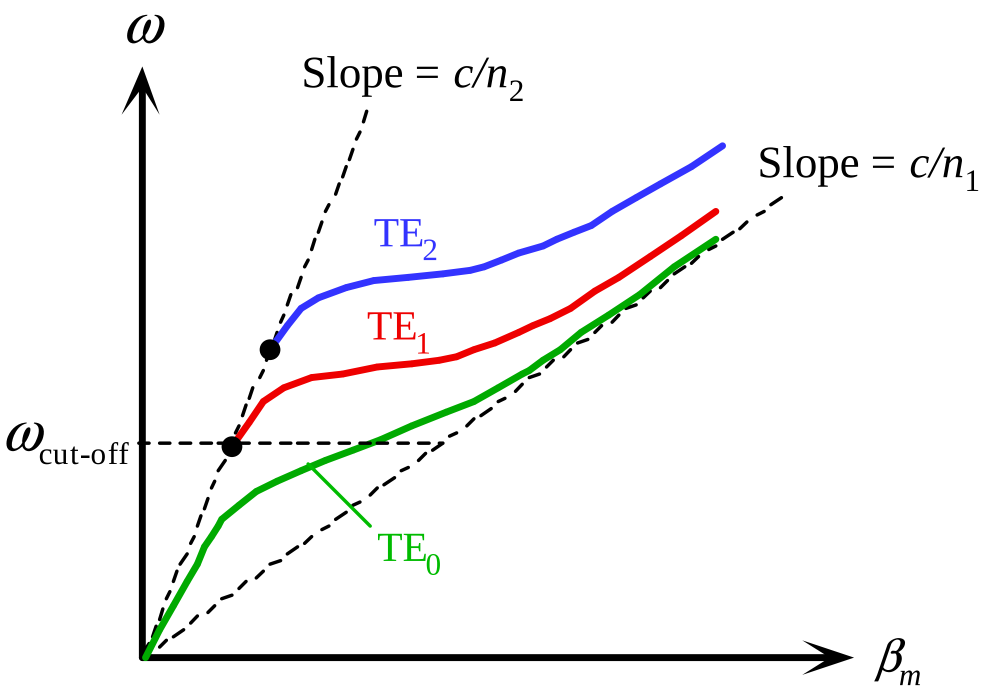

Schematic dispersion diagram, ω vs. β for the slab waveguide for various TE_m. modes. $\omega_{cut-off}$ corresponds to $V = \pi/2$. The group velocity v_g at any ω is the slope of the ω vs. β curve at that frequency.

Velocidade de grupo em função da frequência

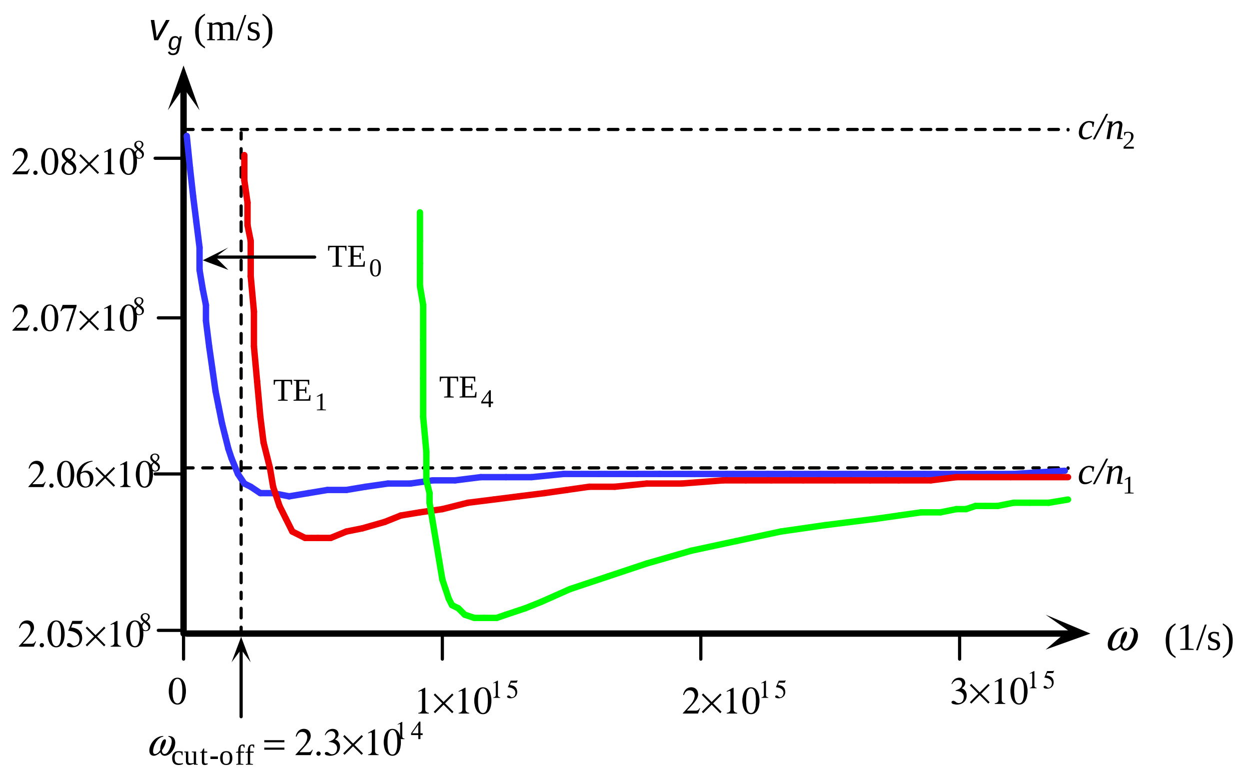

Group velocity vs. angular frequency for three modes for a planar dielectric waveguide which has $n_1 = 1.455$, $n_2 = 1.44$, $a = 10$ μm (Results from Mathview, Waterloo Maple math-software application). TE$_0$ is for $m = 0$ *etc.*

Fibras Óticas

Fibra óptica com perfil de índice em degrau

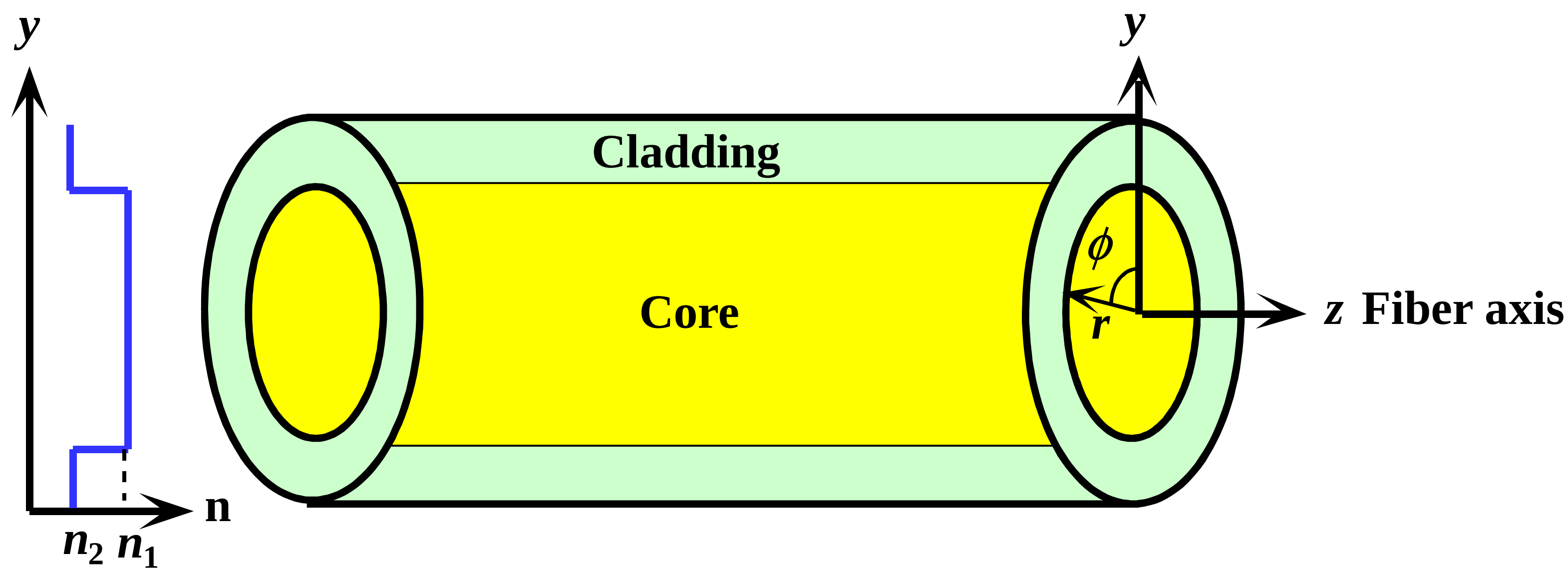

The step index optical fiber. The central region, the core, has greater refractive index than the outer region, the cladding. The fiber has cylindrical symmetry. We use the coordinates r, ϕ, z to represent any point in the fiber. Cladding is normally much thicker than shown.

Secção transversal de uma fibra óptica mono-modo

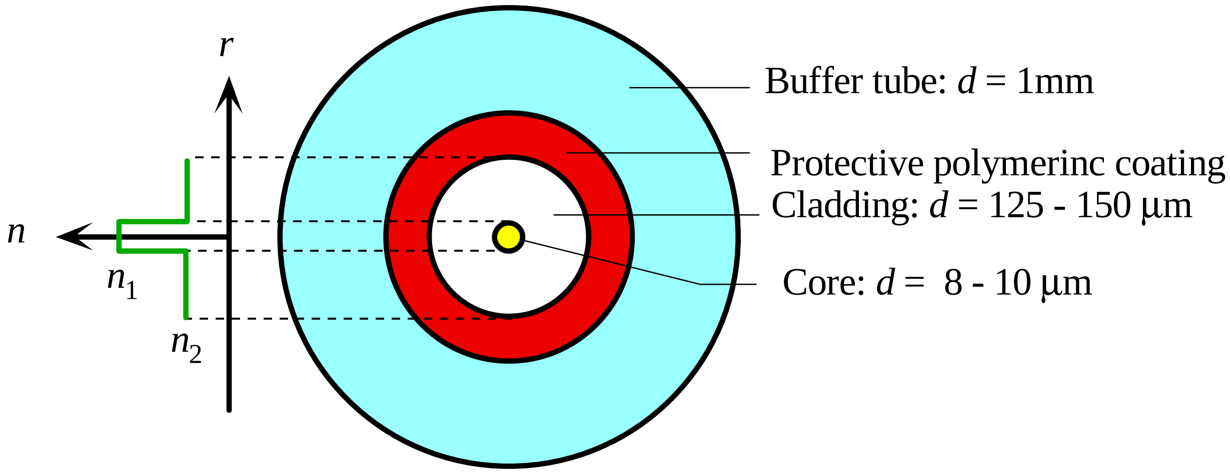

The cross section of a typical single-mode fiber with a tight buffer tube. (d = diameter)

Raios meridionais e raios “skew”

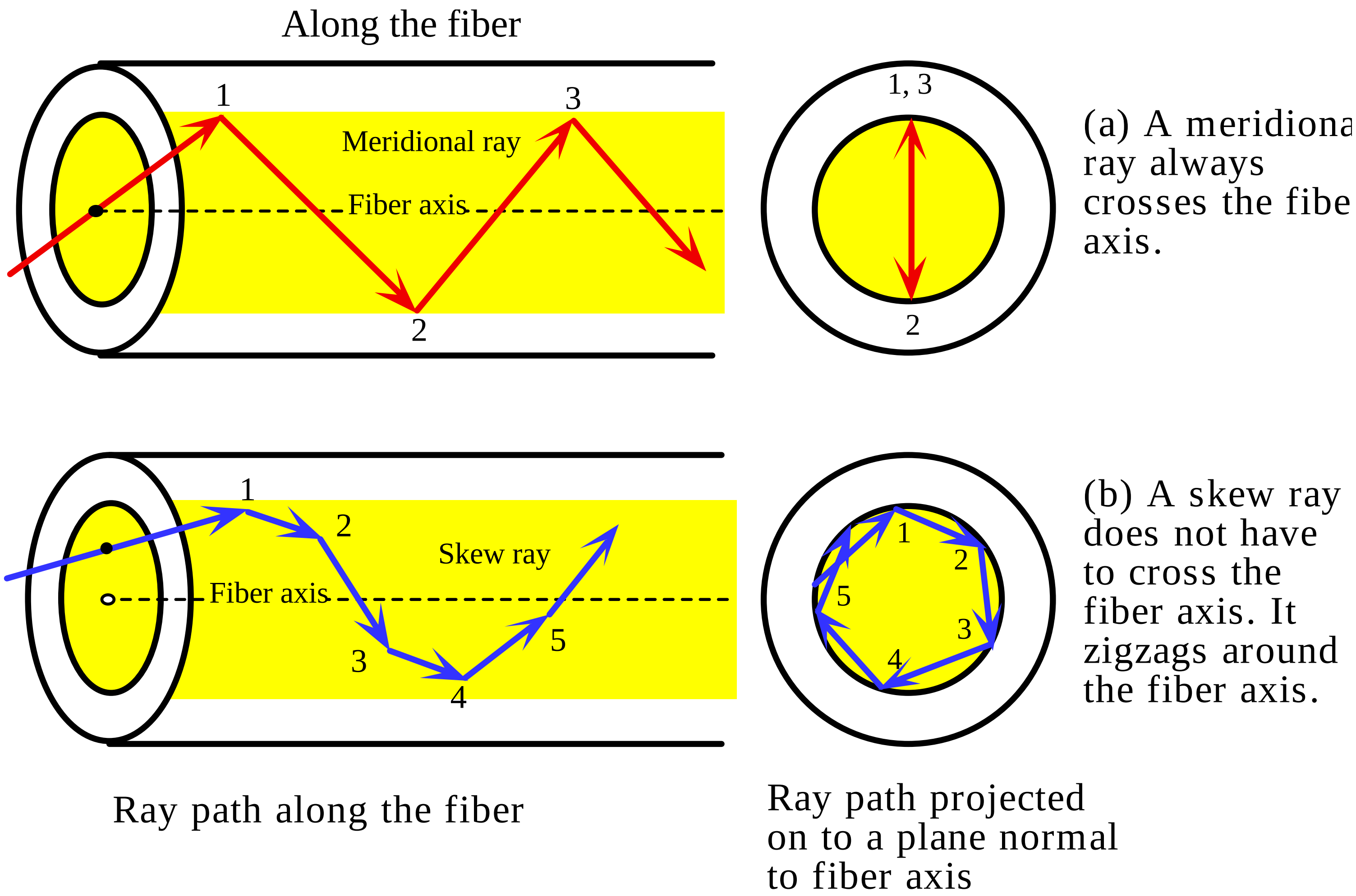

Illustration of the difference between a meridional ray and a skew ray.
Numbers represent reflections of the ray.

Distribuição do campo eléctrico e intensidade luminosa

(a) The electric field of the fundamental mode

(b) The intensity in the fundamental mode LP_{01}

(c) The intensity in LP_{11}

(d) The intensity in LP_{21}

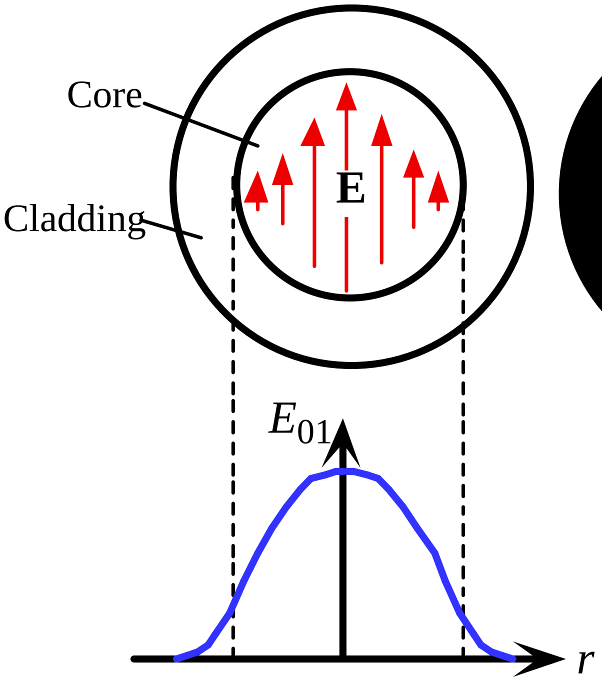

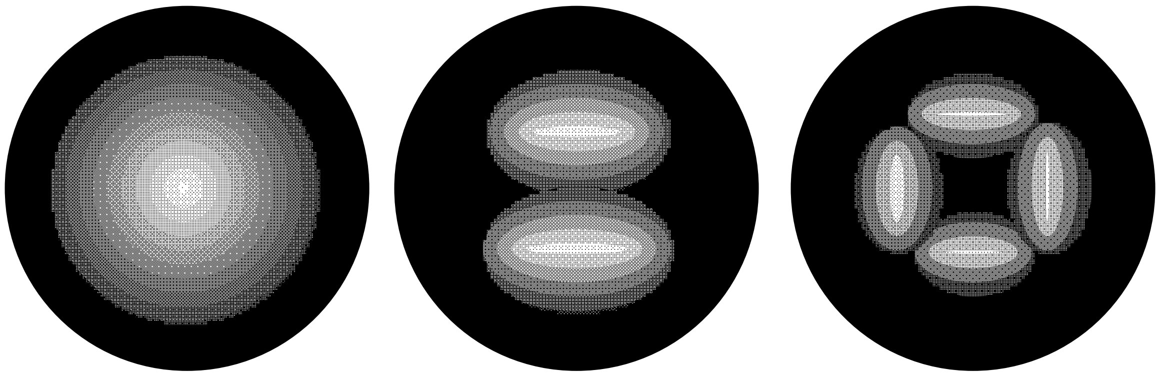

The electric field distribution of the fundamental mod in the transverse plane to the fiber axis z. The light intensity is greatest at the center of the fiber. Intensity patterns in LP_{01}, LP_{11} and LP_{21} modes.

Constante de propagação normaliza vs número *V*

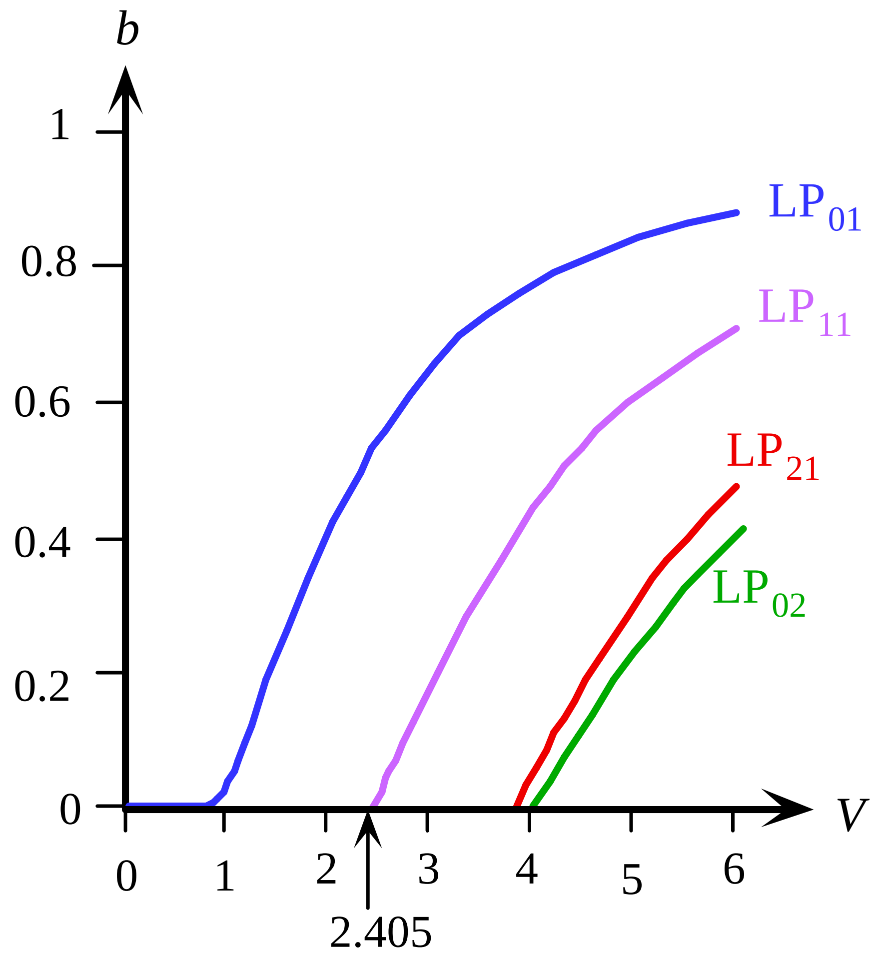

Normalized propagation constant *b* vs. *V*-number for a step index fiber for various LP modes.

Dispersão em fibras mono-modo

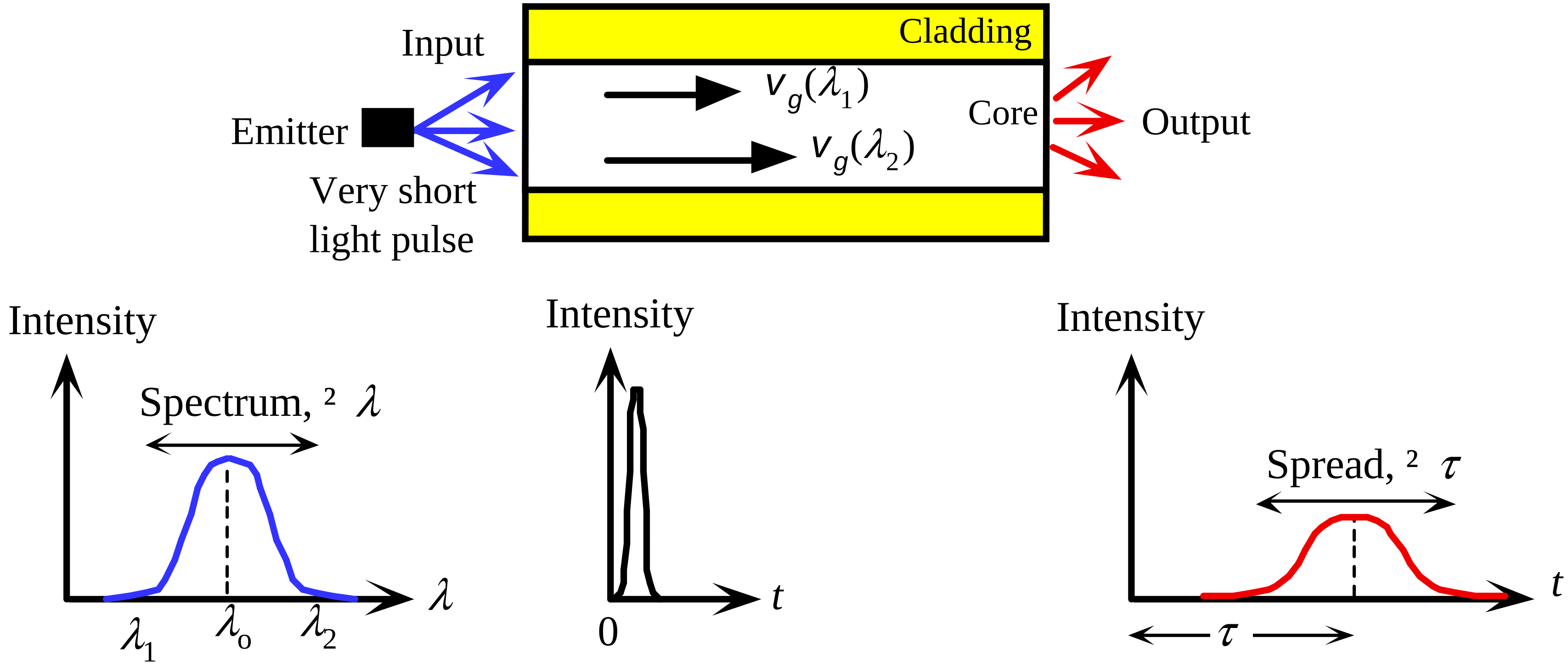

All excitation sources are inherently non-monochromatic and emit within a spectrum, $^2 \lambda$, of wavelengths. Waves in the guide with different free space wavelengths travel at different group velocities due to the wavelength dependence of n_1. The waves arrive at the end of the fiber at different times and hence result in a broadened output pulse.

Dispersão material e dispersão do guia de onda

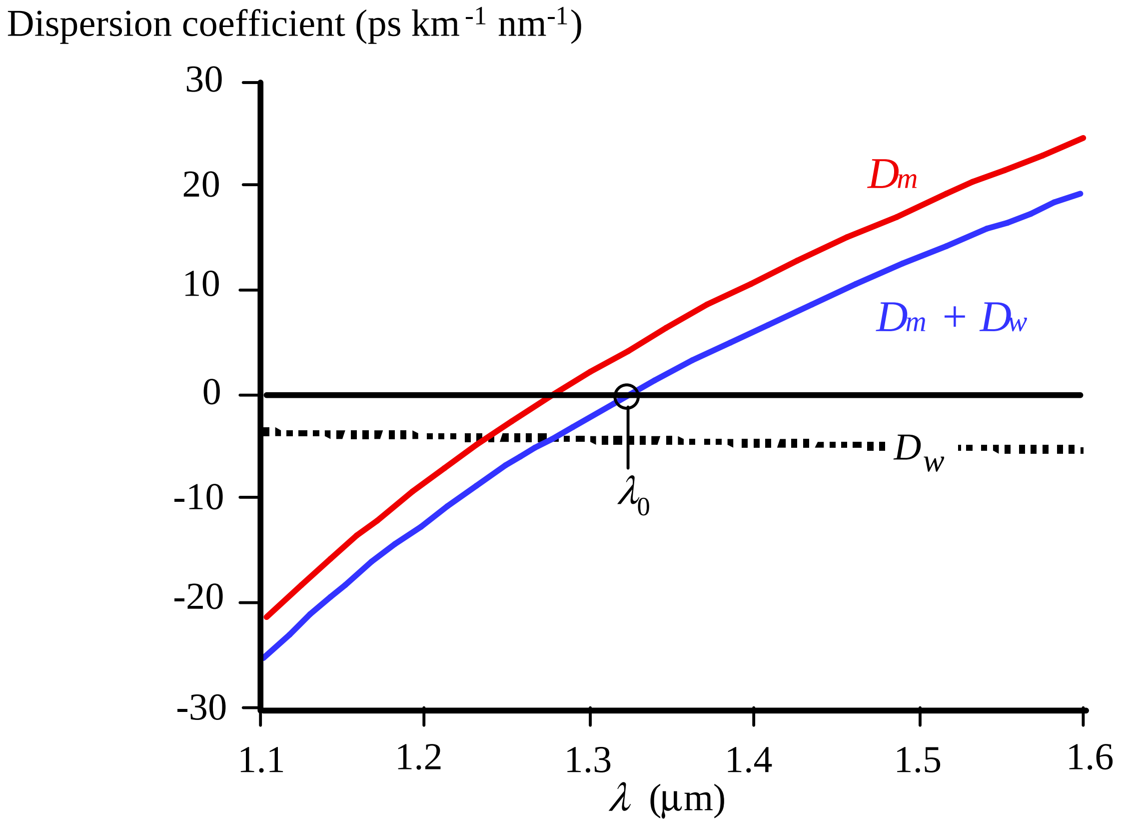

Material dispersion coefficient (D_m) for the core material (taken as SiO_2), waveguide dispersion coefficient (D_w) (a = 4.2 µm) and the total or chromatic dispersion coefficient D_{ch} (= $D_m + D_w$) as a function of free space wavelength, λ.

Dispersão devida à polarização

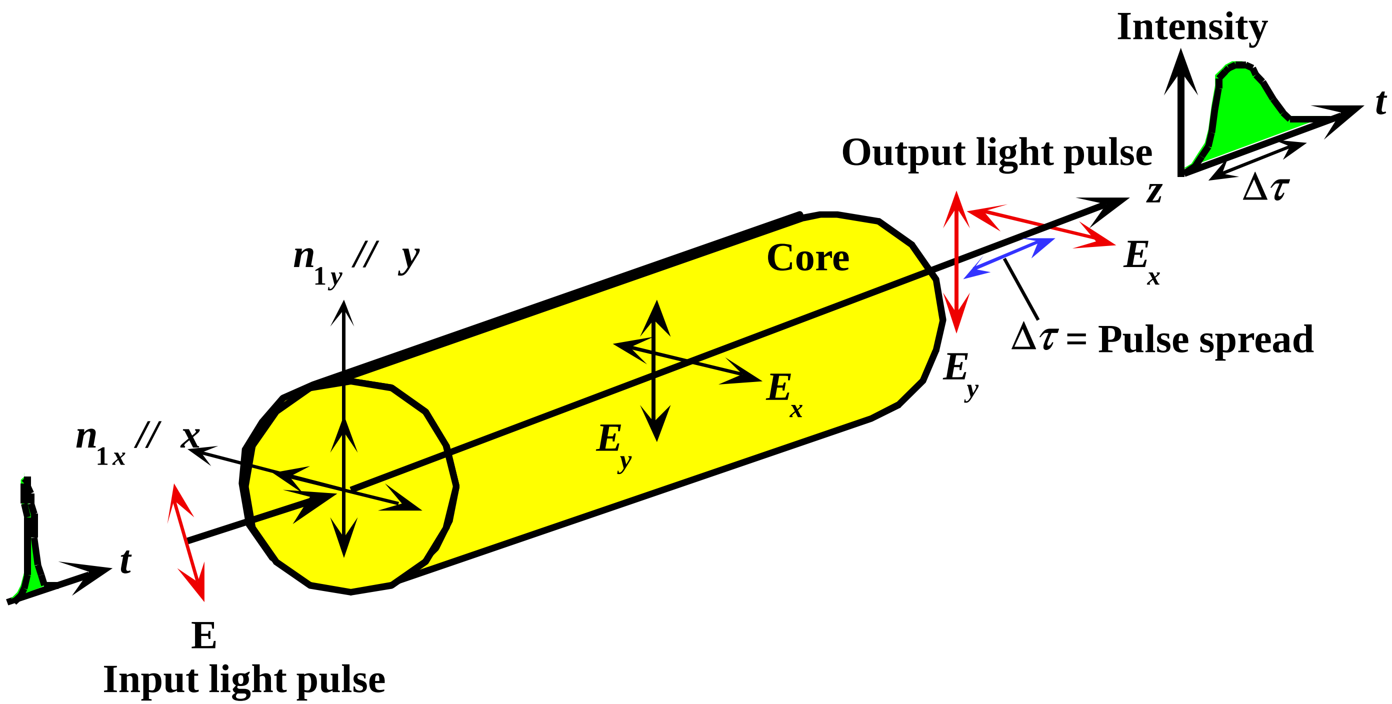

Suppose that the core refractive index has different values along two orthogonal directions corresponding to electric field oscillation direction (polarizations). We can take x and y axes along these directions. An input light will travel along the fiber with E_x and E_y polarizations having different group velocities and hence arrive at the output at different times

Dispersão em fibras "flattened"

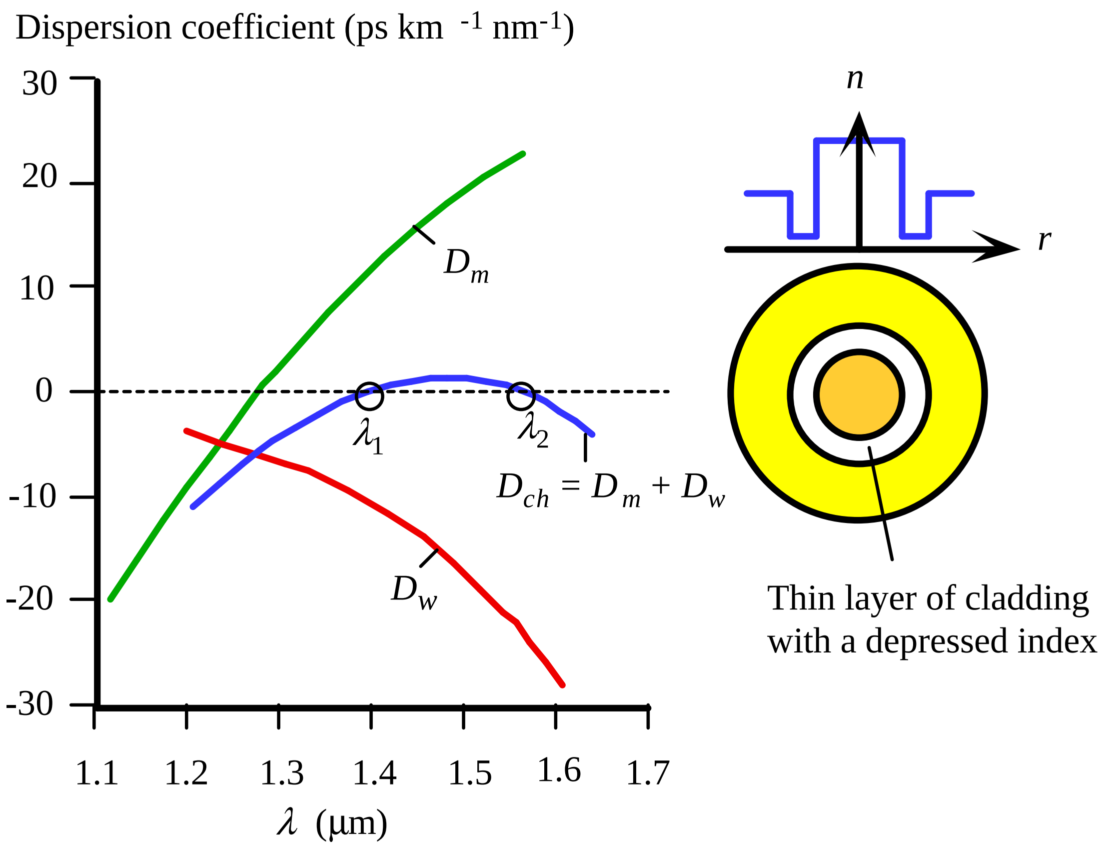

Dispersion flattened fiber example. The material dispersion coefficient (D_m) for the core material and waveguide dispersion coefficient (D_w) for the doubly clad fiber result in a flattened small chromatic dispersion between λ_1 and λ_2.

Dispersão em fibras ópticas de vidro

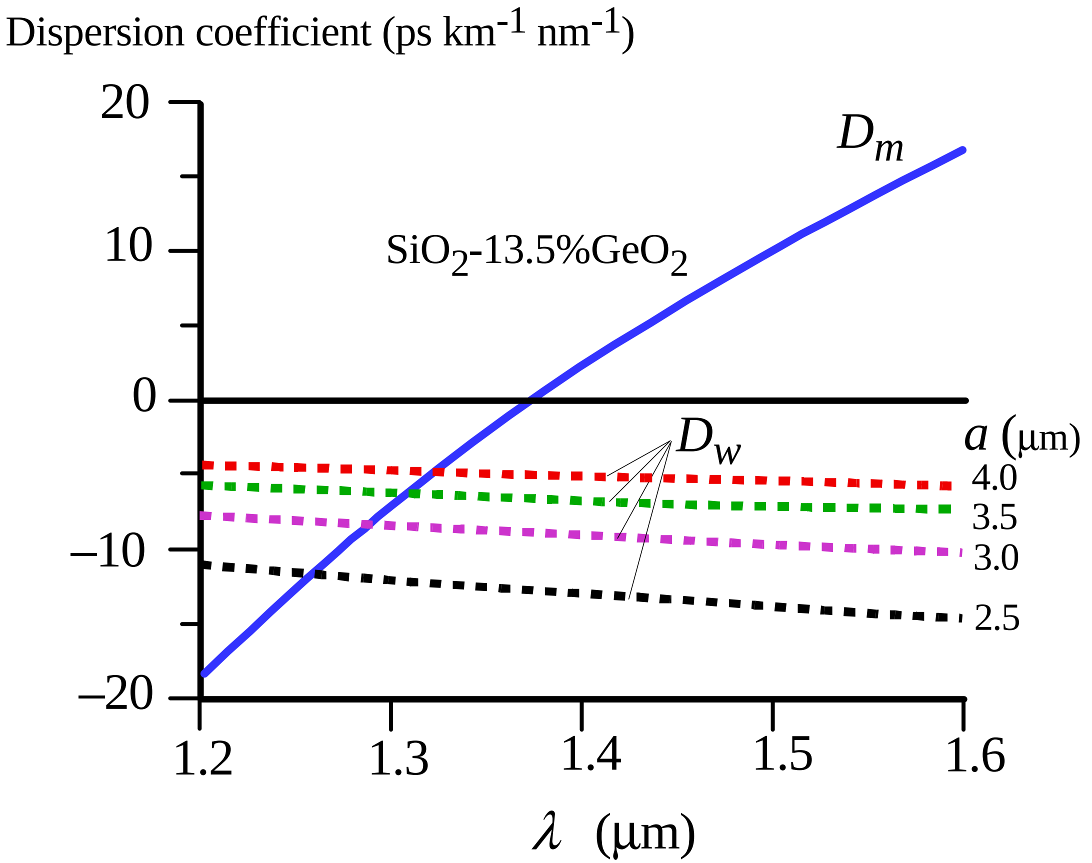

Material and waveguide dispersion coefficients in an optical fiber with a core SiO_2-13.5%GeO_2 for *a* = 2.5 to 4 µm.

"Bit rate" e Dispersão

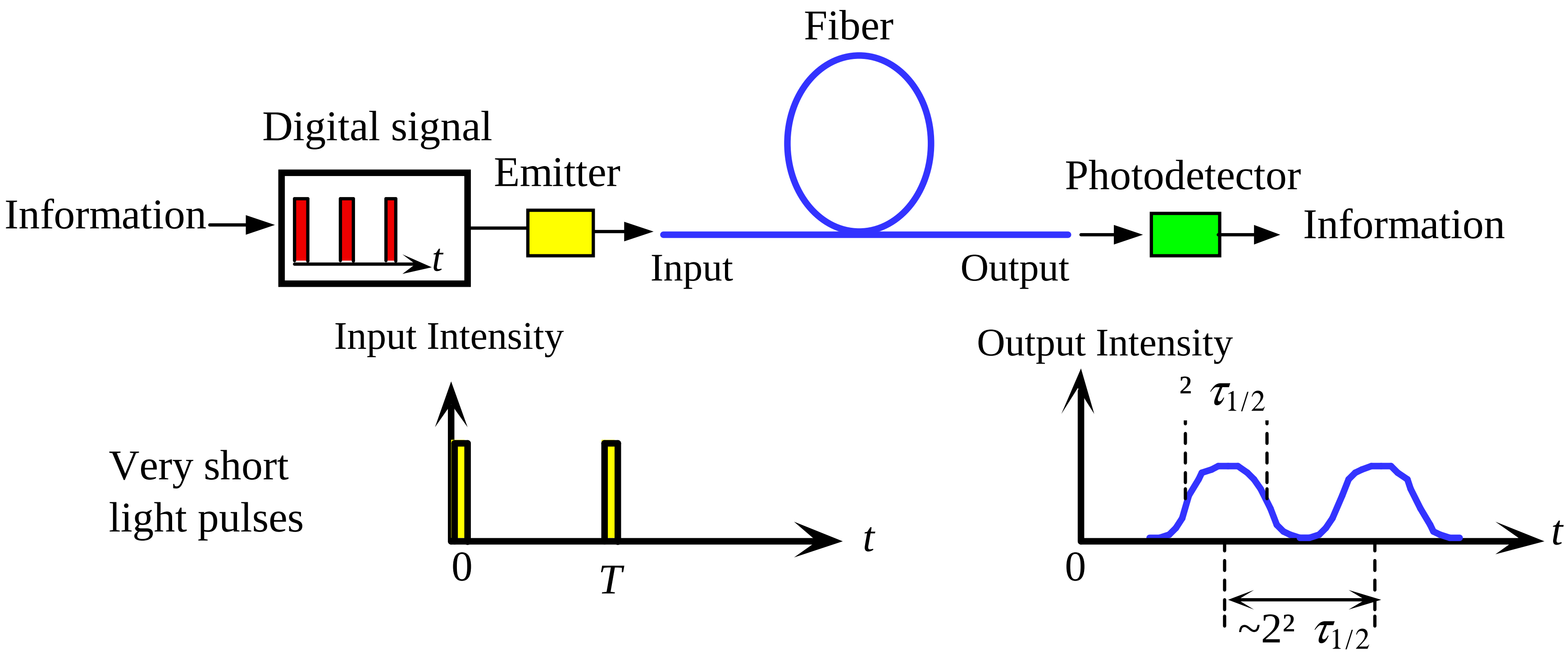

An optical fiber link for transmitting digital information and the effect of dispersion in the fiber on the output pulses.

Interferência intersimbólica tolerável

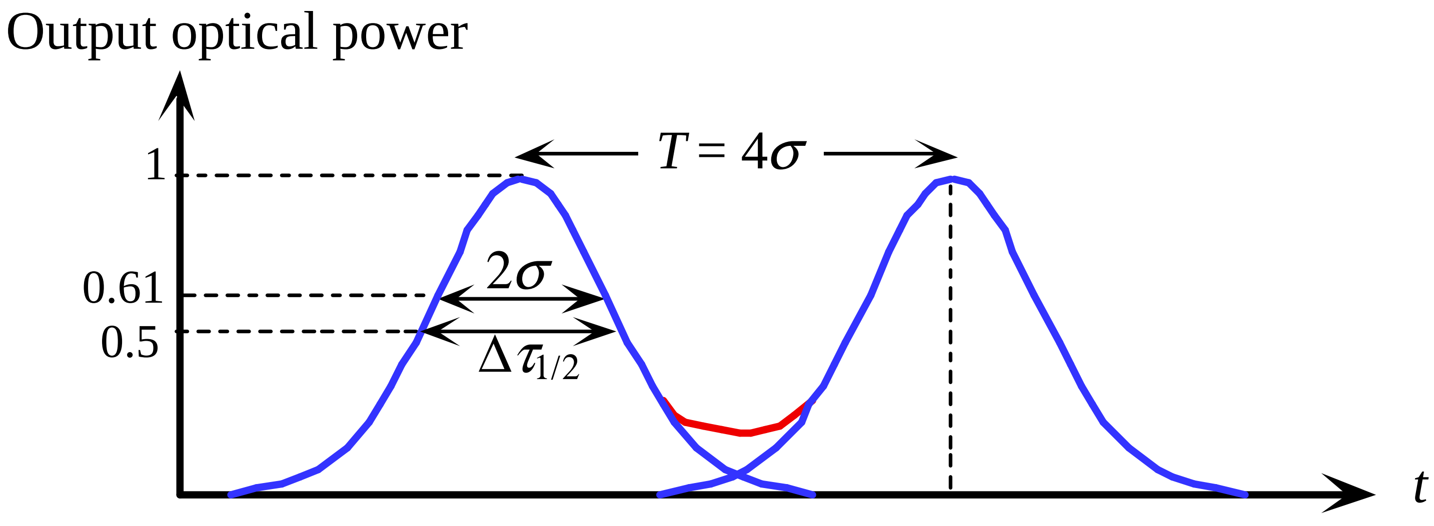

A Gaussian output light pulse and some tolerable intersymbol interference between two consecutive output light pulses (*y*-axis in relative units). At time $t = \sigma$ from the pulse center, the relative magnitude is $e^{-1/2} = 0.607$ and full width root mean square (rms) spread is $\Delta\tau_{rms} = 2\sigma$.

Ligação de fibra óptica analógica e o efeito da dispersão

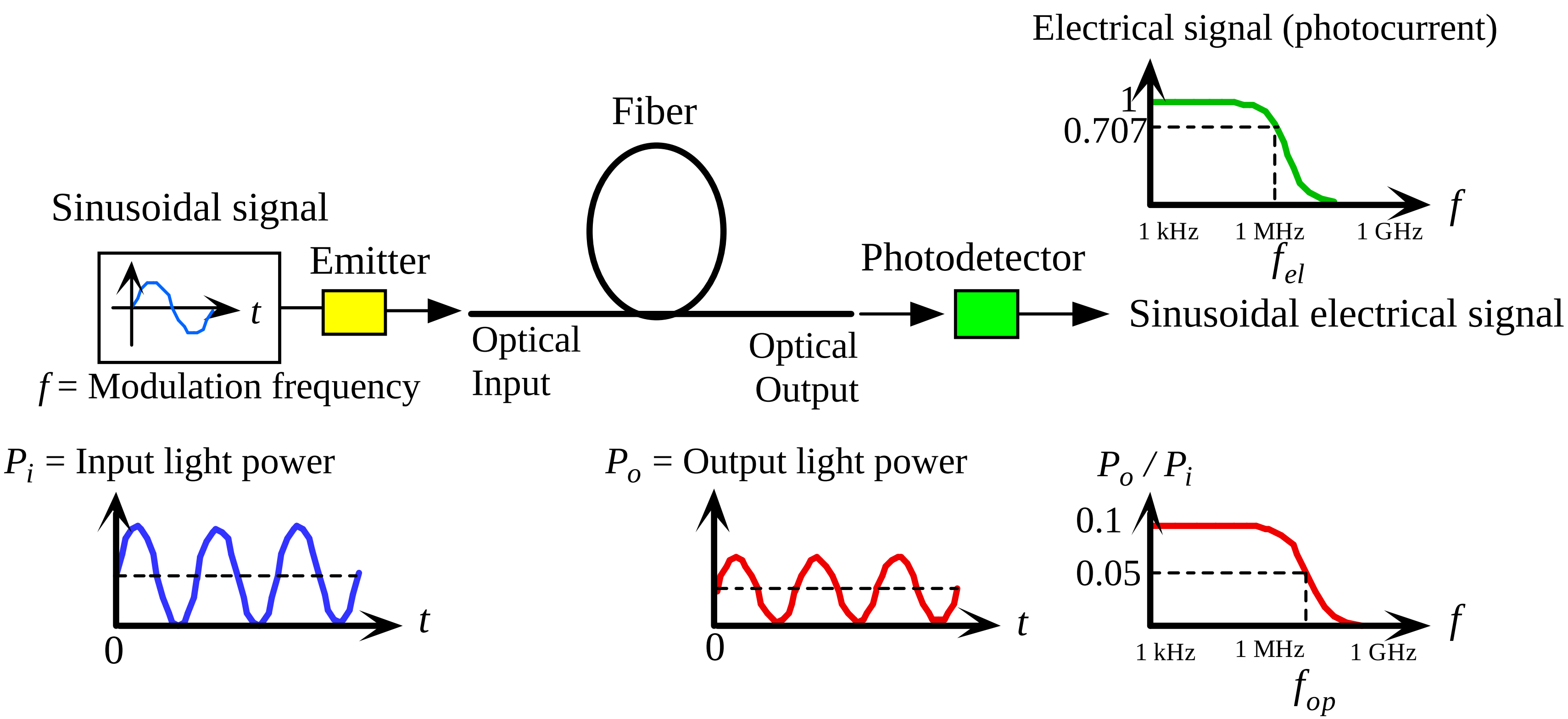

An optical fiber link for transmitting analog signals and the effect of dispersion in the fiber on the bandwidth, f_{op}.

Fibras ópticas com índice gradual

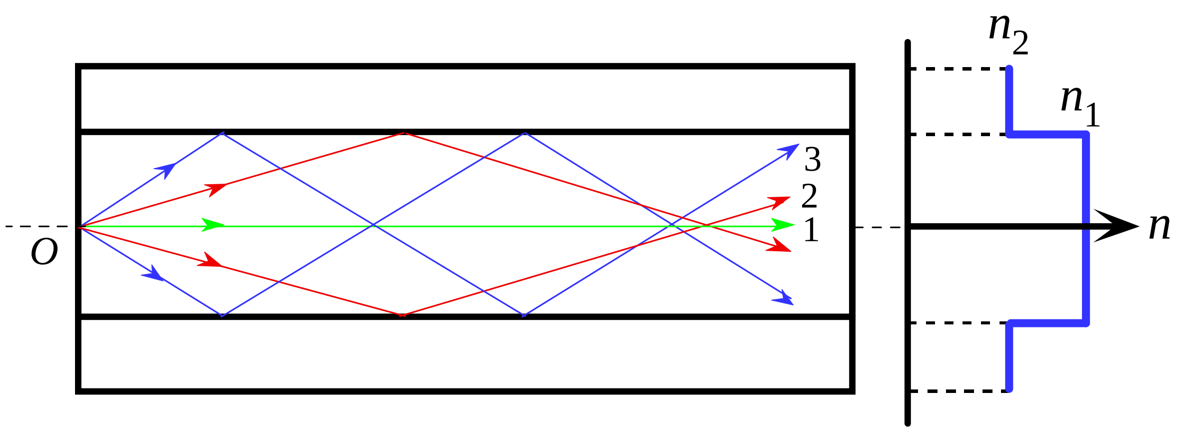

(a) Multimode step index fiber. Ray paths are different so that rays arrive at different times.

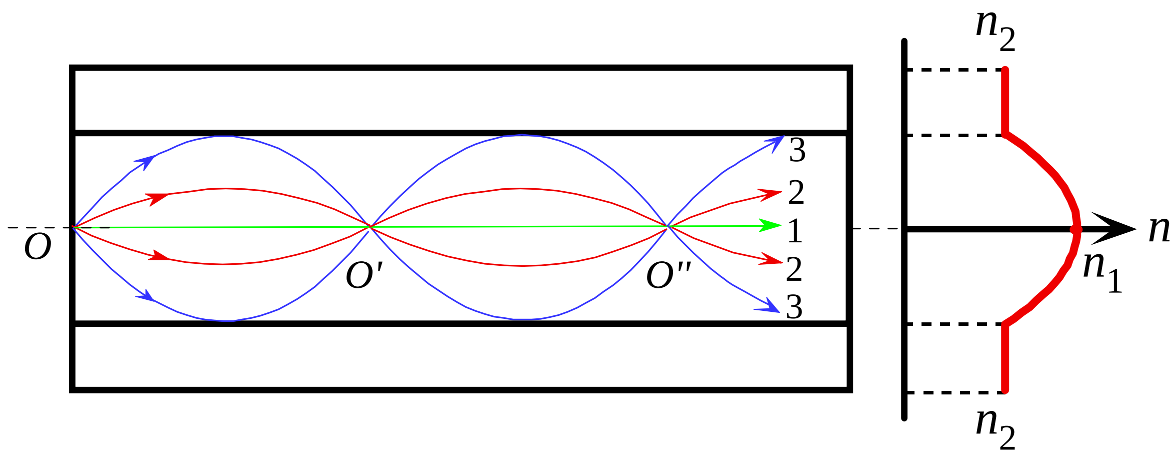

(b) Graded index fiber. Ray paths are different but so are the velocities along the paths so that all the rays arrive at the same time.

Aproximação a uma fibras ópticas com índice gradual

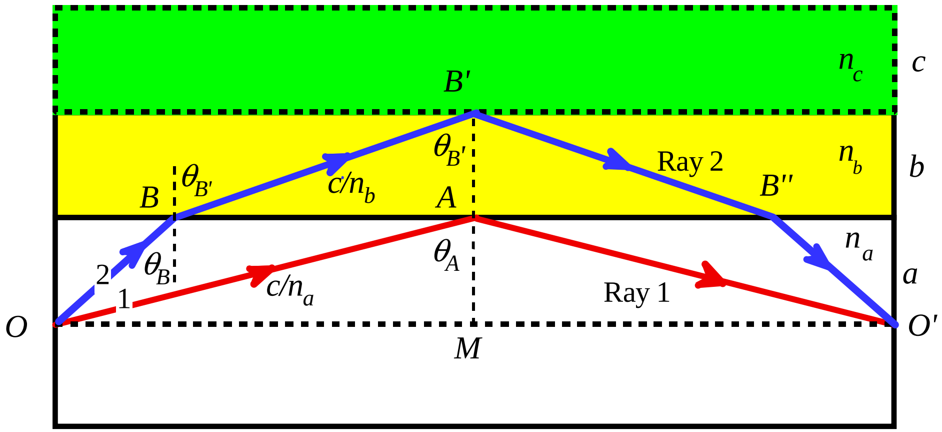

We can visualize a graded index fiber by imagining a stratified medium with the layers of refractive indices $n_a > n_b > n_c$ ... Consider two close rays 1 and 2 launched from O at the same time but with slightly different launching angles. Ray 1 just suffers total internal reflection. Ray 2 becomes refracted at B and reflected at B'.

Propagação de raios num meio estratificado

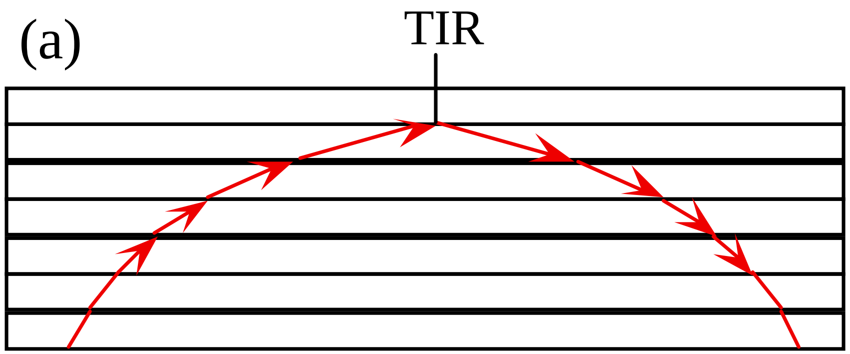

n decreases step by step from one layer to next upper layer; very thin layers.

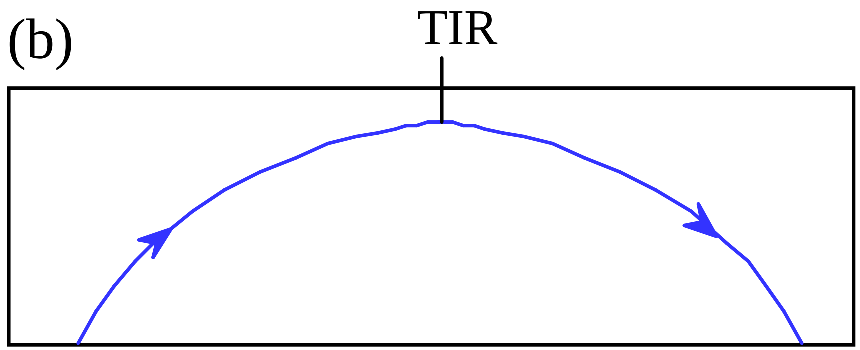

Continuous decrease in *n* gives a ray path changing continuously.

(a) A ray in thinly stratifed medium becomes refracted as it passes from one layer to the next upper layer with lower *n* and eventually its angle satisfies TIR
(b) In a medium where *n* decreases continuously the path of the ray bends continuously.

Lentes com distribuição de índice gradual

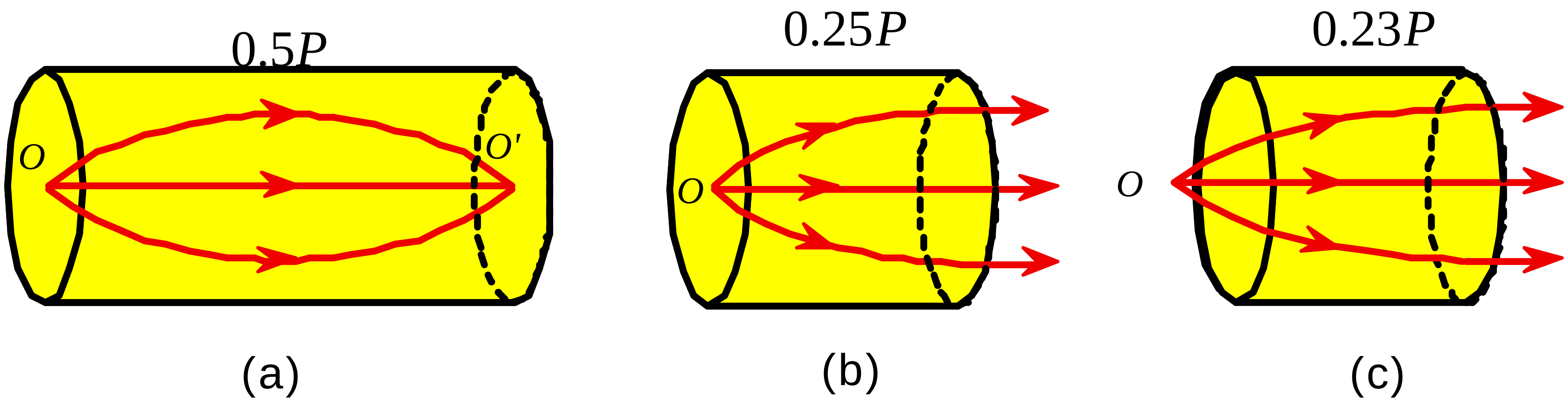

Graded index (GRIN) rod lenses of different pitches. (a) Point *O* is on the rod face center and the lens focuses the rays onto *O'* on to the center of the opposite face. (b) The rays from *O* on the rod face center are collimated out. (c) *O* is slightly away from the rod face and the rays are collimated out.

Absorção da luz em fibras óticas na direção de propagação

Attenuation of light in the direction of propagation.

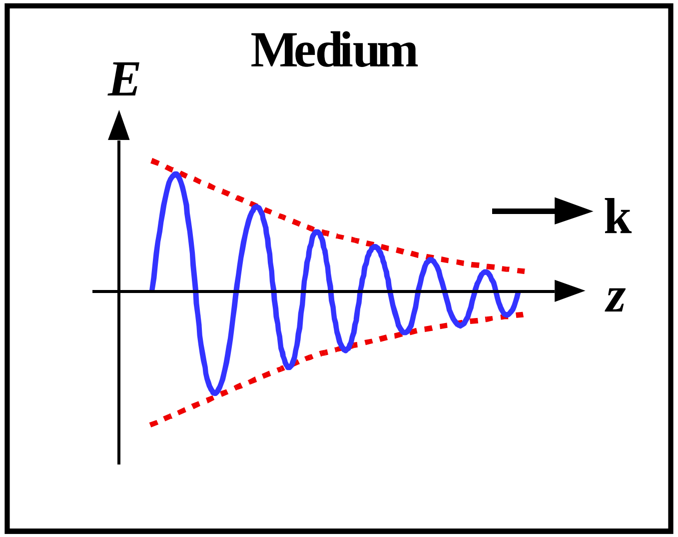

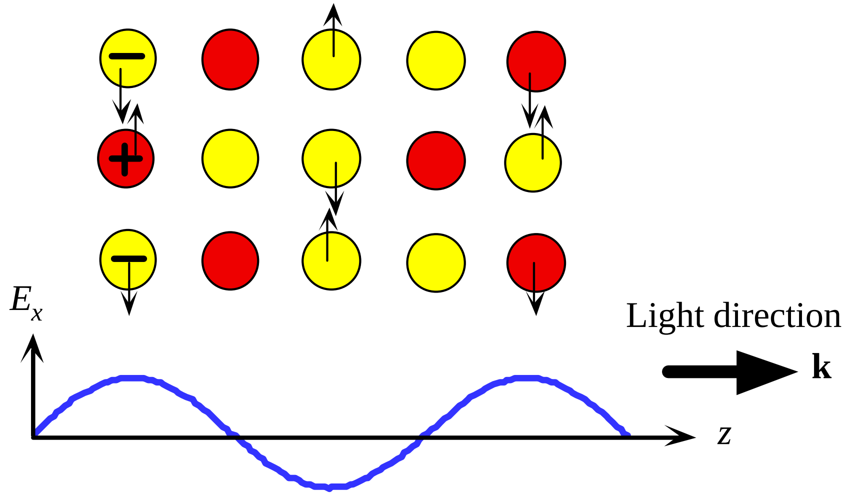

Lattice absorption through a crystal. The field in the wave oscillates the ions which consequently generate "mechanical" waves in the crystal; energy is thereby transferred from the wave to lattice vibrations.

Espalhamento da luz em fibras ópticas

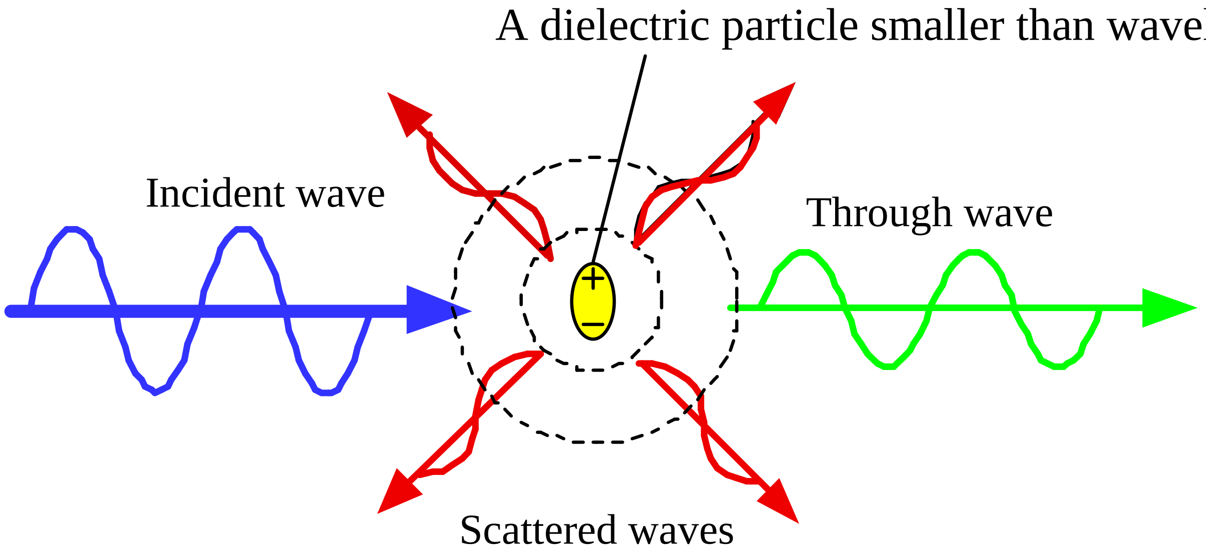

Rayleigh scattering involves the polarization of a small dielectric particle or a region that is much smaller than the light wavelength. The field forces dipole oscillations in the particle (by polarizing it) which leads to the emission of EM waves in "many" directions so that a portion of the light energy is directed away from the incident beam.

Atenuação em fibras ópticas de sílica

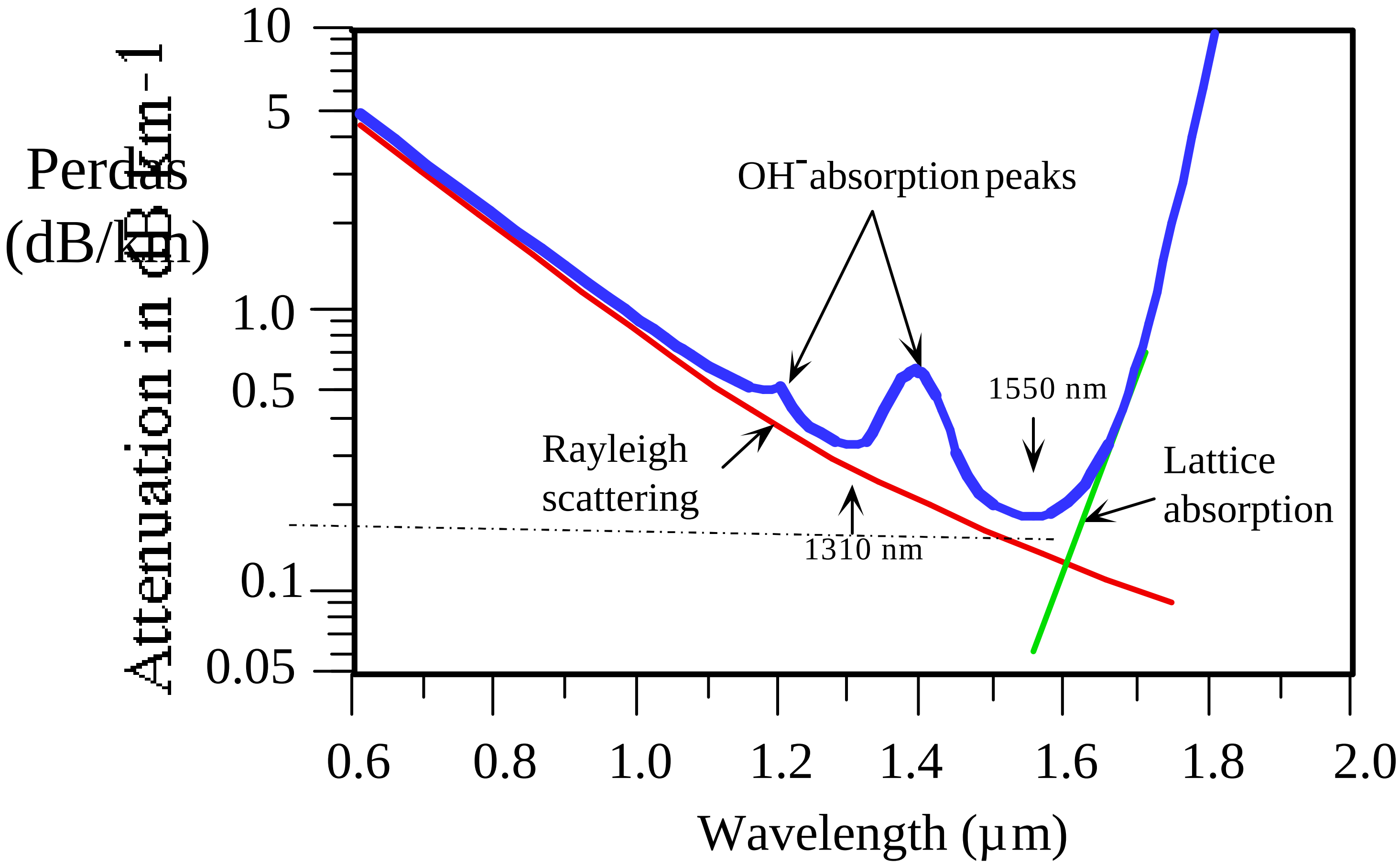

Illustration of a typical attenuation vs. wavelength characteristics of a silica based optical fiber. There are two communications channels at 1310 nm and 1550 nm.

Perdas em fibras ópticas devido a curvaturas

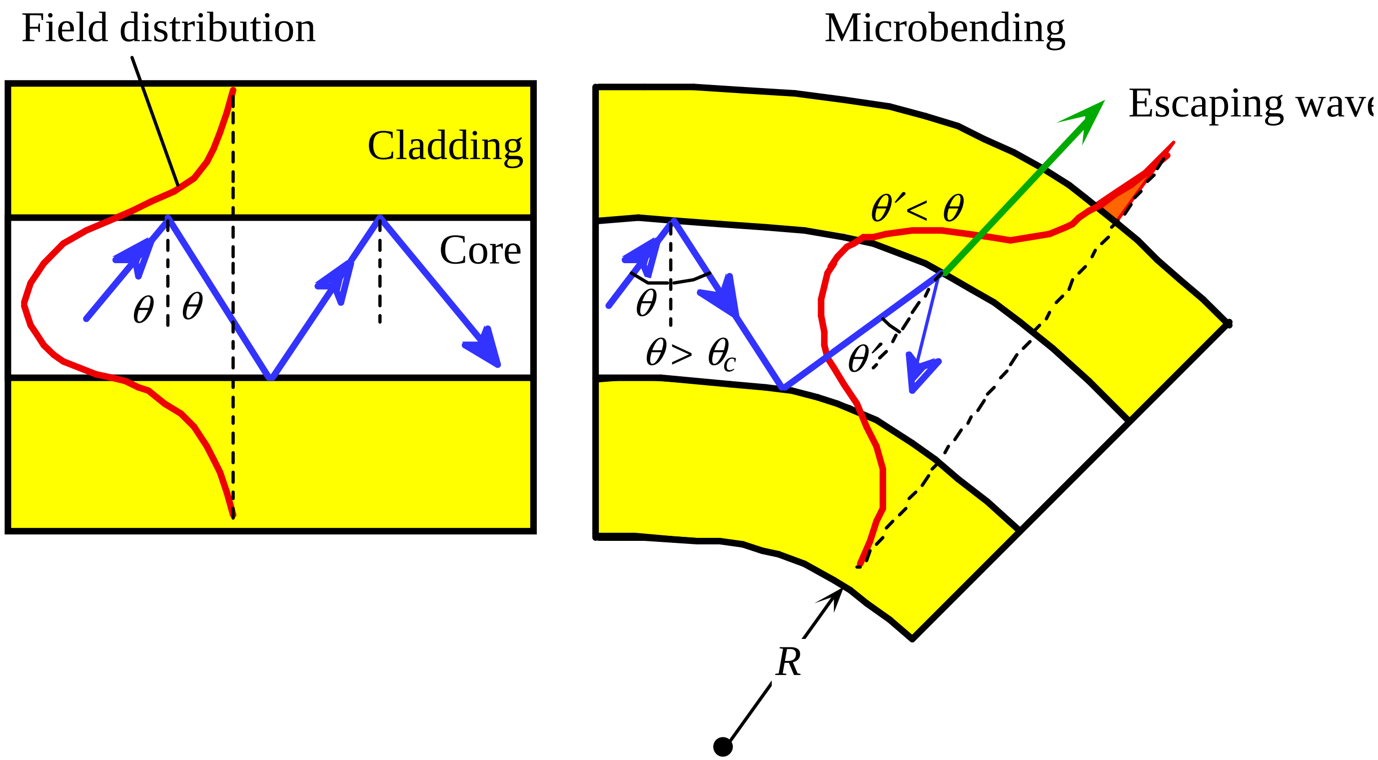

Sharp bends change the local waveguide geometry that can lead to waves escaping. The zigzagging ray suddenly finds itself with an incidence angle θ' that gives rise to either a transmitted wave, or to a greater cladding penetration; the field reaches the outside medium and some light energy is lost.

Perdas em fibras ópticas devido a micro-curvaturas

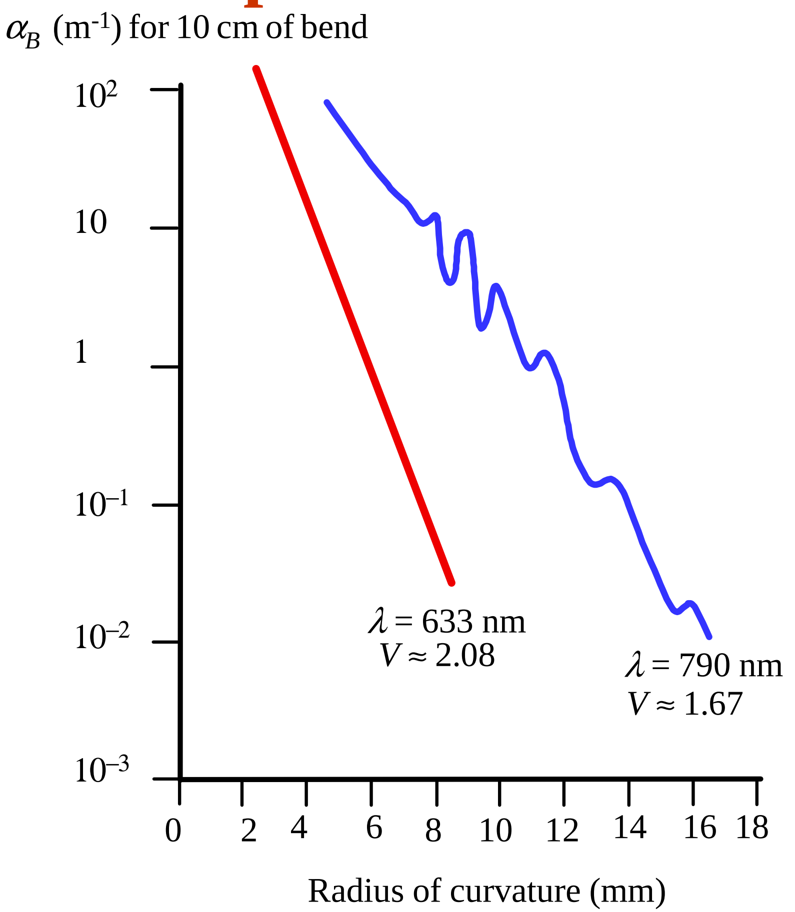

Measured microbending loss for a 10 cm fiber bent by different amounts of radius of curvature *R*. Single mode fiber with a core diameter of 3.9 μm, cladding radius 48 μm, $\Delta = 0.004$, $NA = 0.11$, $V \approx 1.67$ and 2.08 (Data extracted and replotted with Δ correction from, A.J. Harris and P.F. Castle, *IEEE J. Light Wave Technology*, Vol. LT14, pp. 34-40, 1986; see original article for discussion of peaks in α_B vs. *R* at 790 nm).

Processo de produção de fibras ópticas

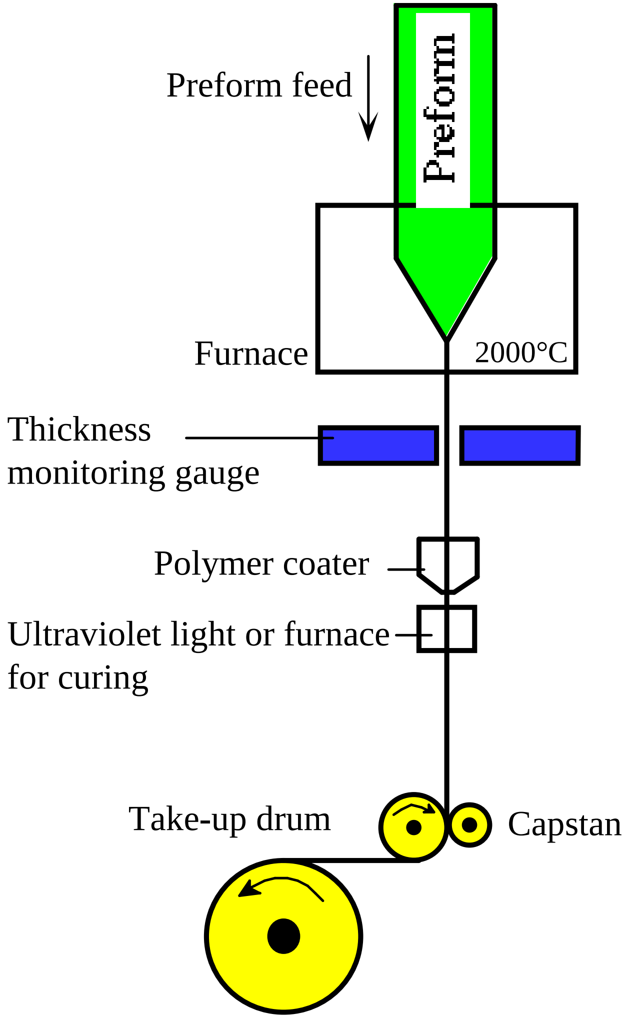

Schematic illustration of a fiber drawing tower.

Processo “outside vapor deposição” de preparação de fibras

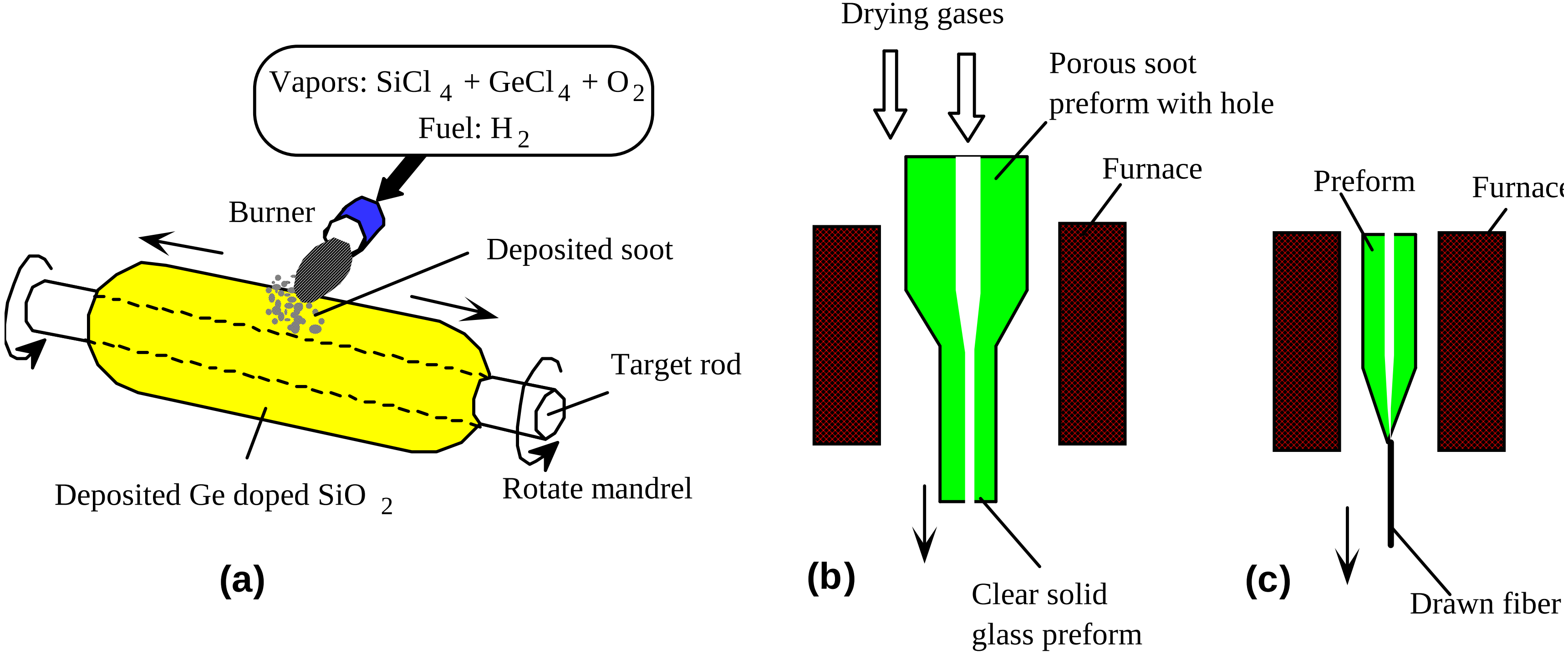

Schematic illustration of OVD and the preform preparation for fiber drawing. (a) Reaction of gases in the burner flame produces glass soot that deposits on to the outside surface of the mandrel. (b) The mandrel is removed and the hollow porous soot preform is consolidated; the soot particles are sintered, fused, together to form a clear glass rod. (c) The consolidated glass rod is used as a preform in fiber drawing.

Secção transversal de uma fibra óptica mono-modo

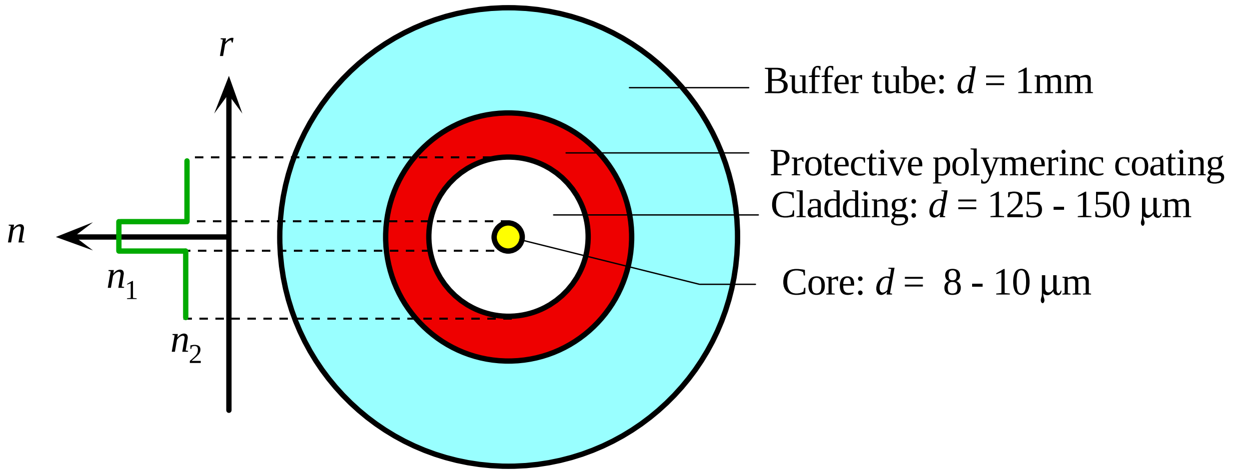

The cross section of a typical single-mode fiber with a tight buffer tube. (d = diameter)

Optoelectrónica e ótica integrada

Efeitos electro-ópticos

Modulador de fase

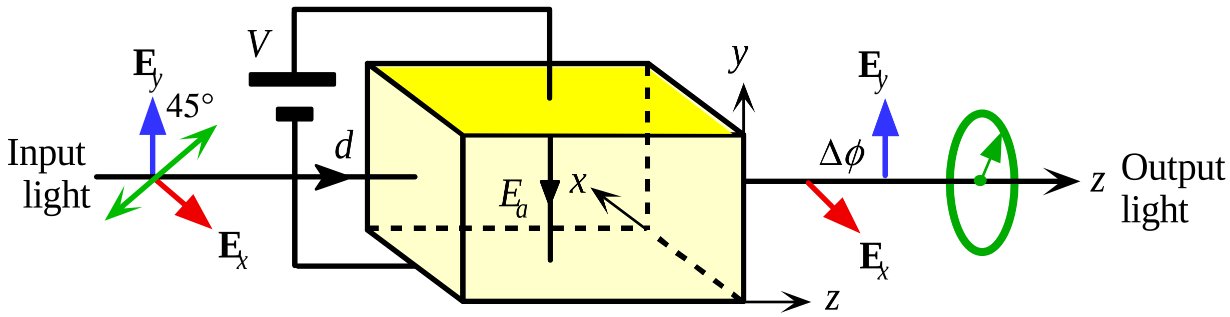

Tranverse Pockels cell phase modulator. A linearly polarized input light into an electro-optic crystal emerges as a circularly polarized light. E_a is the applied field parallel to y.

Modulador de intensidade

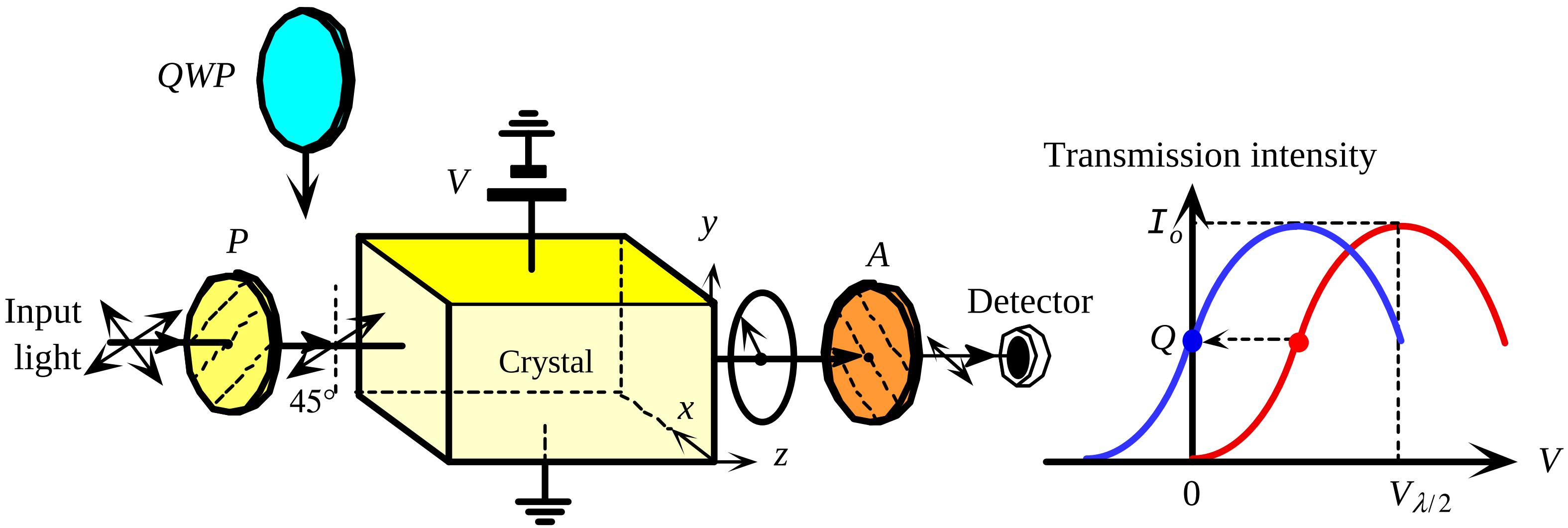

Left: A tranverse Pockels cell intensity modulator. The polarizer *P* and analyzer *A* have their transmission axis at right angles and *P* polarizes at an angle 45° to *y*-axis. Right: Transmission intensity vs. applied voltage characteristics. If a quarter-wave plate (*QWP*) is inserted after *P*, the characteristic is shifted to the dashed curve.

Modulador ópticos integrados

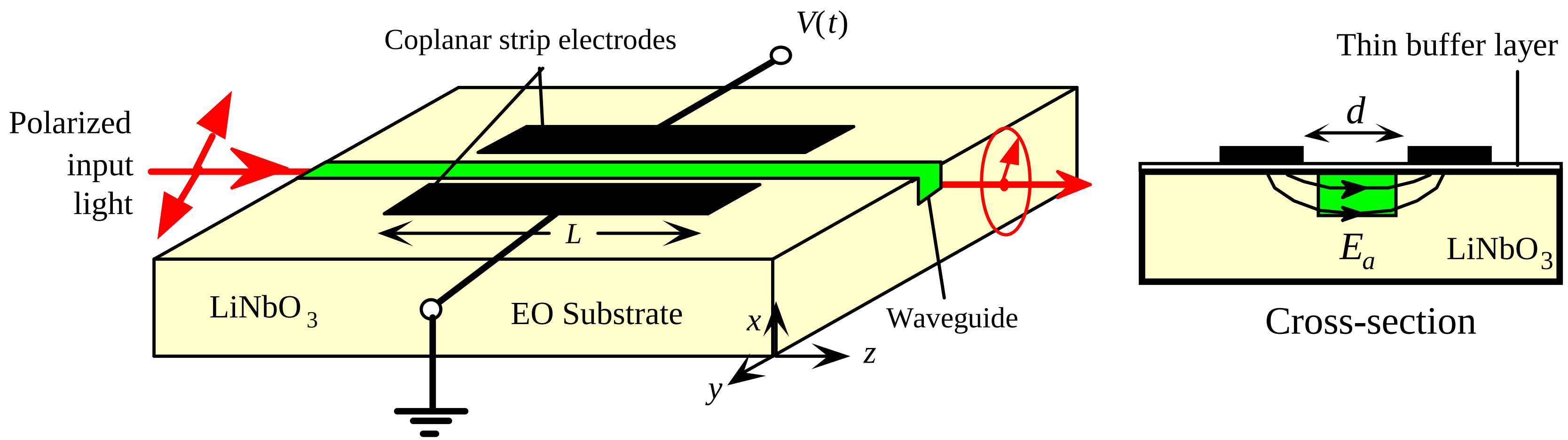

Integrated tranverse Pockels cell phase modulator in which a waveguide is diffused into an electro-optic (EO) substrate. Coplanar strip electrodes apply a transverse field E_a through the waveguide. The substrate is an *x*-cut $LiNbO_3$ and typically there is a thin dielectric buffer layer (*e.g.* ~200 nm thick SiO_2) between the surface electrodes and the substrate to separate the electrodes away from the waveguide.

Modulador Mach-Zehnder

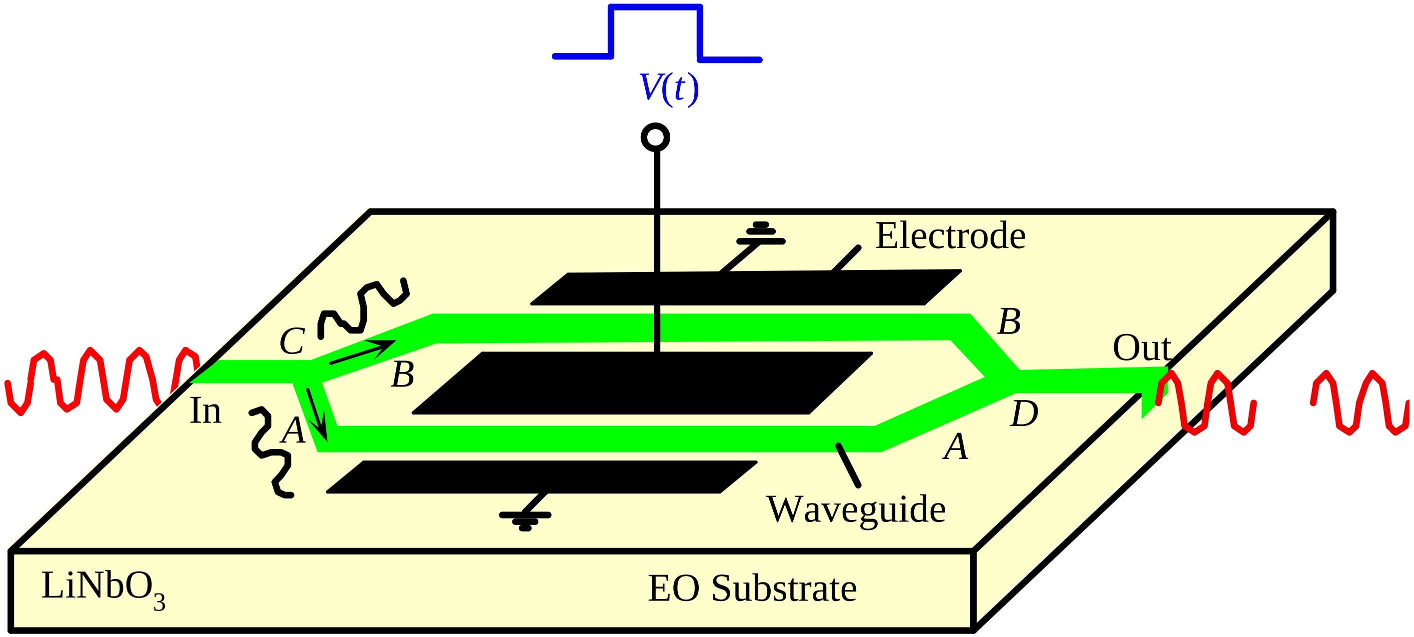

An integrated Mach-Zender optical intensity modulator. The input light is split into two coherent waves *A* and *B*, which are phase shifted by the applied voltage, and then the two are combined again at the output.

Acoplador direccional passivo

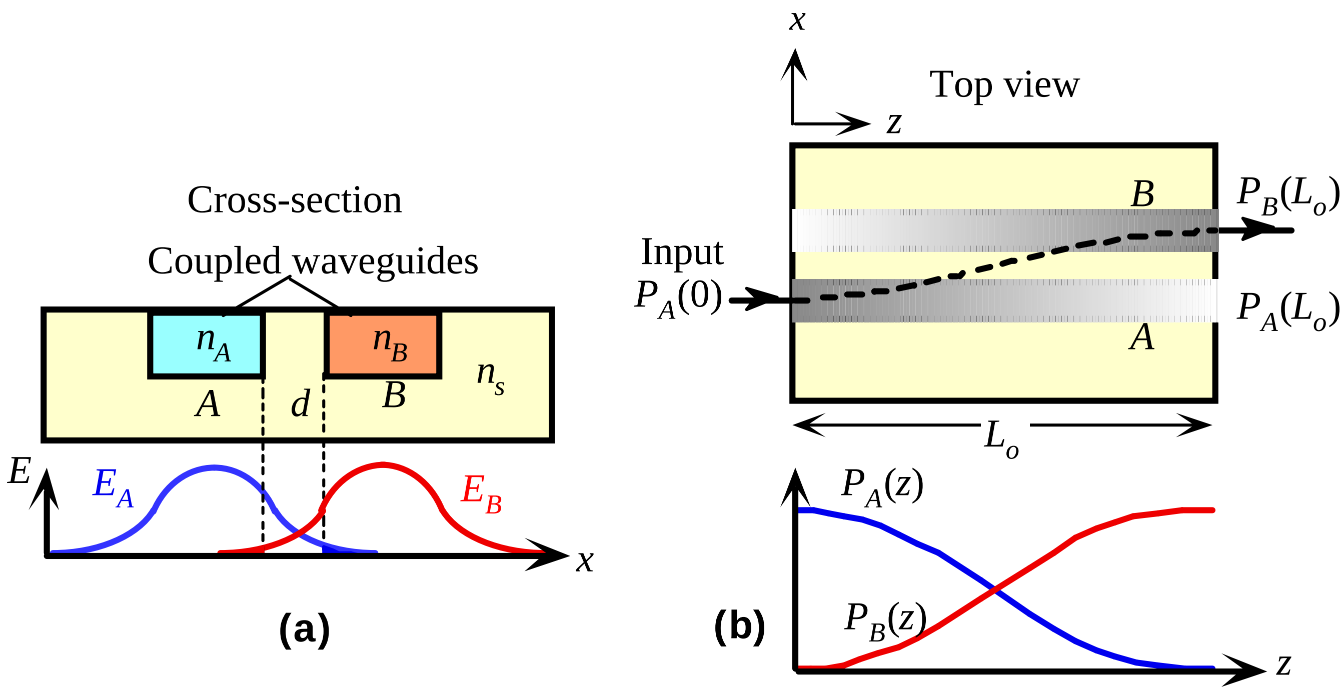

(a) Cross section of two closely spaced waveguides *A* and *B* (separated by *d*) embedded in a substrate. The evanescent field from *A* extends into *B* and vice versa. Note: n_A and $n_B > n_s$ (= substrate index).

(b) Top view of the two guides *A* and *B* that are coupled along the *z*-direction. Light is fed into *A* at $z = 0$, and it is gradually transferred to *B* along *z*. At $z = L_o$, all the light been transferred to *B* . Beyond this point, light begins to be transferred back to *A* in the same way.

Ver também http://w3.ualg.pt/~jlongras/JLFMScThesis.pdf (4º capítulo)

Acoplador direccional activo

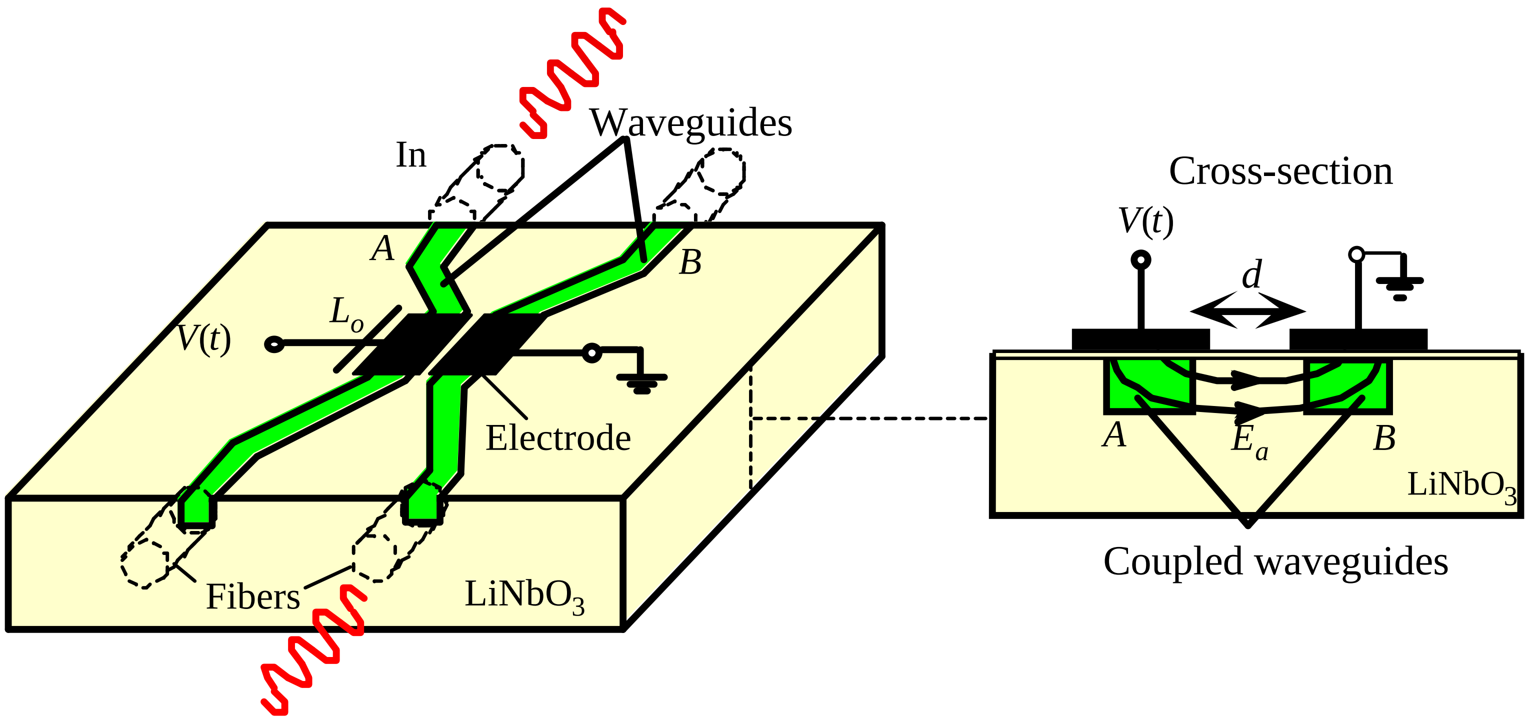

An integrated directional coupler. Applied field E_a alters the refractive indices of th
two guides and changes the strength of coupling.

Moduladores acusto-ópticos

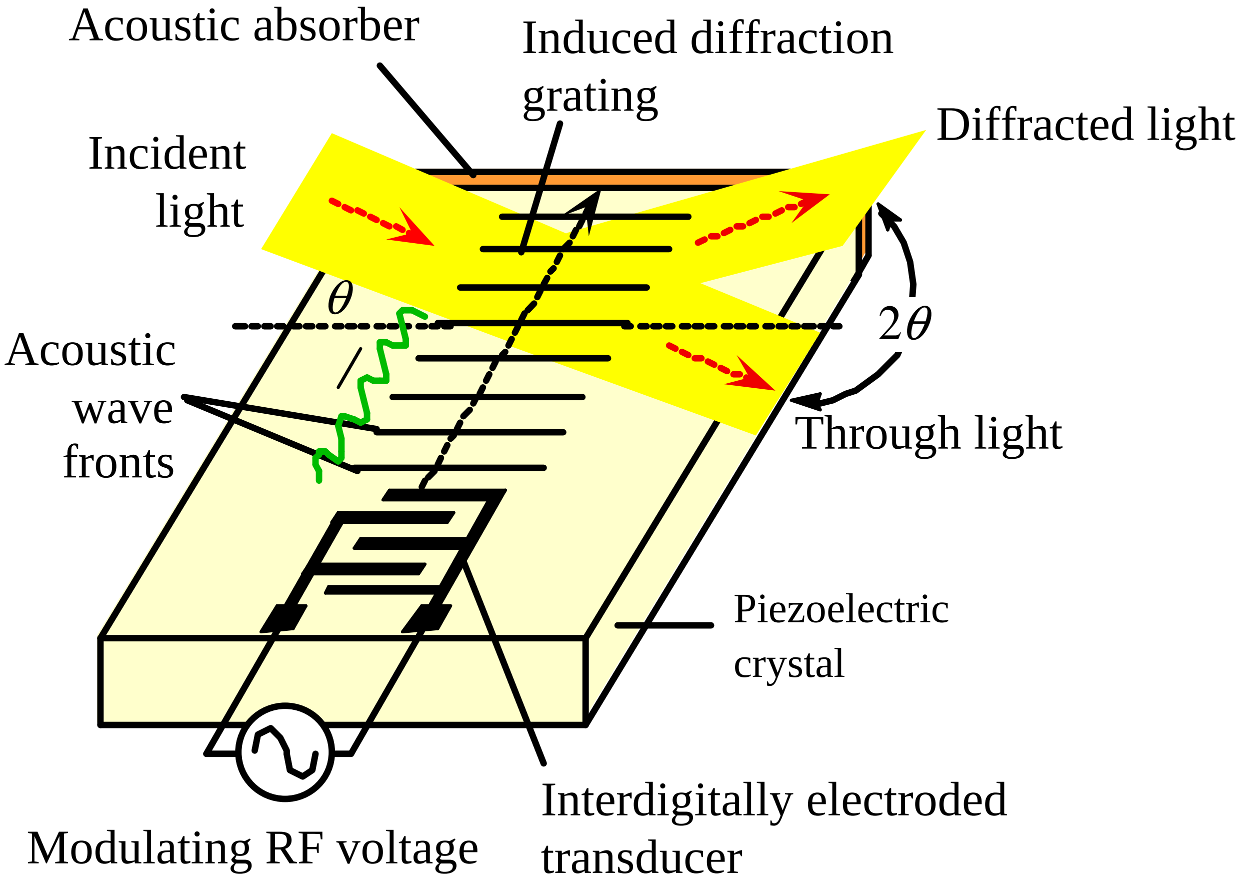

Traveling acoustic waves create a harmonic variation in the refractive index and thereby create a diffraction grating that diffracts the incident beam throug an angle 2θ.

Moduladores acusto-ópticos

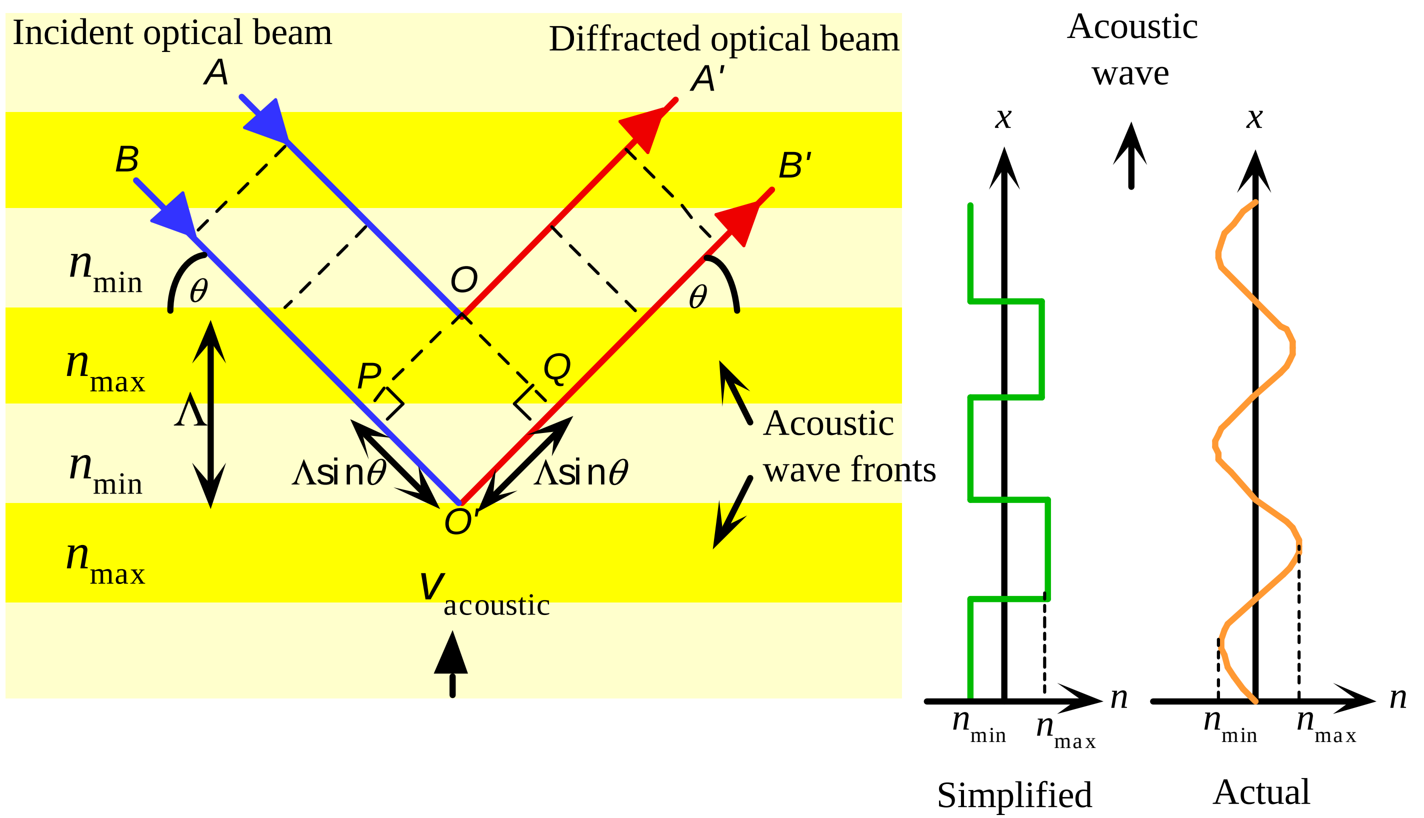

Consider two coherent optical waves *A* and *B* being "reflected" (strictly, scattered) from two adjacent acoustic wavefronts to become *A′* and *B′*. These reflected waves can only constitute the diffracted beam if they are in phase. The angle θ is exaggerated (typically this is a few degrees).

Efeitos magno-ópticos

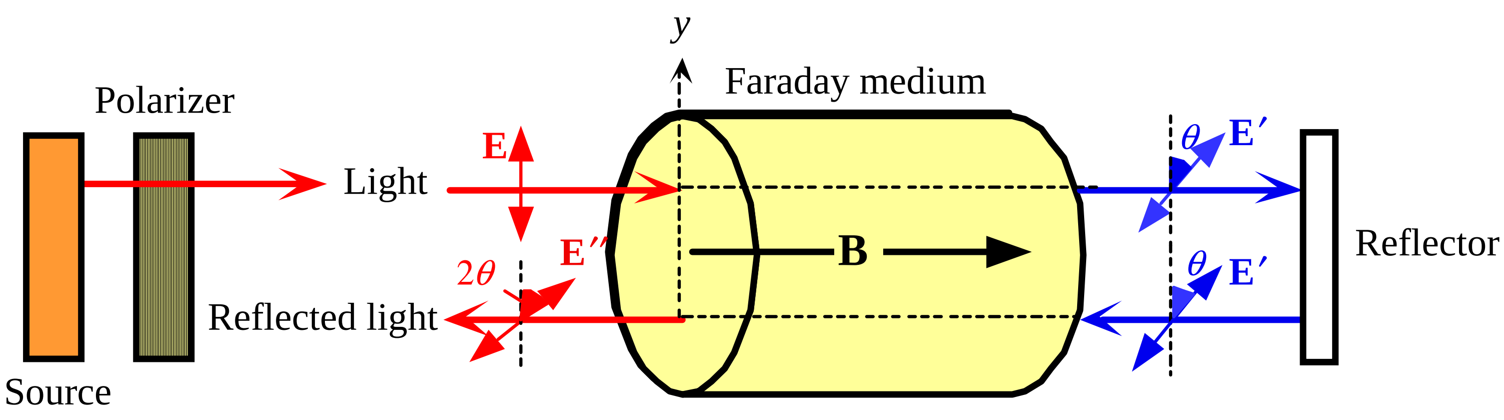

The sense of rotation of the optical field **E** depends only on the direction of the magnetic field for a given medium (given Verdet constant). If light is reflected back into the Faraday medium, the field rotates a further θ in the same sense to come out as **E**″ with a 2θ rotation with respect to **E**.

Efeitos não-lineares e geração do segundo harmónico

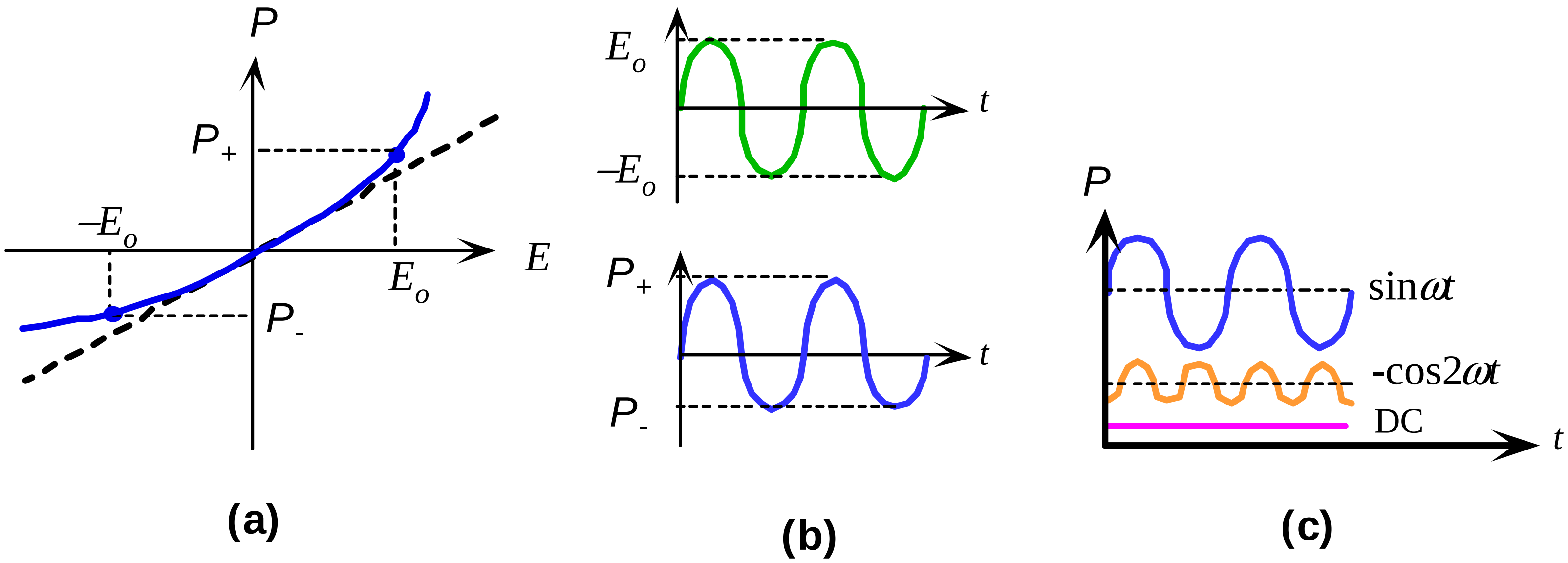

(a) Induced polarization vs. optical field for a nonlinear medium. (b) Sinusoidal optical field oscillations between $\pm E_o$ result in polarization oscillations between P_+ and P_-. (c) The polarization oscillation can be represented by sinusoidal oscillations at angular frequencies ω (fundamental), 2ω (second harmonic) and a small DC component.

Geração do segundo harmónico

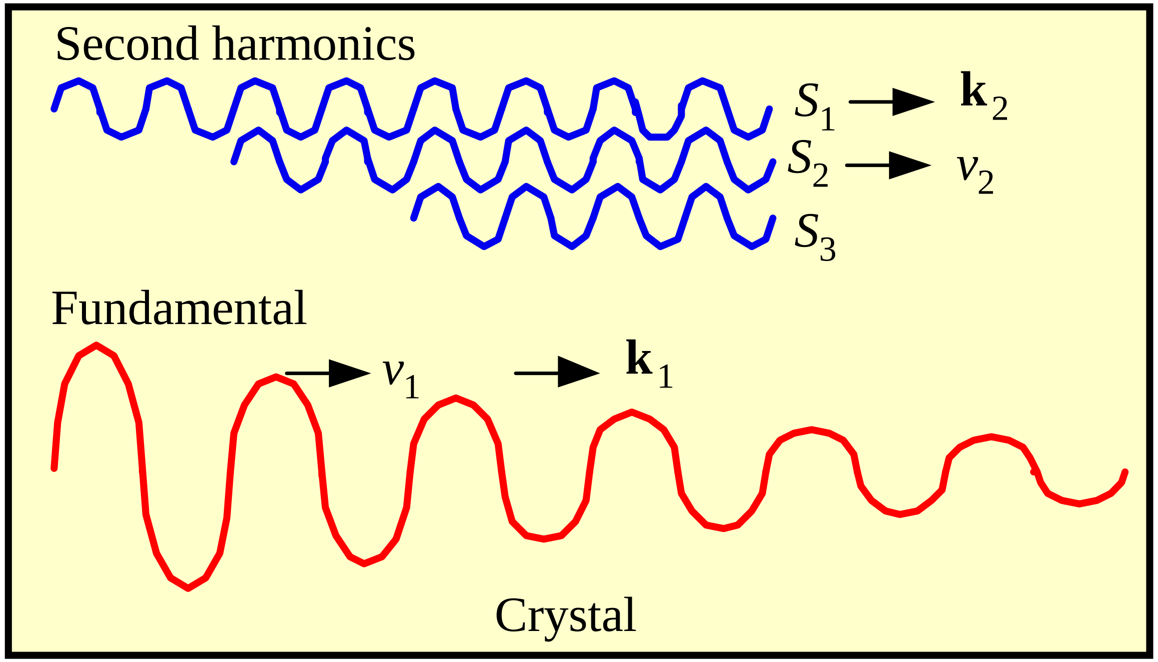

As the fundamental wave propagates, it periodically generates second harmonic waves (S_1, S_2, S_3, ...) and if these are in phase then the amplitude of the second harmonic light builds up.

Duplicação de frequência

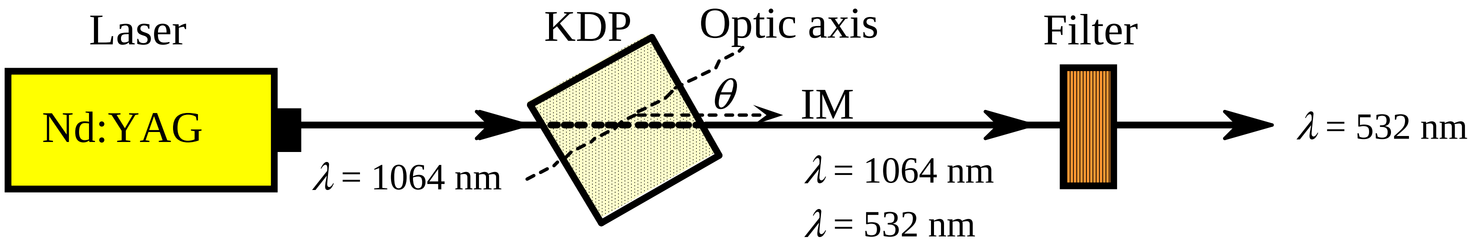

A simplified schematic illustration of optical frequency doubling using a KDP (potassium dihydrogen phosphate) crystal. IM is the index matched direction at ar angle θ (about 35°) to the optic axis along which $n_e(2\omega) = n_o(\omega)$. The focusing o the laser beam onto the KDP crystal and the collimation of the light emerging from the crystal are not shown.

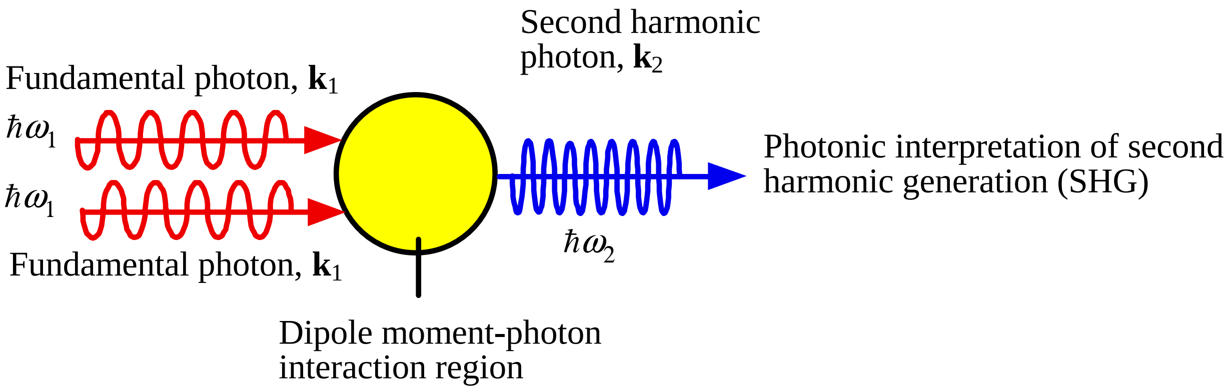

Material semicondutores e sistema MBE

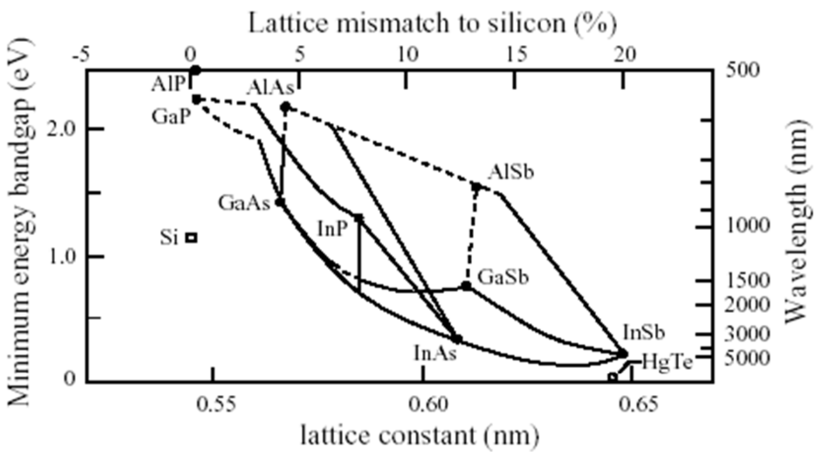

Figure 2.12: Energy bandgap versus lattice constant for some semiconductors [11].

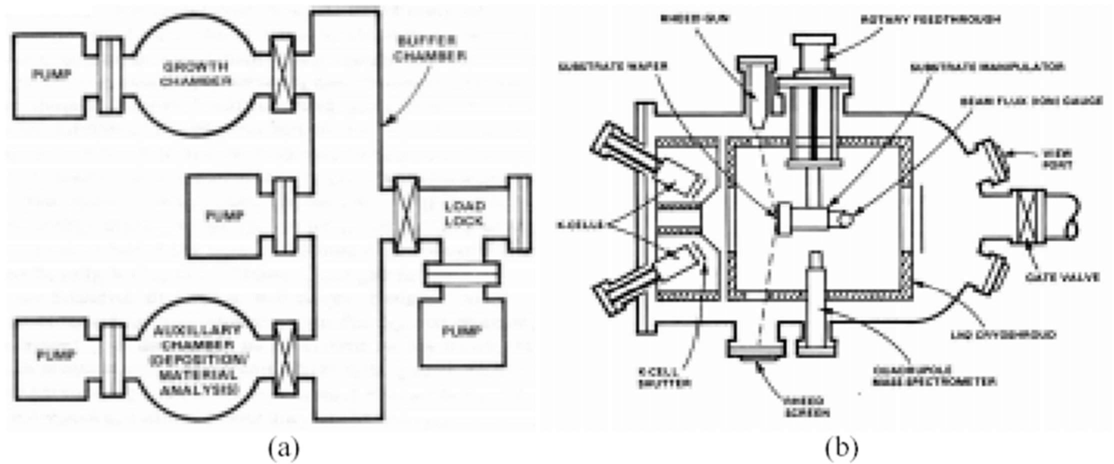

Figure 2.13: (a) Functional schematic of a basic MBE system. (b) Schematic cross-section of a typical MBE growth chamber [57].

Ver também http://w3.ualg.pt/~jlongras/JLFPhDThesis.pdf (2º capítulo)

Heteroestruturas e engenharia de bandas

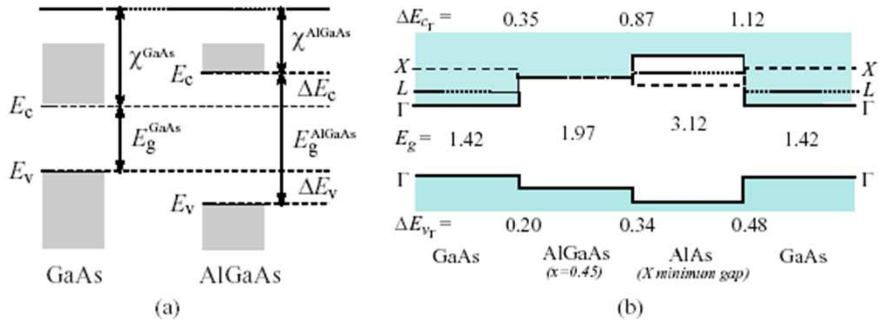

Figure 2.14: Alignment of bands at the heterojunction between GaAs and AlGaAs [23].

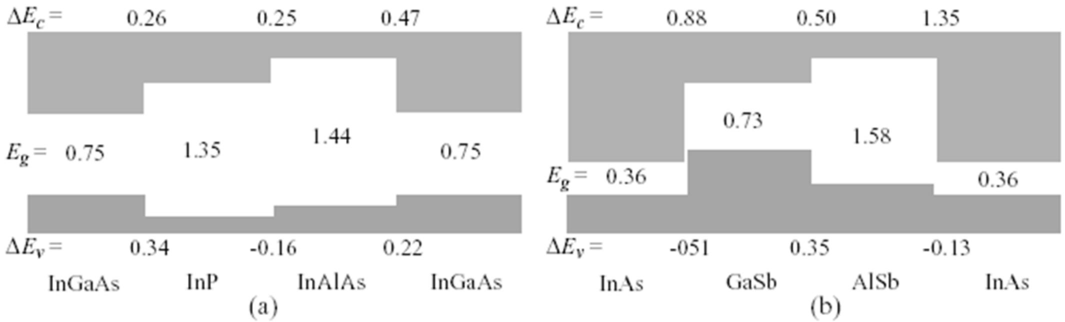

Figure 2.15: Band alignment in InGaAs-InAlAs-InP and InAs-GaSb-AlSb heterostructures [23].

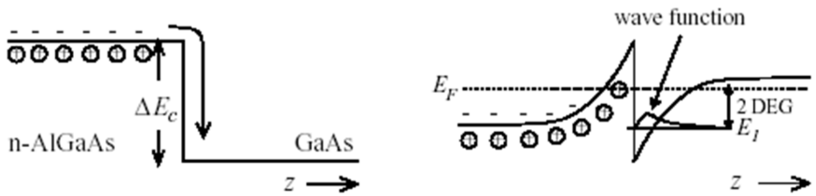

Figure 2.16: Conduction band discontinuity in a n-AlGaAs-undoped GaAs heterojunction [23].

Ver também http://w3.ualg.pt/~jlongras/JLFPhDThesis.pdf (2º capítulo)

Barreiras e poços de potencial

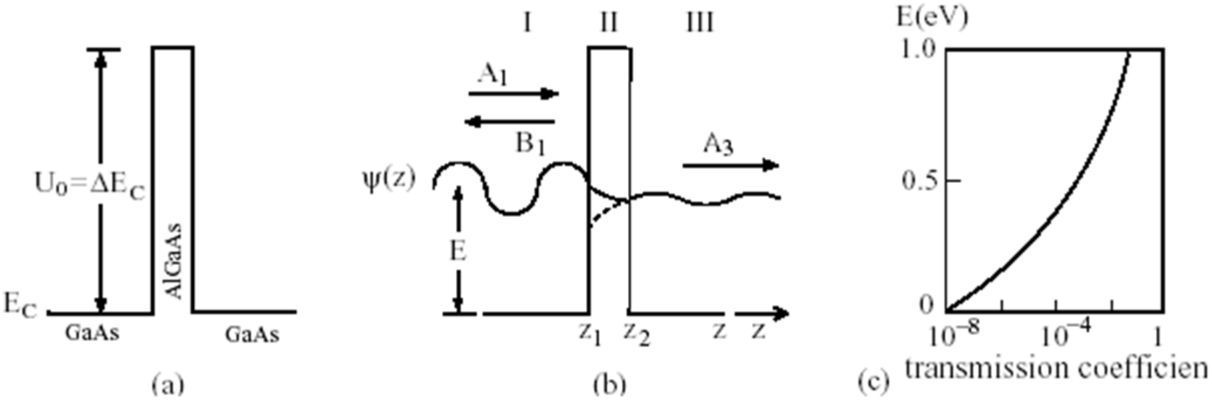

Figure 2.17: Schematic representation of tunnelling in a potential barrier.

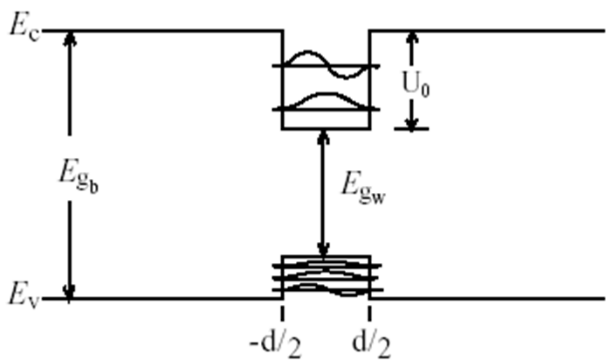

Figure 2.18: Quantum well schematic energy diagram.

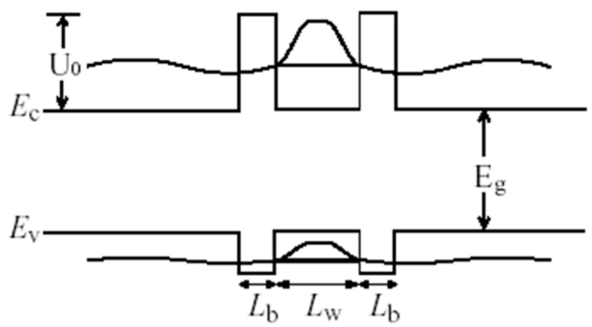

Figure 2.19: Double barrier quantum well.

Ver também http://w3.ualg.pt/~jlongras/JLFPhDThesis.pdf (2º capítulo)

Confinamento ótico e confinamento eletrónico

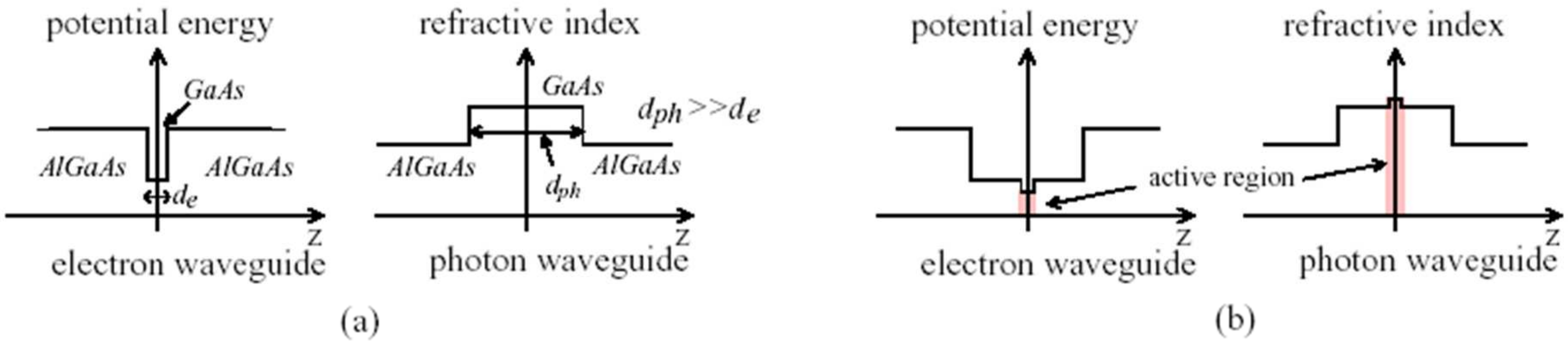

Figure 2.21: (a) Electron and photon confinement in semiconductor heterostructures [30]. The length scales of the confining structures, d_e and d_{ph}, are rather different, because the wavelength is around 1 μm for near infrared light but only about 50 nm for electrons. (b) *Separate confinement heterostructure* (SCH).

Ver também http://w3.ualg.pt/~jlongras/JLFPhDThesis.pdf (2º capítulo)

Guias de onda

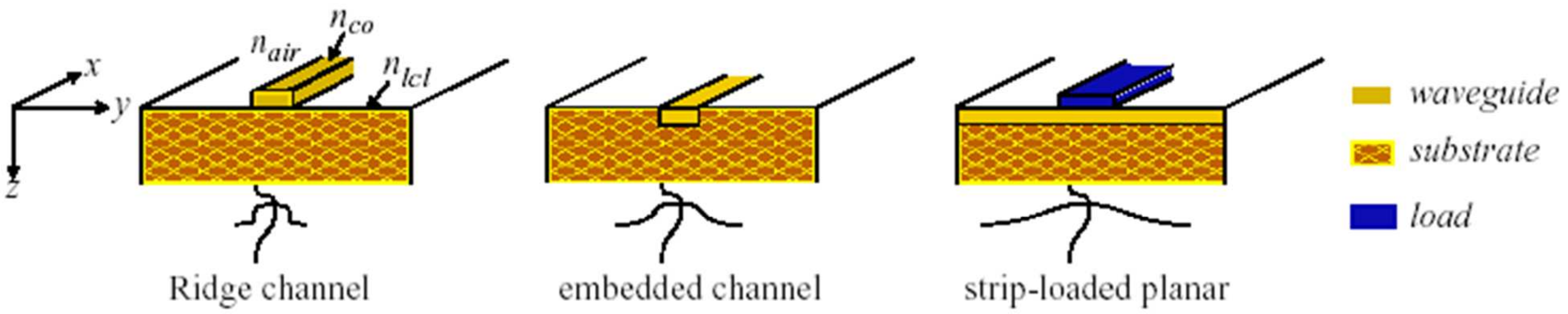

Figure 2.22: Diagrams of basic channel waveguide configurations [58].

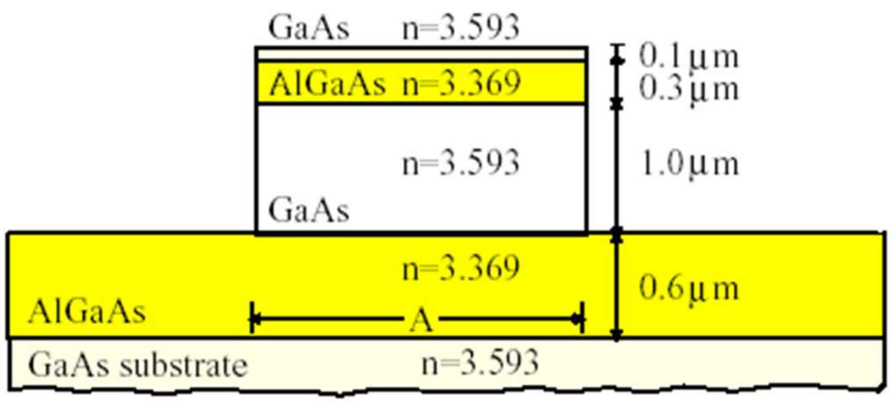

Figure 5.1: AlGaAs/GaAs ridge waveguide cross section schematic.

Fabricação de dispositivos óticos integrados em semicondutores

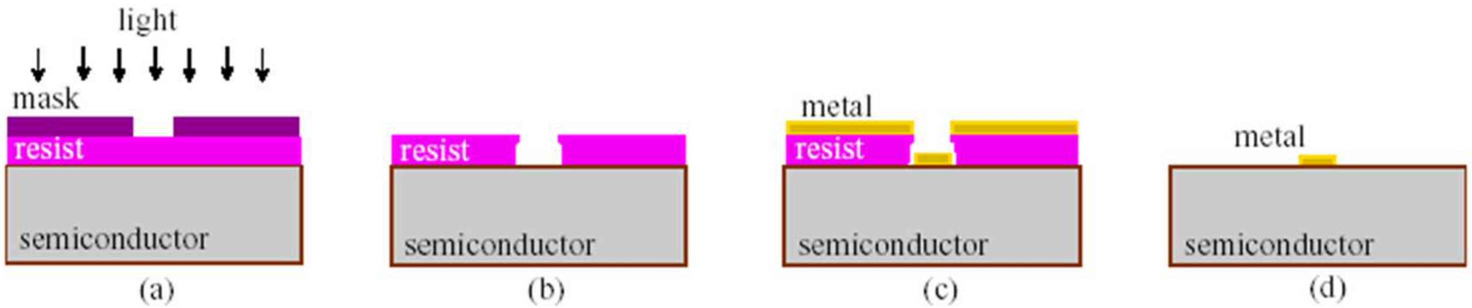

Figure 4.9: Lift-off process used in RTD-EAM fabrication.

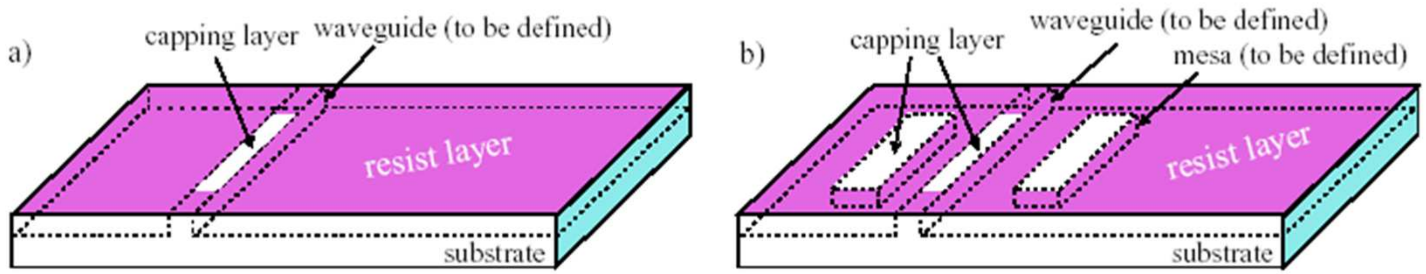

Figure 4.8: RTD-EAM ohmic contact pattern, without and with mesa configurations.

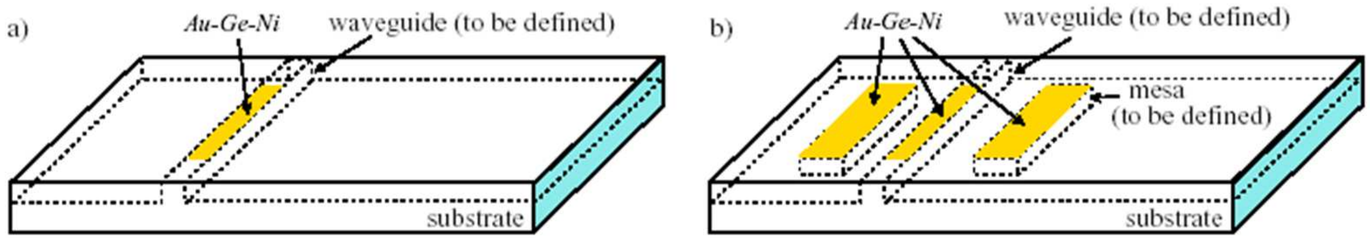

Figure 4.10: RTD-EAM ohmic contacts, without and with mesas.

Fabricação de dispositivos óticos integrados em semicondutores

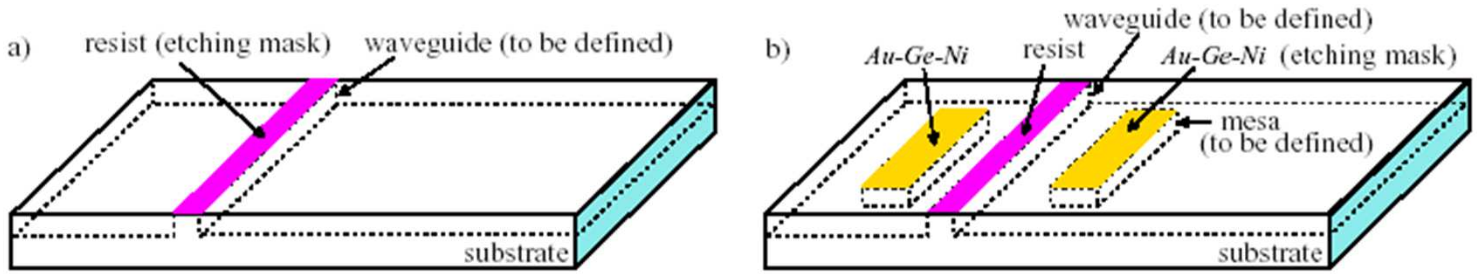

Figure 4.12: RTD-EAM waveguide pattern configuration.

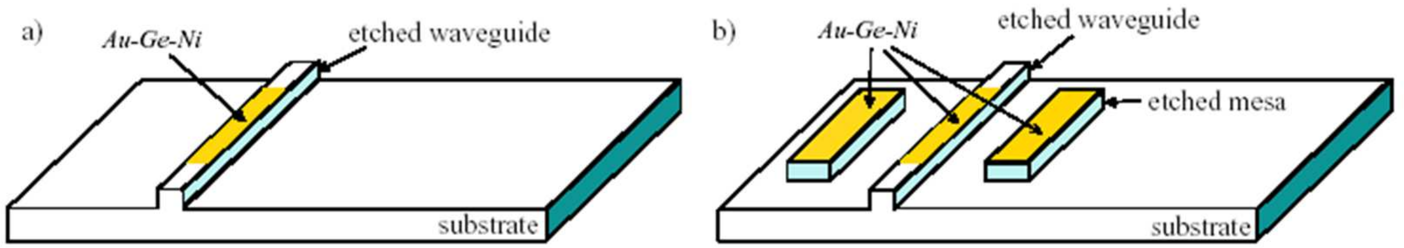

Figure 4.13: Scheme of etched RTD-EAM waveguide.

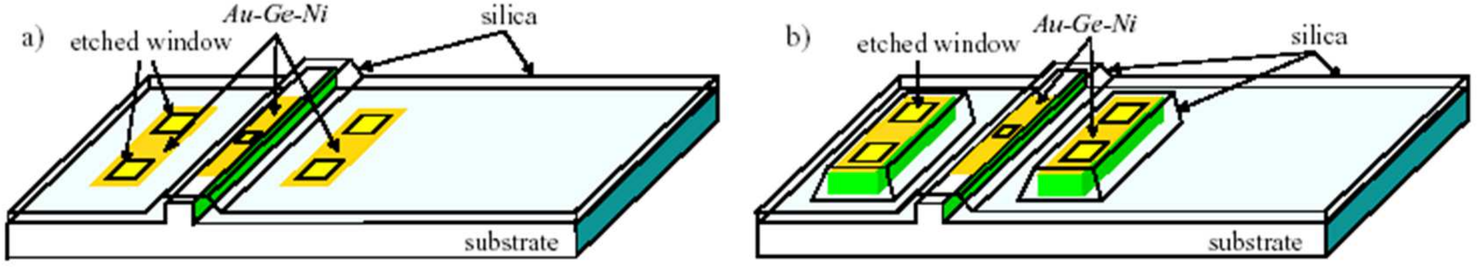

Figure 4.14: RTD-EAM SiO_2 passivation/insulation, showing access contact windows.

Modos em guias de onda semicondutores

mode	$n_{\text{eff,TE}}$	$n_{\text{eff,TM}}$	*FWave IV* mode profile
1st	3.573	3.572	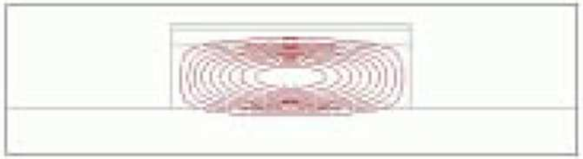
2nd	3.567	3.567	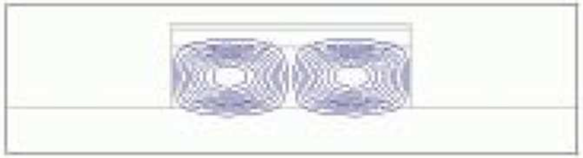
3rd	3.558	3.558	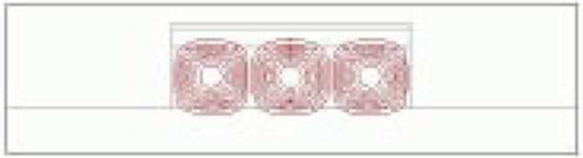

Table 5.1: First three guided modes effective refractive index and profile, for the case of a 4 μm wide 1.4 μm ridge waveguide ($\lambda = 900$ nm).

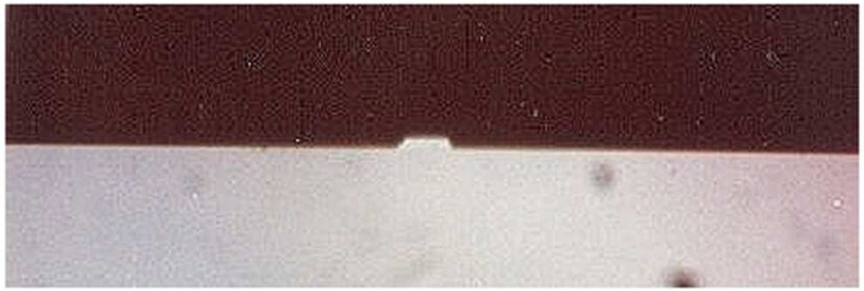

Figure 6.4: Side view of the InGaAlAs waveguide (ridge depth: 1.4 μm; width: 4 μm).

Perdas em guias de onda

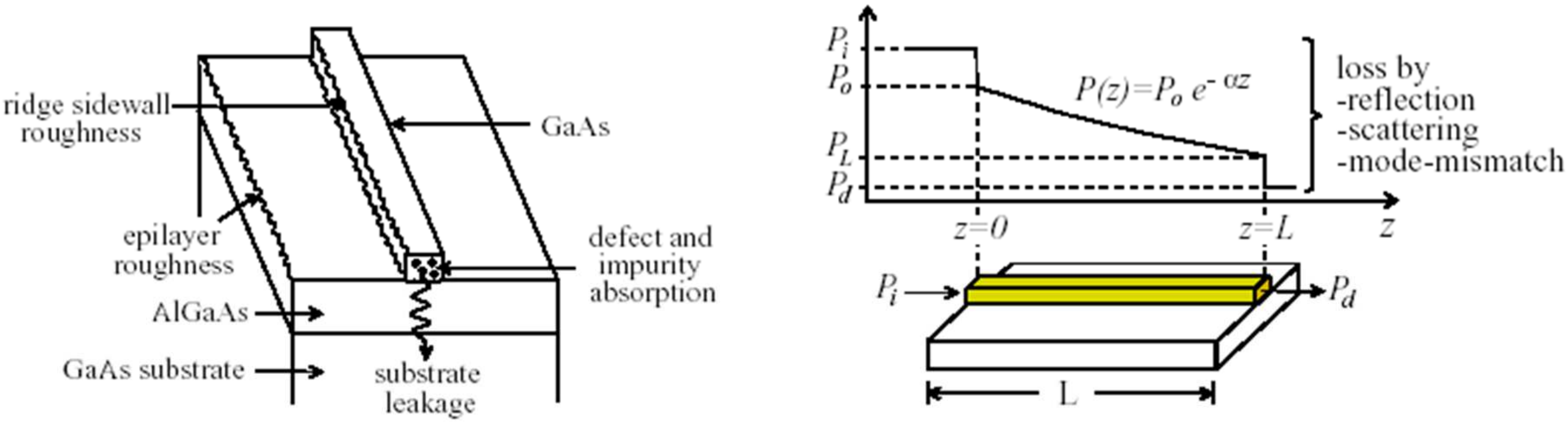

Figure 2.23: Loss mechanisms in ridge waveguides [69].

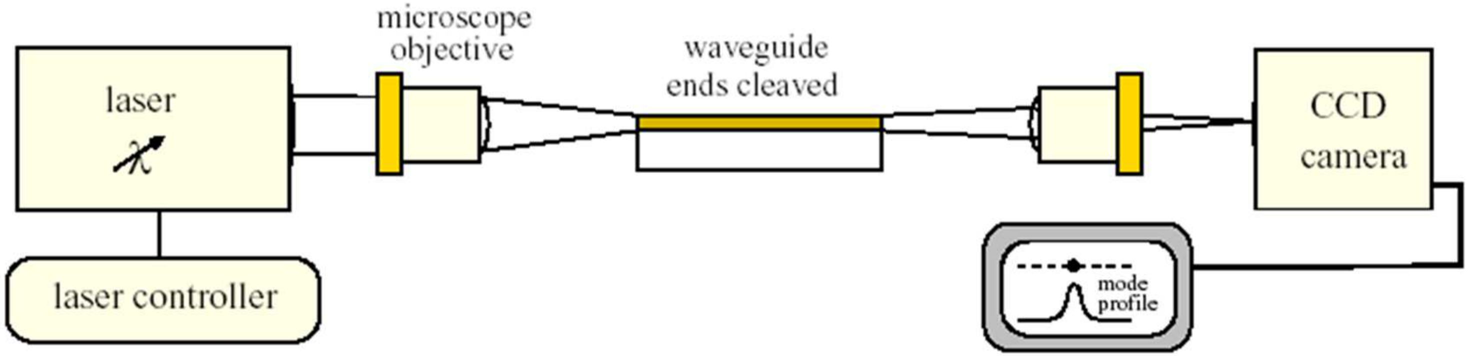

Figure 4.21: Experimental apparatus for observation of optical waveguiding [58].

Ver também http://w3.ualg.pt/~jlongras/JLFPhDThesis.pdf (2º capítulo)

Dispositivos electro-óticos

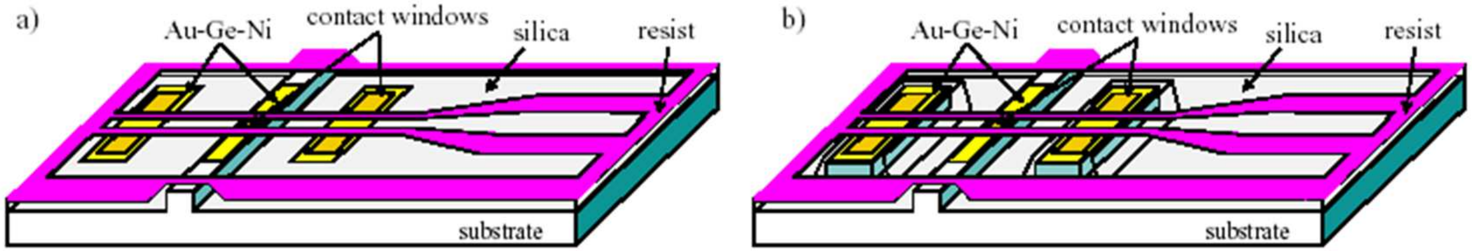

Figure 4.15: RTD-EAM high frequency bonding pads lithography.

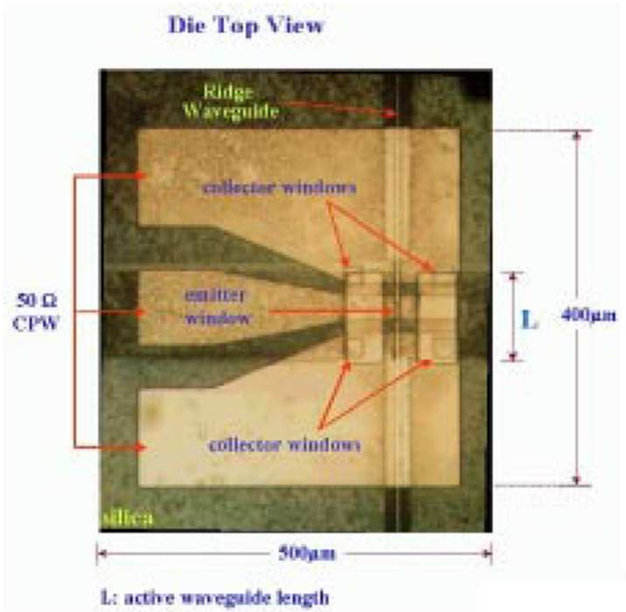

Figure 4.16: RTD-EAM die top view, showing the CPW

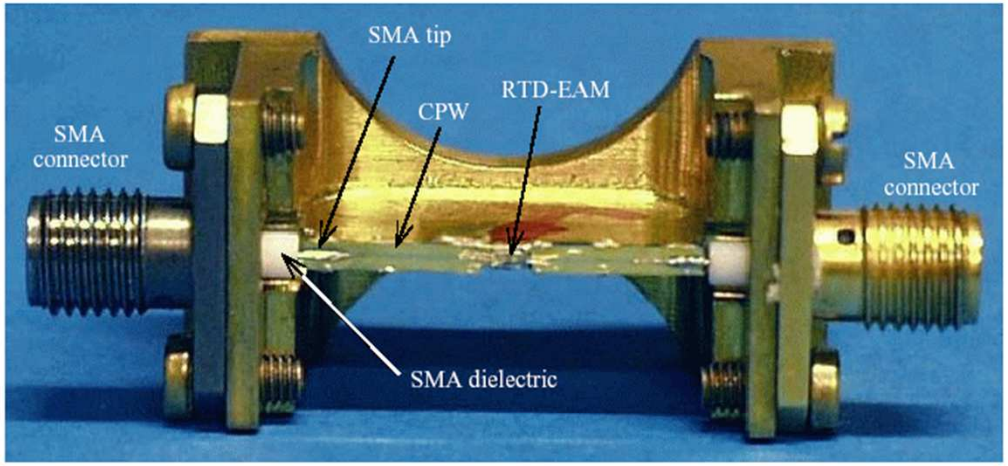

Figure 4.18: Photograph of the RTD-EAM package implemented.

Figure 4.17: Side view picture of a RTD-EAM ridge waveguide (ridge: 1.4 μm).

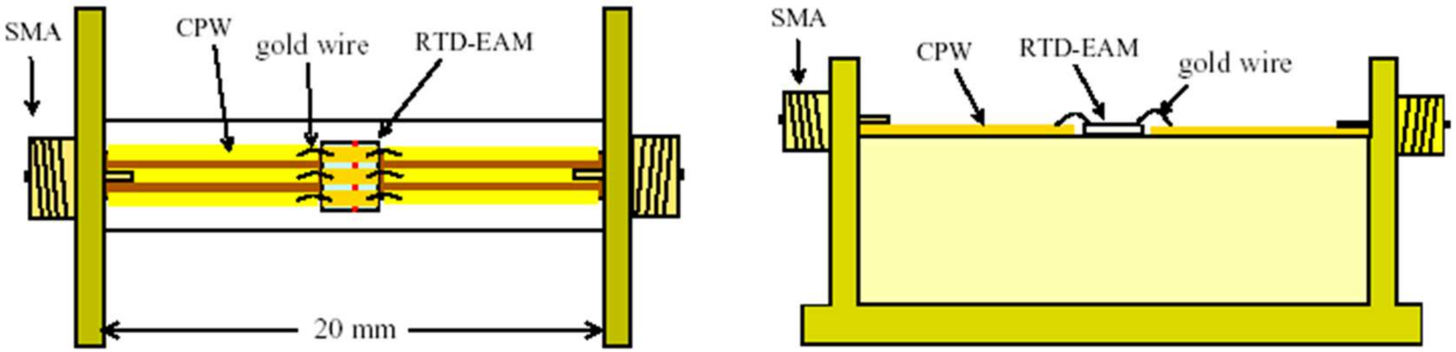

Figure 4.19: Schematic representation of a packaged RTD-EAM device.

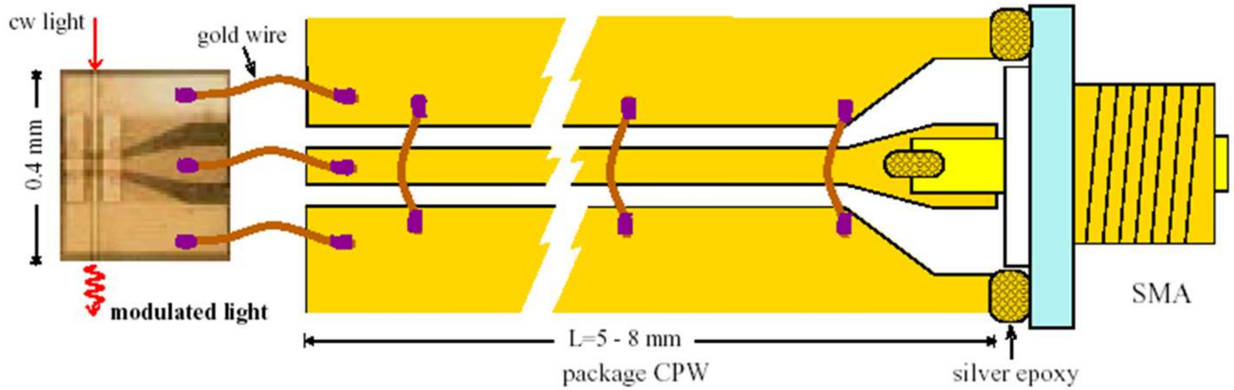

Figure 4.20: Schematic of the RTD-EAM and SMA connection to the CPW package.

Moduladores óticos

Esquemas de modulação

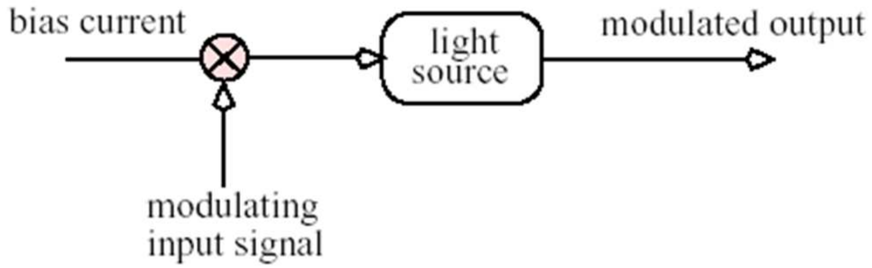

Figure 2.29: Diagramatic represention of direct modulation [14].

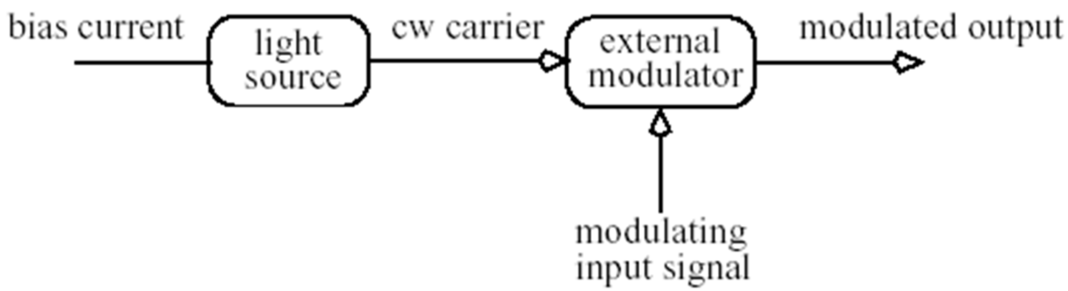

Figure 2.30: Schematic represention of external modulation [14].

Modulação externa por electrorefração e por electro-absorção

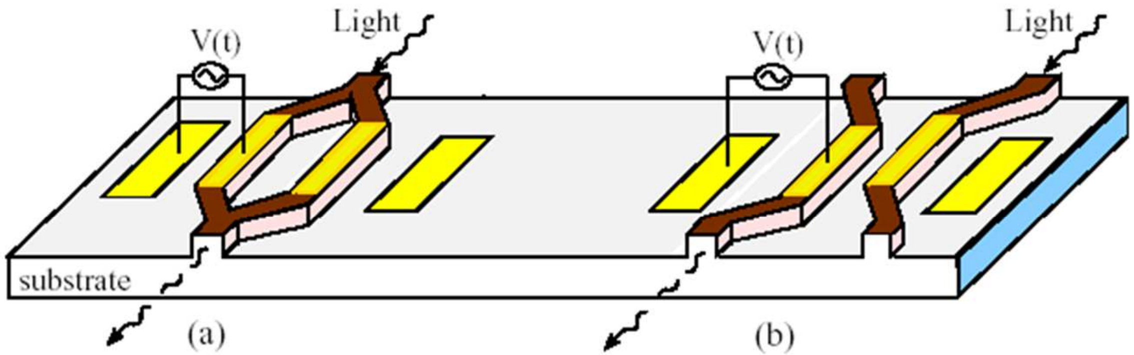

Figure 2.31: (a) Mach-Zehnder modulator. (b) Directional coupler electro-optic switch.

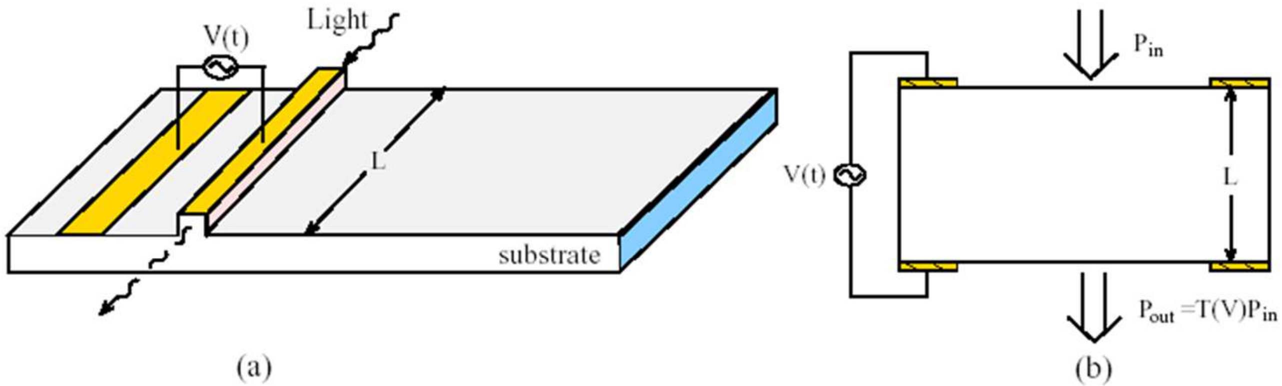

Figure 2.32: Electro-absorption modulator types. a) Waveguide modulator. b) Transverse transmission modulator [58].

Electroabsorção em semicondutores

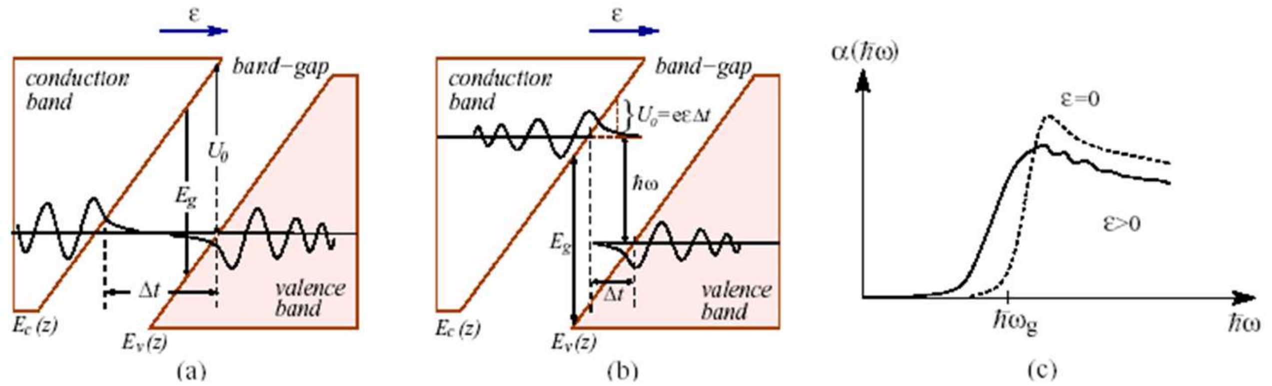

Figure 2.26: Energy band diagram under an electric field, without (a) and with (b) photon absorption. Absorption edge broadening (c) [23].

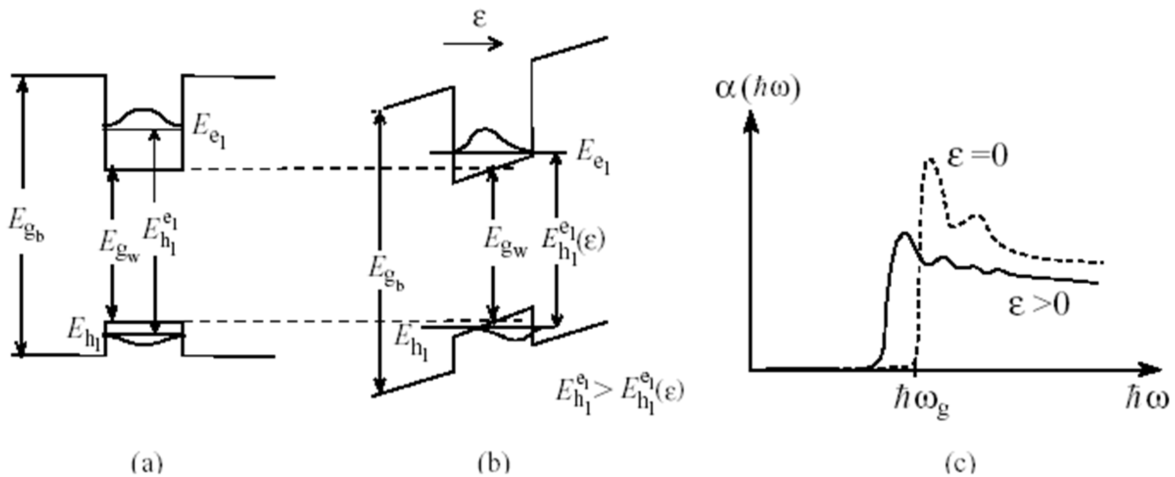

Figure 2.27: Quantum-confined Stark effect (QCSE) in semiconductor quantum wells [23].